Università degli Studi di Ferrara

PH.D. Course
in
Evolutionary Biology and Ecology

In cooperation with:
Università degli Studi di Parma
Università degli Studi di Firenze

CYCLE XXXII

COORDINATOR Prof. Guido Barbujani

# DNA methylation and Cr(VI) stress responses in *Scenedesmus acutus*: a focus in Sulfur pathway

Scientific/Disciplinary Sector (SDS) BIO/01

**Candidate**
Dott. Ferrari Michele

**Supervisor**
Prof. Torelli Anna

Year 2016/2019

Università degli Studi di Ferrara

PH.D. Course
in
Evolutionary Biology and Ecology

In cooperation with:
Università degli Studi di Parma
Università degli Studi di Firenze

CYCLE XXXII

COORDINATOR Prof. Guido Barbujani

# DNA methylation and Cr(VI) stress responses in *Scenedesmus acutus*: a focus in Sulfur pathway

Scientific/Disciplinary Sector (SDS) BIO/01


**Candidate**
Dott. Ferrari Michele

_____
*(signature)*

**Supervisor**
Prof. Torelli Anna

_____
*(signature)*


Year 2016/2019

# Table of Contents

CHAPTER

1

# *Introduction*

## 1.1 - DNA methylation

DNA methylation is a conserved epigenetic modification that is crucial for various biological processes, including gene and transposon silencing, imprinting and X chromosome inactivation. Together with other epigenetic marks, such as the histone code, DNA methylation contributes to chromatin remodelling processes and it is involved in the regulation of gene expression but does not alter the primary DNA sequence (Law and Jacobsen, 2010; He et al., 2011).

Albeit all nucleotides can be methylated, DNA methylation generally refers to an addition of a methyl group onto the C5 position of cytosine to form 5-methylcytosine (5-mC), through a covalent modification (Kalisz and Purugganan, 2004). DNA methylation can be found both in prokaryotes and eukaryotes. In bacteria, its major function is to act as a defence mechanism against invading phage, in fact methylation differentiate host from phage genome, which becomes the preferential target of cleavage action of host restriction enzymes. Moreover, it plays also an important role in DNA repair and replication (Chinnusamy and Zhu, 2009). In eukaryotes, DNA methylation is a fundamental mechanism for the maintenance of genome stability and the regulation of gene expression in response to both external and internal stimuli thus playing a relevant role in plant diversity and development (Becker et al., 2011; Lauria and Rossi, 2011; Schmitz et al., 2011; Zhang et al., 2018).

In plants, DNA methylation is more extensive and affects a wider sequence diversity than in animal genomes. Plants have relatively high concentrations of 5-mC compared to non-plant species because cytosine methylation occurs in three sequence contexts: symmetric CG and CHG and asymmetric CHH (in which H = A, T or C) (Henderson and Jacobsen, 2007). In animals, cytosine methylation is instead mainly restricted to the symmetric CpG dinucleotide, with the exception of the embryonic stem cells (Ramsahoye et al., 2000), the adult mouse cortex and human brain (Lister et al., 2013), where CpH methylation was found.

DNA methylation can be distinguished in *de novo* methylation and maintenance methylation. *De novo* methylation consists in the methylation of DNA sequences not previously methylated and an RNA-directed DNA methylation pathway is crucial in plants for this process (Matzeke and Mosher, 2014). It is involved in the rearrangement of methylation pattern during the embryogenesis and in the cell differentiation processes during development (Razin and Cedar, 1993). Maintenance methylation preserves the

methylation status of symmetric (palindromic) sites after DNA duplication through recognition of hemimethylated sites and methylation of the newly synthesized filament (Finnegan and Dennis, 1993; Saze et al., 2003) (Fig.1.1).

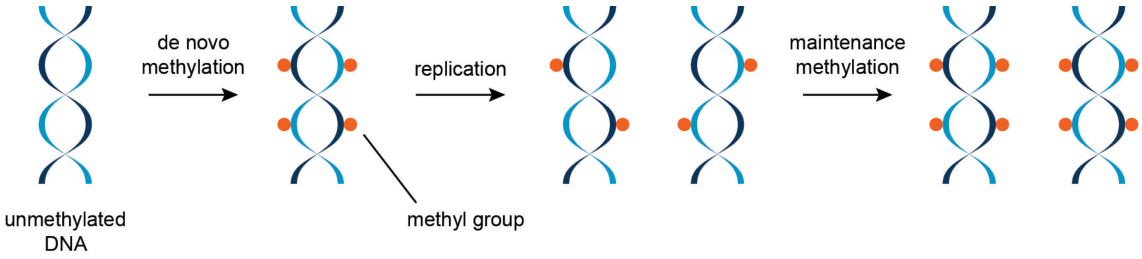


**Figure 1.1 - Schematic representation of *de novo* methylation and maintenance methylation of DNA** (www.atdbio.com/content/56/Epigenetics).

### 1.1.1 - DNA Methyltransferases

DNA methylation in plants, as in animals, relies on different families of DNA methyltransferases (MTasi) with distinct substrate specificity and different modes of action. A large family of DNA methyltransferases, including six subfamilies characterized by conserved active domains associated with distinct N-terminal or C-terminal extensions, catalyses methylation at the C5 position of cytosine (C5-MTasi) (Goll and Bestor, 2005; Ponger and Li, 2005; Huff and Zilberman, 2014). In land plants, three DNA methyltransferase subfamilies have been implicated in the establishment and/or maintenance of DNA methylation (Goll and Bestor, 2005; Du et al., 2015). CG methylation is maintained by enzymes belonging to the Dnmt1/MET1 subfamily (with strong preference for hemimethylated DNA), CHG methylation is mediated by the plant specific CMT3 chromomethylase, and CHH methylation is mainly dependent on the Dnmt3/DRM (Domains Rearranged Methyltransferase) enzymes (Du et al., 2015). Symmetrical CG methylation in certain eukaryotes is carried out by a divergent cytosine methyltransferase, Dnmt5 (Ponger and Li, 2005; Huff and Zilberman, 2014). These enzymes recognize the specific DNA sequences through their variable N-terminal domain and transfer a methyl group from S-adenosyl-L-methionine (S-AdoMet) to carbon 5 of cytosine residues through the activity of the C-terminal catalytic domain (Kumar et al., 1994; Pavlopoulou and Kossida, 2007).

The plant homolog of mammalian Dnmt1, namely DNA METHYLTRANSFERASE 1 (MET1), is the major CG maintenance methyltransferase and it may also contribute to CG *de novo* methylation. In plant are also present DNMT2 homologs that, like

mammalian DNMT2, possess transfer RNA (tRNA) methylase activity (Goll et al., 2006); however, no catalytic activity on DNA has been reported for these enzymes.

The plant DOMAINS-REARRANGED METHYLTRANSFERASEs (DRM) and their mammalian homologs, the Dnmt3 group, are predominantly *de novo* methyltransferases. The domains of amino- and carboxy-terminal halves of DRM proteins are arranged in reverse order when compared with Dnmt3 (domains VI–X are followed by I–V) (Fig. 1.2). DRM2 catalyses cytosines methylation in all sequence contexts and is the prominent cytosine methyltransferase in the RNA-directed DNA methylation pathway (Pikaard and Scheid, 2014).

CHROMOMETHYLASEs (CMTs), a family of DNA methyltransferases identified exclusively in plant, are characterized by the presence of an amino acid chromodomain motif between the conserved motifs II and IV that binds to methylated histones. CHROMOMETHYLASE 3 (CMT3) is the enzyme primarily responsible for CHG maintenance methylation. The chromodomain of CMT3 binds the histone H3 that is dimethylated on lysine 9 (H3K9me2). CHG methylation, in turn, provides a binding site for the SET- AND RING- ASSOCIATED (SRA) domain of the H3K9 methyltransferase SUVH4, leading to H3K9 dimethylation. In such a way, CHG and H3K9me2 modifications reinforce each other through a positive regulatory feedback (Stroud et al., 2013; Du et al., 2014).

CHROMOMETHYLASE 2 (CMT2) plays a role in maintaining CHH methylation in specific genomic contexts, such as the central regions of large transposable elements, presumably via cross talk with histone modifications like its paralog, CMT3 (Zemach et al., 2013).

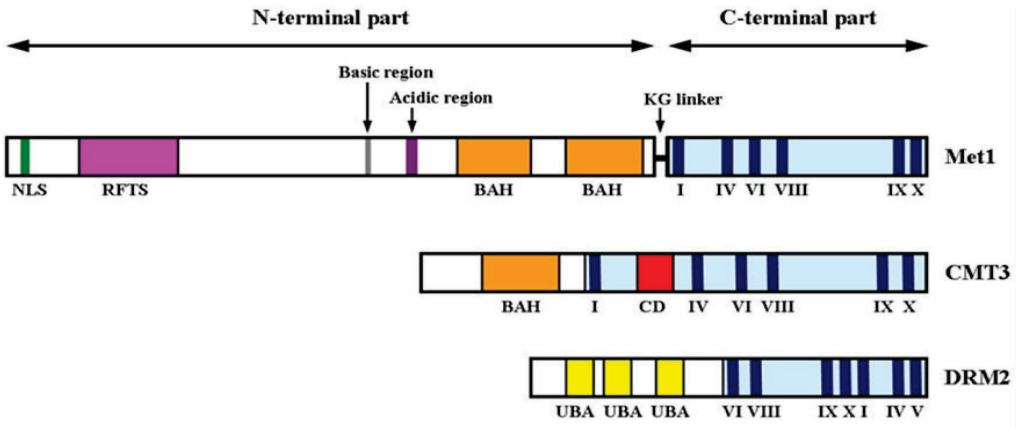


**Figure 1.2 - Comparative schematic structures and relatedness of plant cytosine DNA methyltransferases**. Llight blue filling marks the catalytic domains. Roman numerals indicate the conservative motifs of C5-DNA MTases. *BAH*, bromo-adjacent homology domain; *CD*, chromodomain; *NLS*, nuclear localization signal; *UBA*, ubiquitin association domain (Ryazanova et al., 2013).

### *1.1.1.1 - DNA methyltransferases in algae*

Analysis of phylogenesis and DNA cytosine methyltransferases domain organization in microalgae have been conducted by Ma et al. (2017), through a survey on 12 complete or near-complete Archaeplastida algal genomes for the presence of genes encoding the corresponding enzymes (Fig. 1.3). These authors have observed that DNA cytosine methyltransferases are widely distributed among Archaeplastida microalgae, but in a patchy pattern, with specific subfamily enzymes largely limited to subgroups of organisms. In fact, only *Klebsormidium flaccidum* appears to have a set of DNA cytosine methyltransferases similar to that found in land plants, whereas homologues from other Archaeplastida algae tended to cluster independently within each subfamily. In particular, MET1 homologues are the methyltransferases with the widest distribution, including species belonging to Trebouxiophyceae (*Chlorella sorokiniana* and *Chlorella variabilis*) and Chlorophyceae (*Chlamydomonas reinhardtii* and *Volvox carteri*) classes, as well as to the Charophyta division (*K. flaccidum*). Algal MET1 proteins share high sequence similarity in the DNA methyltransferase catalytic domain with the land plant polypeptides (Fig. 1.3).

Additionally, most of these algal proteins possess D-RFD (DNA methyltransferase replication foci domain) and bromo adjacent homology (BAH) motifs (Fig. 1.3) in their N-terminal extensions, as observed in the canonical enzyme. Besides, in *C. reinhardtii* two additional MET1-related polypeptides, localized in the chloroplasts and influencing plastid DNA methylation, were found. These paralogues, lacking conserved motifs in the N-terminal region, have been termed DMT1a and DMT1b as novel DNA methyltransferase with nonselective *de novo* cytosine methylation activity (Nishiyama et al., 2004; Lopez et al., 2015). Chromomethylase-like methyltransferases, structurally similar to land plant CMT3 except for the lack of the chromodomain in the *Chlorella* enzymes, seemed to be restricted to the chlorophytes *C. sorokiniana* and *C. variabilis* and to the charophyte *K. flaccidum*. Moreover, homologues of Dnmt3/DRM proteins, implicated in *de novo* DNA methylation, were found exclusively in the red alga *Cyanidioschyzon merolae* and the charophyte *K. flaccidum*. Intriguingly, the *C. merolae* predicted polypeptide showed a structural organization similar to the vertebrate Dnmt3s, whereas the *K. flaccidum* proteins appeared more closely related to land plant DRMs. In contrast, Dnmt5-related enzymes appeared limited to the Mamiellophyceae class (*Bathycoccus prasinos*, *Micromonas pusilla* and *Ostreococcus lucimarinus*). The glaucophyte *Cyanophora paradoxa* contains a single DNA methyltransferase that cannot

be unequivocally categorized, maybe because this algae genome has not been completely characterized and some proteins may be missing in the database.

Among the DNA methyltransferases encoded by microalgae there are also other enzymes that cannot be clearly categorized. These predicted proteins contain catalytic domains somewhat related to those of the MET1 and/or the CMT subfamilies but lacking either N-terminal extensions or conserved domains in the N-terminal extensions (Ma et al., 2017). *Chlamydomonas* DMT4 belongs to this group and it is tempting to speculate that some of these enzymes might be responsible for DNA methylation processes unique to microalgae (Lopez et al., 2015).

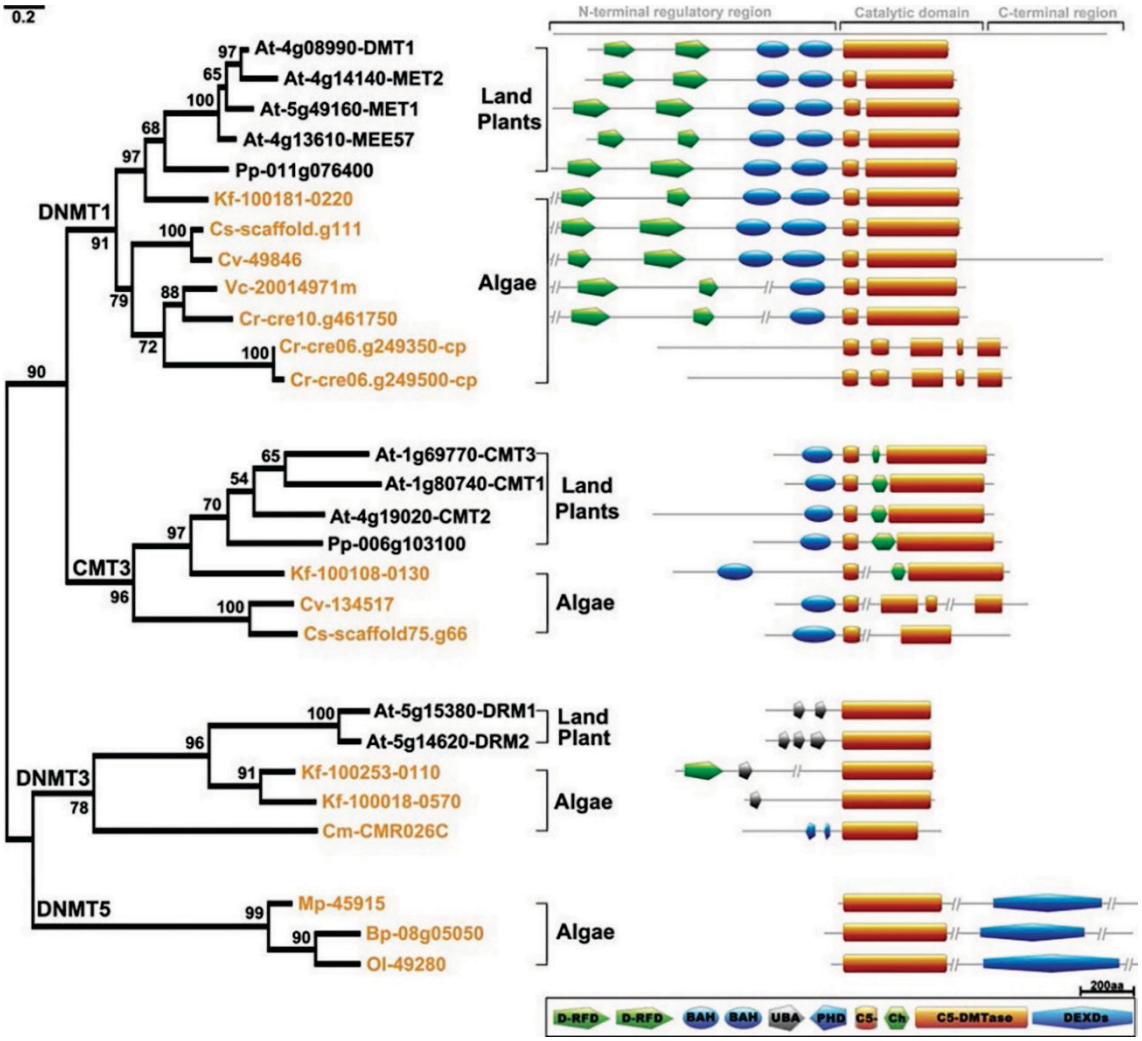


**Figure 1.3** - **Phylogenetic relationship among DNA cytosine methyltransferases**. Species are designated by a two-letter abbreviation preceding the name of each protein: At, *A. thaliana*; Bp, B. prasinos; Cm, *C. merolae*; Cr, *C. reinhardtii*; Cs, *C. sorokiniana*; Cv, *C. variabilis* NC64A; Kf, *K. flaccidum*; Mp, *M. pusilla* CCMP1545; Ol, *O. lucimarinus*; Pp, *P. patens*; and Vc, *V. carteri*. The protein domain organization is indicated on the right. Domain abbreviations: D-RFD, DNA (cytosine-5) methyltransferase Replication Foci Domain; BAH, Bromo Adjacent Homology domain; UBA, UBiquitin-Associated domain; PHD, Plant Homeo Domain zinc finger domain; C5- or C5-DMTase, C-5 DNA Methyltransferase; Ch, Chromo-like domain; and DEXDs, DEXD-like helicases superfamily (Ma et al., 2017).

### 1.1.2 - Maintenance of DNA Methylation

Maintenance of plant DNA methylation depends on the cytosine sequence context and it is catalysed by DNA methyltransferases that in their turn are regulated by different mechanisms. The maintenance of already established DNA methylation patterns occurs in all the different sequence contexts: CG, CHG and CHH. The maintaining of CG methylation in plants requires the activity of MET1, the VARIANT IN METHYLATION (VIM) and the DDM1 chromatin remodelling factor. VIMs are a family of SRA domain proteins orthologs of mammalian ubiquitin-like PHD and RING finger domains 1 (UHRF1) (Law and Jacobsen, 2010), thus suggesting that both plants and mammals maintain CG methylation in a similar manner. MET1 is associated with DNA replication sites, recognizes hemi-methylated CG dinucleotides following DNA replication and methylates the unmodified cytosine in the daughter strand. MET1 has been proposed to be recruited to DNA by VIM proteins in a similar way as DNMT1 is recruited by UHRF1 (Fig. 1.4) (Zhang et al., 2018).

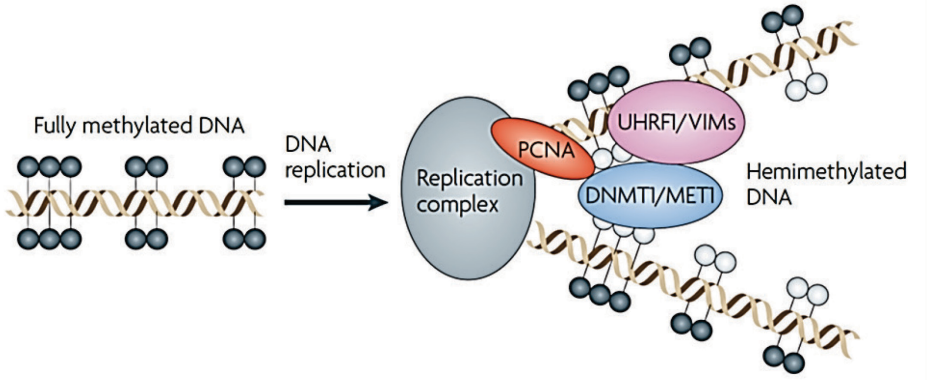


**Figure 1.4 - Maintenance of DNA methylation in plants and mammals.** DNMT1 is proposed to be recruited to replication foci through interactions with UHRF1 that specifically interacts with hemimethylated DNA and with proliferating cell nuclear antigen (PCNA). After been recruited, DNMT1 functions to maintain methylation patterns by restoring the hemimethylated DNA to a fully methylated state. In plants, MET1 and the VIM are likely to function in a similar manner to maintain CG methylation patterns. Black and white circles represent methylated and unmethylated cytosines, respectively (Law and Jacobsen, 2010).

The maintenance of methylation at CHG sites seems not depending on the palindromic symmetry of the sequence. CHG methylation is thought to be maintained through a mechanism involving histone and DNA methylation (Johnson et al., 2007). Genome wide analyses showed that histone H3K9 dimethylation and DNA methylation are highly correlated (Bernatavichute et al., 2008). CMT3 indeed is the DNA methyltransferase largely responsible for maintaining CHG methylation (Lindroth et al., 2001; Bartee et al., 2001) and its activity is strongly associated with dimethylation of lysine 9 on histone 3

where the dual recognition of H3K9me2 by BAH (Bromo Adjacent Homology) and CHROMO domains of CMT3 leads the methylation of CHG sites (Du et al., 2012).

In more details, SUVH4, also known as histone H3K9 methyltransferase KRYPTONITE (KYP), has been demonstrated able to bind methylated mCHH or mCHG of the DNA through its SRA (SET and RING-associated) domain (Jackson et al., 2002). CMT3 is recruited by H3K9me and further methylates CHG sites of the DNA to create binding sites for KYP, resulting in a self-reinforcing feedback loop (Fig. 1.5) (Law and Jacobsen, 2010). A loss of these two components results in a dramatic decrease in DNA methylation (Jackson et al., 2002). Two other H3K9 histone methyltransferases, SUVH5 and SUVH6, also contribute to global levels of CHG methylation (Ebbs et al., 2005). Such interplay between DNA and histone methylation is also observed in mammals and, in many cases, the connection between these modifications appears to involve protein-protein interactions between the histone and DNA methyltransferases themselves. Whereas the direct protein interactions between CMT3 and KYP help to maintain CHG methylation in mammals, this mechanism has yet to be verified in plants.

Methylation in the CHH asymmetric context is maintained by DRM2 and RNA-directed DNA methylation (RdDM), which is involved in *de novo* methylation. However, at some loci this kind of methylation is provided by CMT3 and DRM2 (Cao et al., 2003).

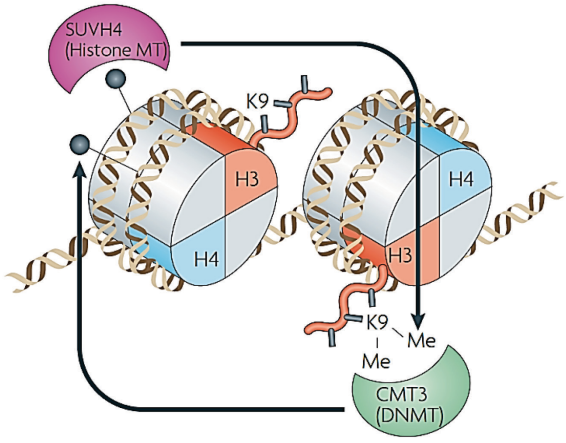


**Figure 1.5 - Model depicting the maintenance of CHG methylation in plants.** A reinforcing loop of DNA and histone methylation is proposed to maintain CHG methylation in plants. The CMT3 maintains methylation in the CHG context, recognized by the SRA domain of the SUVH4 (also known as KYP) histone methyltransferase (histone MT). SUVH4 catalyses H3K9me2, required for the maintenance of CHG methylation, and the chromodomain of CMT3 binds methylated H3 tails (Law and Jacobsen, 2010).

### 1.1.3 - *De novo* DNA Methylation

In plants, *de novo* DNA methylation is mediated through the RNA- directed DNA methylation (RdDM) pathway, which involves small interfering RNAs (siRNAs) and Scaffold RNAs in addition to an array of proteins. The mechanism for RdDM has been divided into the canonical (RNA Polymerase (RNA Pol) IV) and non-canonical (RNA Pol II) pathways (Figure 1.6). Both rely on the generation of siRNA molecules that direct the activity of DRM methyltransferases towards targets through sequence homology (Lister et al., 2008; Matzke et al., 2009).

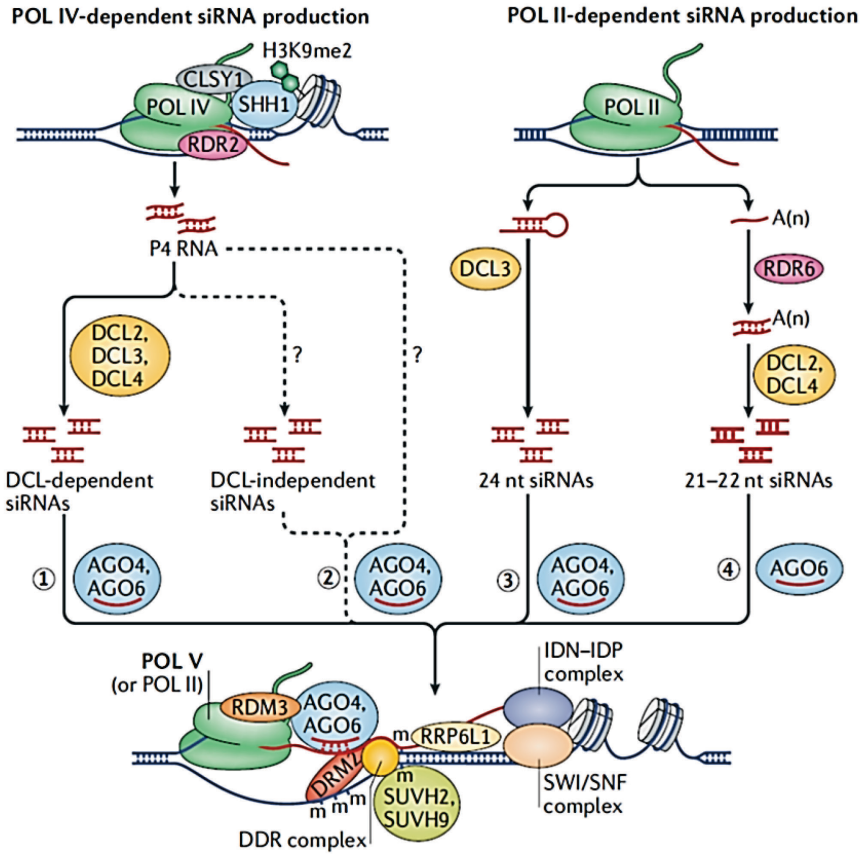


**Figure 1.6 - RNA-directed DNA methylation pathways in *Arabidopsis thaliana*.** In RdDM pathway (step 1), POL IV generates non-coding RNAs (P4 RNAs) functioning as templates for RDR2-mediated production of ds RNAs, which in turn are cleaved by DCL3, DCL2 and DCL4 to yield mainly 24-nt siRNAs. Subsequently, siRNAs, bound by AGO4 or AGO6, pair with POL V-transcribed scaffold RNAs to recruit DRM2, which methylates (m) the DNA. POL IV is recruited to RdDM loci by SHH1, which binds H3K9me2. The chromatin remodeller SNF2 DOMAIN- CONTAINING PROTEIN CL ASSY 1 (CLSY1) interacts with POL IV and is required for POL IV- dependent siRNA production30,31. The majority of RdDM targets remain methylated in the *dcl1–dcl2–dcl3–dcl4* quadruple mutant, implying DCL-independent RdDM may be mediated by DCL- independent siRNAs or directly by P4 RNAs43 (step 2). At some RdDM loci, POL II can produce 24- nucleotide siRNAs and scaffold RNAs45 (step 3). At some activated transposons, POL II and RDR6 collaboratively produce precursors of 21-nucleotide or 22-nucleotide siRNAs that mediate DNA methylation similarly to 24-nucleotide siRNAs47–49 (step 4). AGO4 and/or AGO6 directly associate with POL V, and the association is enhanced by RDM3. Production of scaffold RNAs by POL V requires the DDR complex, consisting of the chromatin remodeller DEFECTIVE

IN RNA- DIRECTED DNA METHYL ATION 1, DEFECTIVE IN MERISTEM SILENCING 3 and RDM1, which associates with both AGO4 and DRM2 and may bind single- stranded methylated DNA. The DDR complex interacts with SUVH2 and SUVH9, which bind to pre-existing methylated cytosines and can recruit POL V. The retention of nascent POL V- transcribed RNA on the chromatin may be facilitated by the RRP6L1 and the IDN2–IDP complex, which interacts with a SWI/SNF chromatin-remodelling complex (Zhang et al., 2018).

The canonical RdDM pathway relies on the activity of two plant-specific RNA Pol II paralogs, RNA Pol IV and RNA Pol V (Haag and Pikaard, 2011). Canonical RdDM initiates with the recruitment of RNA Pol IV, preferentially towards heterochromatic regions by SAWADEE HOMEODOMAIN HOMOLOG 1 (SHH1) (Law et al., 2013; Blevins et al., 2014) and by RNA-DIREECTED RNA POLYMERASE 2 (RDR2), to produce double-stranded RNA (dsRNA) (Blevins et al., 2015). The putative chromatin remodeler CLASSY 1 (CLSY1) is also required for a correct RNA Pol IV and RDR2 recruitment and generation of the corresponding transcripts (Li et al., 2015). The dsRNA is processed by DICER-LIKE 3 (DCL3) into 24-nucleotide siRNAs that are subsequently methylated at their 3′ ends by HUA ENHANCER 1 (HEN1) and incorporated into ARGONAUTE 4 (AGO4). Pol V, in the nucleus, transcribes a scaffold RNA that base-pairs with AGO4-bound siRNAs. A key role is played by RNA-DIRECTED DNA METHYLATION 1 (RDM1), the only protein that interacts with both AGO4 and DRM2 thus creating a bridge between them (Gao et al., 2010). Through this action, the canonical RdDM machinery acts to maintain methylation levels, predominantly in the mCHH context, through *de novo* methylation at heterochromatic regions for continued silencing (Li et al., 2015).

The canonical RdDM pathway utilizes transcripts produced by RNA Pol II to *de novo* initiate new regions for silencing independently from RNA Pol IV (Stroud et al., 2013). RDR6 converts the RNA Pol II-mediated transcripts into dsRNA molecules that are subsequently processed by DCL2 and DCL4 to produce 21-22nt siRNA (McCue et al., 2012; Nuthikattu et al., 2013). These 21-22nt siRNA can then be loaded into either AGO4 or AGO6 to direct methylation in mCHH context in an RNA Pol V- and DRM- dependent manner as described above (McCue et al., 2015). The non-canonical pathway could be considered to act as a surveillance mechanism aimed to identify and target actively transcribed regions for silencing, such as at active TE elements potentially due to loss of silencing factors or recent transposition (Panda et al., 2016).

In order to prevent aberrant hyper-methylation, the activity of RdDM is antagonized, and therefore moderate, by that of REPRESSOR OF SILENCING 1 (ROS1) (Lei et al., 2015; Williams et al., 2015). ROS1 is a DNA glycosylase, involved in the base-excision repair

pathway, which preferentially excises methylated cytosine and, thus, is crucial for the removal of methyl groups that prevents gene hyper-methylation and the spreading of methylation from methylated TEs into genes (Gong et al., 2002; Tang et al., 2016).

### 1.1.4 - DNA Methylation landscape of algae genome

Albeit to date DNA methylation has been studied in many plant species, ranging from algae, cereal crops, vegetables, to trees, the role of DNA methylation in microalgae is still poorly understood. Nuclear genome 5-mC patterns have been recently profiled in several microalgae, including *C. variabilis*, *V. carteri*, *C. reinhardtii* and some Mamiellophyceae members (Feng et al., 2010; Zemach et al., 2010; Huff and Zilberman, 2014; Lopez et al., 2015). In *C. reinhardtii*, DNA cytosine methylation was initially observed in chloroplast DNA during gametogenesis and implicated in the uniparental inheritance of mating type plus chloroplast DNA (Umen and Goodenough, 2001; Nishiyama et al., 2004). Recent findings indicate that the nuclear genome of this alga is methylated at low levels (5.4%, 2.6%, 2.5% in CG, CHG and CHH context, respectively) (Feng et al., 2010; Niederhuth et al., 2016). *Chlorella sp.* Shows even lower CG methylation levels (4–5%), without the clear drop near the transcription start site, but with higher methylation in exons compared to introns (Vandegehuchte and Janssen, 2014).

By contrast, land plants have in general much higher levels of DNA methylation, especially at CG and CHG contexts. For example, in *A. thaliana* leaves, 30.5%, 10.0%, 3.9% methylation occurs in CG, CHG, CHH sites, respectively; rice leaves have an intermediate level of DNA methylation with 58.4% in CG, 31.0% in CHG and 5.1% in CHH sites; *Beta vulgaris* (beet) leaves show the highest levels of DNA methylation with 92.6%, 81.2% and 18.9% in CG, CHG and CHH sites respectively (Niederhuth et al., 2016).

*C. reinhardtii* genome exhibits one of the highest levels known in gene body methylation, with approximately 90% methylation of CG sites. Interestingly, in *Chlorella sp.* there is a large drop in methylation in the promoter region near the transcription start site, where CG methylation level is negatively correlated to gene transcription. However, *C. reinhardtii* had higher levels of CHG and CHH methylation throughout the genome than *Chlorella sp.*, in which CHG methylation is confined to repeats (Vandegehuchte and Janssen, 2014). Intriguingly, CHG and CHH methylation is also observed uniformly along chromosomes and shows little enhancement in transposons/repeats (Feng et al., 2010). In *C. variabilis*, genes are universally CG methylated within their bodies (Zemach

et al., 2010). CHG methylation is also substantial but, similarly to what occur in land plants, is concentrated in repetitive (presumably transposon) sequences and excluded from genes (Zemach et al., 2010).

The genome of the green alga *V. carteri* shows much lower methylation and exclusively in the CG context; transposons and repeats are preferentially methylated but a weak negative correlation between promoter methylation and transcript abundance was also observed (Zemach et al., 2010). In *Volvox*, DNA methylation seems to be implicated in the transcriptional silencing of introduced transgenes and a MET1-like methyltransferase was suggested to be involved in the maintenance of transgene and transposon methylation (Babinger et al., 2007).

*Chlamydomonas* does not contain CMT3 or Dnmt3/DRM homologues, responsible for the CHG and CHH methylation (Feng et al., 2010). In *Chlamydomonas,* DNA cytosine methylation has also been associated with the transcriptional silencing of transgenes, particularly tandem repeats (Cerutti et al., 1997). In contrast, DNA methyltransferases of the Dnmt5 subfamily are present in the Mamiellophyceae microalgae such as *O. lucimarinus*, *M. pusilla* and *B. prasinos.* Moreover, these algae exhibit densely clustered CG methylation in nucleosome linkers, probably contributing to nucleosome positioning and chromatin compaction in very small nuclei (Huff and Zilberman, 2014).

In some microalgae preferential DNA methylation occurs on transposable elements, repetitive sequences and gene bodies(Feng et al., 2010; Zemach et al., 2010; Lopez et al., 2015), consistently with a role of 5-mC in the repression of transgenes, transposons and some protein coding genes (Cerutti et al., 1997; Babinger et al., 2007; Zemach et al., 2010; Du et al., 2015).

Some species of *Chlorella* exhibits a 5-mC pattern of the nuclear genome and a complement of DNA methyltransferases (except for the lack of a Dnmt3/DRM homologue) very similar to those observed in land plants. Other Chlorophyceae i.e. *C. reinhardtii* and *V. carteri* preferentially methylate transposons and repeats in the CG, rather than in the CHG/ CHH, context, reflecting the divergence of their DNA cytosine methyltransferases from land plants.

As for as the chloroplast genome, *Chlamydomonas* chloroplastic DNA was dynamically methylated throughout all the life cycle: 5-mC level was low in vegetative cells; increased during gametogenesis reaching a peak during zygote development probably related to the packaging and protection of chloroplast DNA in the zygospores (Lopez et al., 2015).

Some microalgae, such as *C. reinhardtii*, also exhibit DNA adenine methylation in the nuclear genome, catalysed by an undefined methyltransferase. N6-methyladenine mainly locates at AT dinucleotides near transcription start sites, shares little correlation with 5-mC and seems to mark the transcriptional start sites of active genes (Fu et al., 2015).

Thus, the distribution and function(s) of DNA methylation in microalgae appear to be highly varied. In some cases, 5-mC seems to be associated with gene silencing – particularly of transposons/repeats, as in higher eukaryotes – but in other instances DNA methylation appears to reflect algal-specific processes that remain to be fully characterized.

### 1.1.5 - DNA methylation in responses to abiotic stress

The role of DNA methylation response to stress has been widely investigated in plants, whereas in algae very few data about DNA methylation and response to environmental stressor are reported. It is note that in plants, abiotic stress (including heavy metals, drought and cold) can trigger DNA methylation changes at a genome-wide scale (Vandegehuchte and Janssen, 2014). So, the single genome in a plant cell could give rise to multiple epigenomic changes in response to developmental and environmental cues. In fact, stresses can induce changes in gene expression through hypomethylation or hypermethylation of DNA (Chinnusamy and Zhu, 2009) but also in genome regions which have an adaptive significance during stress responses and can direct genome evolution (Boyko and Kovalchuk, 2008).

Indeed, modifications in DNA methylation pattern, allowing rapid and reversible changes in the chromatin structure, can enable the activation of defence pathways through the combination of genetic and epigenetic mechanisms (Peng et al., 2009). Moreover, in presence of a persistent stress, the epigenetic mechanism establishes a DNA methylation-dependent stress memory in plants, mainly due to GC-rich sequences methylation (Jiang et al., 2014; Sanchez et al., 2014; Wibowo et al., 2016); this mechanism ensures the faithfully transfer of the "memory" to the offspring (Mathieu et al., 2007).

Both biotic and abiotic stresses were found to induce modifications in DNA methylation pattern, both genome-wide and at specific loci, usually associated to transcriptional regulation of genes involved in plant stress responses (Yong et al., 2015; Xu et al., 2015; Zhang et al., 2016). These genes, in their turn, control important genetic functions like

transcription, replication, DNA repair, gene transposition and cell differentiation (Madlung and Comai 2004; Angers et al., 2010; Sahu et al., 2013).

Literature data reported that DNA methylation plays an important role in the adaptation of the red alga *Gracilariopsis lemaneiformis* to temperature stress (Peng et al., 2018). By using MSAP technique (methylation sensitive amplified polymorphism), it was observed that both high and low temperature stress induced some changes in the methylation pattern of this alga. In particular, high temperature could induce more cytosine methylation/demethylation transform than low temperature treatment (Peng et al., 2018). Notwithstanding, in plant, as *Zea mays,* cold stress induced a decrease of the level of genomic methylation. This modification seems to be organ- and site-specific, with a decrease of DNA methylation in roots in Ac/Ds transposons, suggesting a possible role for transposable elements in stress response (Shan et al., 2013). In *Solanum lycopersicum*, cold determines the downregulation of the DNA demethylase DME-LIKE 2 (*DML2*) gene, leading to a hypermethylation and silencing of genes involved in the biosynthesis of volatile compounds, thus causing the loss of flavour of *S. lycopersicum* fruits under cold storage (Zhang et al., 2016). In *Mesembryanthemum crystallinum* exposed to salt stress, water deficit caused by the osmotic pressure determines the switching to the Crassulacean acid metabolism (CAM) (Bohnert et al., 1988). This switchover to the CAM pathway is accompanied by satellite DNA hypermethylation probably allowing the simultaneous regulation of expression of the genes involved in the CAM pathways (Dyachenko et al., 2006).

Many data report DNA methylation variations induced by heavy metals in plants. Mercury (Hg) exposed rice plants were self-pollinated and three further non-exposed generations were evaluated. In many cases altered methylation patterns were transferred to the first offspring generation (F1), often accompanied by extra methylation changes. For most of the tested loci this new methylation pattern was then stably transferred to the second offspring generation (F2). In the third generation (F3), all methylation changes that were originally induced in the Hg-exposed plants were stably inherited. Strikingly, the F1 and F2 progeny of Hg-exposed ancestors exhibited a higher resistance to Hg-exposure compared to the progeny of control plants. These plants might thus have acquired a transgenerational epigenetic memory of stress, resulting in an increased tolerance respect to progeny of non-exposed plants (Ou et al., 2012).

A reduction of DNA methylation has been detected in *Trifolium repens* and *Cannabis sativa* after exposure to nickel, cadmium and chromium (Aina et al., 2004), while in

*Brassica napus* heavy metal exposure promoted genomic methylation (Li et al., 2016). Labra et al. (2004) evaluated genetic damage and epigenetic alteration induced by Cr(VI) in *B. napus*. The Authors observed an increased global DNA methylation in the CCGG-DNA sequence after treatment with 10–200 mg/l potassium dichromate and the methylation levels were positively correlated to the metal concentration. The Authors suggested that the global DNA hypermethylation was associated to plant self-protection mechanisms, which induced cell cycle arrest with the consequent reduction of plant growth and development (Labra et al., 2004).

In marine environment, *Posidonia oceanica* exposed to Cd stress, showed a DNA methylation increase (evaluated by MSAP technique) and an overexpression of a chromomethylase gene *(PoCMT)* (Greco et al., 2012). On the contrary, Cd exposure stimulated DNA demethylation events in the red seaweed *Gracilaria dura* genome, resulting in 18.1% of hypomethylation (Kumar et al., 2012).

These data suggest that methylome dynamic under stressful condition depends on both the plant species and the kind of heavy metal. Therefore, further studies are required to fully elucidate the network of processes "acting on" and "regulated by" DNA methylation, mainly under stress conditions, expecially in algae for which very few data are known.

## 1.2 - Chromium

Heavy metals (HMs) belong to group of non-biodegradables, persistent inorganic chemical constituents with the atomic mass over 20 and the density higher than 5 $g \cdot cm^{-3}$ and showing cytotoxic, genotoxic and mutagenic effects on humans or animals and plants (Flora et al., 2008). In the soils there are two kinds of metals which are referred to as essential micronutrients for normal plant growth (Fe, Mn, Zn, Cu, Mg, Mo and Ni) and nonessential elements with unknown biological and physiological function (Cd, Sb, Cr, Pb, As, Co, Ag, Se and Hg). The essential elements play a pivotal role in the structure of enzymes and proteins. Plants require them in tiny quantities for their growth, metabolism and development; however, the availability of both essential and nonessential metals represents only one important factor in the growing process of plants because also their exceeding concentration can lead to the reduction and inhibition of in plant growth (Emamverdian et al., 2015 and references therein).

Chromium (Cr) is a common heavy metal and it is well documented as a toxic agent for plant growth and development. In addition, chromium is known as one of the causes of environmental pollution (Emamverdian et al., 2015 and references therein), which has gained substantial consideration worldwide because of the high levels of the metal disperse in the water and soil by numerous natural and anthropogenic activities (Ashraf et al., 2017). Chromium concentration ranges from 0.1 to 117 mg $L^{-1}$ and from 0.2 - 50 mg $L^{-1}$ in fresh and sea water respectively (Nriagu, 1988).

Many human activities contribute to chromium release, mainly in its hexavalent form, in water, air and soil matrices. In particular, chromium is utilised in the metallurgical and chemical industry in processes such as metalworking and pigment production (Tchounwou, 2012).

Chromium has several oxidation states (-2 to +6), but hexavalent chromate (Cr(VI)) and trivalent chromite (Cr(III)) are the most common and stable forms in the natural environment (Ashraf et al., 2017). Cr(III), being necessary for lipid and sugar metabolism (Bai et al., 2015), is an essential trace element for human and animal health (Prasad, 2013; Eskin, 2016), however, it is not required by plants (Shanker et al., 2005). Cr(VI) usually occurs in the anionic chromate ($CrO_4^-$) and dichromate ($Cr_2O_4^{2-}$) forms. It can form water-soluble compounds such as, for example, sodium chromate ($Na_2CrO_4$) and potassium chromate ($K_2CrO_4$) or non-water-soluble compounds such as barium ($BaCrO_4$) and lead chromate ($PbCrO_4$) (IARC).

In plants, Cr is found as Cr(III) and Cr(VI) species, where the former is considered more toxicant than the latter. Despite this, Cr(III) is a less mobile than Cr(VI), which instead as $Cr_2O_7^{2-}$, can readily enter cells through nonspecific anion channel (Guo et al., 2019). Under reducing condition, Cr(VI) is converted to its more toxic form Cr(III), which can indirectly influence and change soil pH to both alkalinity or acidity extremes, depending on prevailing condition in soil subsurface. This phenomenon might perturb the nutrients bioavailability and their sorption by plants. The highest concentration of Cr occurs in the root rather than other parts of plants (Emamverdian et al, 2015 and references therein).

### 1.2.1 - Toxicity of chromium

Chromium does not have any known biological role in physiological and biochemical metabolism of plants but it is known that an excessive Cr level in plant tissues can

provoke numerous physiological, morphological and biochemical toxic effects (Shahid et al., 2017 and references therein).

Cr(VI) is highly toxic since it easily crosses cell membranes thrugh sulfate channels. The toxic effects occur during its reduction to Cr(III), via the Fenton and Haber-Weiss reactions, resulting in the production of radical oxygen species (Shi and Dalal, 1990) and the subsequent interaction of the Cr(III) with DNA (Vignati et al., 2010) that induces genotoxic effects (Warren et al., 1981; Medeiros et al., 2003).

Chromium toxicity is well reported to reduce plant growth, cause ultrastructural modifications of the cell membrane and chloroplast, induce chlorosis in leaves, damage root cells, reduce pigment content, disturb water relations and mineral nutrition and alter enzymatic activities (Ali et al., 2015; Reale et al., 2016).

The mentioned alterations can be caused either by a direct effect on enzymes and metabolites or by the formation of reactive oxygen species that determine oxidative stress. The toxic action of chromium at the photosynthesis level occurs in terms of reduction in carbon dioxide fixation, inhibition of the electron transport chain and of enzymes involved in Calvin cycle and photophosphorylation. The effects exerted by chromium on mineral nutrition concern the interaction on absorption of many essential elements for plants such as N, P, Fe, K, Mg, Mn and others. Chromium also affects the production of pigments necessary for plant life such as chlorophylls and anthocyanins (Shanker et al, 2005).

High Cr levels also induce changes in plant physiology and morphology due to enhanced generation of reactive oxygen species (ROS). When generated at high levels, ROS may provoke cell death because of oxidative processes such as DNA and RNA mutation, enzyme inhibition, lipid peroxidation and protein oxidation (Shahid et al., 2017 and references therein).

Numerous studies report that Cr toxicity suppresses the functioning and regulation of various proteins (Dotaniya et al., 2014) and causes chromosomal aberrations in plant tissues (Kranner and Colville, 2011).

Chromium induces oxidative stress due to its reduction from Cr(VI) to Cr(III), a reaction that generates various radical oxygen species including superoxide anions, hydrogen peroxide and hydroxyl radicals. Oxygen toxic species cause peroxidation of membrane lipids with the consequent destabilization of cell membranes and loss of membrane functions, such as decreased photosynthetic efficiency and consequent loss of biomass (Liu et al., 2008; Ali et al., 2013; Gill et al., 2015; Ma et al., 2016).

In the green alga *Chlorella pyrenoidosa* (growing both in the sea and in fresh water) Cr(VI) causes an accelerated photo-destruction and/or slowing down in the repair of the PSII reaction centers. This does not occur if the algae are exposed to chromium in the dark. This suggests that Cr(VI) uptake is a light dependent process or, more likely, that the inhibitory effects on PSII are caused by other injurious effects on the photosynthetic system, due to photo-destruction and/or to the slowing down in the repair of its reaction centers for electron transport (Horcsik et al., 2007).

In the green alga *Desmidium swartzii*, Cr(VI) causes morphological alterations visible to the optical microscope, such as contraction of chloroplasts and cellular structure alterations; the reduction of biomass and photosynthetic efficiency have also been recorded (Andosch et al., 2015). Similar effects were also observed in *Micrasterias denticulata*, in which the reduction of cell viability was also observed (Volland et al., 2012). Electron microscopy analysis of *M. denticulata* showed alterations in cell morphology, including the appearance of vacuoles containing electron-dense material, swollen mitochondria, a high number of starch granules in chloroplasts and destruction of the ultrastructure of the photosynthetic organelle (Volland et al., 2012, 2014). Both in *D. swartzii* and in *M. denticulata* accumulations of chromium have been observed in vesicular structures attached to the inner side of the cell walls.

### 1.2.3 - Responses to Cr(VI) toxicity

In order to cope with high levels of ROS produced under biotic and abiotic stresses, plants have developed numerous and complex adaptive strategies, including chelation by organic molecules followed by sequestration within vacuoles. Plants also possess a secondary mechanism of producing antioxidant enzymes to scavenge the enhanced levels of Cr-mediated ROS (Shahid et al., 2017 and references therein).

Different mechanisms for coping heavy metal toxicity (in particular of chromium), have been reported in microorganisms and in plants: (i) decrease in chromium accumulation, (ii) chelation or external complexation, (iii) compartmentalization or formation of intracellular chromium-binding complexes, (iv) activation of the antioxidant system, (v) reduction of Cr(VI) to Cr(III) and (vi) efflux of the chromate (Cervantes et al., 2001; Mallick and Rai, 2002).

i. Chromium accumulation can be reduced by decreasing the number of sulfate transporters. *Neurospora crassa* mutants with a reduced number of sulfate

transporters are able to tolerate chromium (Marzluf, 1970; Paietta, 1990). The inhibition of sulfate assimilation, due to the presence of chromium, was also observed in the unicellular algae *C. reinhardtii* and *Monoraphidium braunii* (Perez-Castineira et al., 1998).

ii. The complexation of extracellular chromium through wall polysaccharides, or mucilage was reported in the cyanobacterium *Nostoc muscorum* (Weckesser et al., 1988) and in the bacterium *Enterobacter cloacae* (Iyer et al., 2004). Extracellular metal chelation has been observed in unicellular green algae (Kaplan et al., 1987), such as *Euglena gracilis* that, in the presence of chromium, secretes molecules such as malate, whose synthesis pathway is upregulated, able to chelate metal ions through their carboxyl groups (Lira-Silva et al., 2011). The same mechanism has been observed in a high number of brown algae (Davis et al., 2003), which, due to the peculiar structure of their cell walls, are among the best existing bio-adsorbents (Wang and Chen, 2009).

iii. In *Micrasterias* chromium has been observed to accumulate in bag-like structures close to the cell wall (Volland et al., 2012). The intracellular Cr can be inactivated by chelating peptides such as reduced glutathione (GSH), the main detoxifying product of the sulfate assimilation pathway. GSH is a tripeptide with multiple functions in plant metabolism. Its biosynthesis is limited to plastids and cytosol, from where it is then transported to different organelles (Moran et al., 2000; Zechmann et al., 2008), as in mitochondria where it is also found at concentrations higher than in chloroplast (Zechmann et al., 2008; Kolb et al., 2009; Volland et al., 2012). GSH plays an important role in Cr(VI) detoxification, thanks to the formation of a GS-$CrO^{3-}$ complex through the binding with its sulfhydryl groups, the reduction from Cr(VI) to Cr(V) (Brauer and Wetterhahn, 1991) and the detoxification of chromium induced ROS (Panda, 2007; Pandey et al., 2009; Upadhyay and Panda, 2010). Moreover, there are several other sulfur metabolites, besides GSH, suitable for detoxification and chelation of heavy metals and useful against the pathogens attack. Among these metabolites have been reported phytochelatins, glucosinolates and cysteines, such as γ-glutamylcysteine, N-acetylcysteine and free cysteines (Bloem et al., 2015).

iv. Plants and algae respond to chromium exposure by activating the synthesis of antioxidant enzymes, such as superoxide dismutase and catalase, in order to

reduce ROS, thus preventing lipid peroxidation and the consequent damage to cell membranes (Pinto et al., 2003; Rai et al., 2004; Gill et al., 2015).

v. Bacteria possess NADH and NADPH dependent systems able to reduce chromium from Cr(VI) to Cr(III) within the cells (Thacker and Madamwar, 2005).

vi. An active chromate transport mechanism directed outside the cells was found in some bacteria and archaea, the involved proteins, called CHromate Resistance (CHR), belong to a chromate/sulfate antiport transporters family (Nies et al., 1998).

### 1.2.4 - Crosstalk between chromium and sulfur

An important link between sulfur and chromium derives from the strict similarity in the chemical/physical characteristics of chromate and sulfate anions (Fig. 1.7) which allow chromate to enter the cell through sulfate transporters.

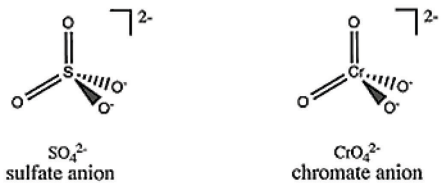


**Figure 1.7 – Structures of sulfate and chromate anions.** A possible competitive interaction for the absorption between chromate ($CrO_4^{2-}$) and sulfate ($SO_4^{2-}$) is due to their similar size.

Cr uptake *via* sulfate transporters has been demonstrated in a wide range of organisms, ranging from bacteria and yeast to plant and mammalian (Holland and Avery, 2011). Paietta in 1990s observed that the repression of sulfate permeases, in presence of high sulfur concentrations, conferred chromate resistance to a wild type strain of *Neurospora crassa*. In contrast, a mutant that was unable to suppress the sulfate permease genes was sensitive even at low chromate concentrations. In transgenic plants of *Nicotiana tabacum*, the over-expression of a yeast transcription factor involved in the accumulation of chromium, induced an increase in chromium and sulfur accumulation and in chromium tolerance. In these transgenic plants was observed an increase in the synthesis of the SLT1 homologous transporter (*NtSLT1*), suggesting that chromate and sulfate are absorbed through the same transporter.

Some researchers investigated the transport and reduction of chromium in the presence and absence of exogenously applied sulfate and suggested that proper sulfate concentration is beneficial to chromate transport into cells. Experiments conducted on yeast cells have led to the hypothesis that chromate toxicity can also be affected by sulfate concentration: in the presence of high sulfate concentrations (30 mM) chromate was toxic between 200 and 400 µM, whereas in standard sulfate condition (100 µM) lower chromate concentrations (15-20 µM) were enough to cause a considerable growth inhibition. The protein expression profile of yeast cells treated with 15-20µM chromate at low sulfate concentration was very similar to that of cells treated with 200 µM chromate at high sulfate concentration (Pereira et al., 2008). The reduced sulfur influx in presence of chromium could explain why chromate is able to induce the expression of genes involved in sulfate assimilation (such as ATP sulfurylase, APS reductase and GSH synthetase), thus promoting the accumulation of this pathway end-products: cysteine and glutathione that could therefore be involved in chromium tolerance processes (Schiavon et al., 2008). Ali et al. (2013), examined the effect of hydrogen sulfide ($H_2S$) derived from NaHS in alleviating chromium stress in barley grown in hydroponic condition. They concluded that $H_2S$ could enhance plant tolerance under Cr stress in as much as NaHS addition slightly enhances plant growth and photosynthesis compared with the control. Moreover, NaHS alleviated the inhibition of plant growth and photosynthesis induced by Cr stress (Ali et al., 2013).

Ding et al. (2019) demonstrated the alleviation of Cr toxicity in *Arabidopsis thaliana* by adding exogenous $SO_4^{2-}$ in the nutrient media. Results displayed that plants growth parameters, including root length and seedling biomass, were considerably recovered by the exogenous addition of sodium sulfate 100 µM. S supply can reduce chromium accumulation in roots, increase its transport from roots to leaves and decrease malonyldialdehyde (MDA) production under Cr exposure. Furthermore, the content of GSH, chlorophylls *a* and *b*, superoxide dismutase (SOD), peroxidase (POD) and catalase (CAT) showed various degrees of recovery. In addition, in presence of $SO_4^{2-}$, the number of dead cells in roots declined and the chloroplasts were undamaged (Ding et al., 2019).

The accumulation of proteins involved in sulfate assimilation has been suggested to correlate with the increase in scavenging of ROS and to the adaptive response to other heavy metals beyond chromium (Mustafa and Komatsu, 2016). Moreover chromium was reported to induce the synthesis of important defence compounds such as the small cysteine-rich peptides, phytochelatins (PCs), metallotioneins (MTs) (Cobbett, 2000;

Cobbett and Goldsbrough, 2002) and reduced glutathione (GSH). These molecules are involved both in metal chelation and in scavenging potential oxidative stress resulting from ROS production (Grill et al., 2004; Panda, 2007; Upadhyay and Panda, 2010; Volland et al., 2011). Hence sulfur availability can lead to an increased capacity to cope with biotic and abiotic stresses, a phenomenon known as SIR/SED (Sulfur Induced Resistance or Sulfur Enhanced Defence) (Nocito et al., 2006; Höller et al., 2010; Nazar et al., 2011; Bloem et al., 2015). Although only few reports suggest the involvement of PCs or MTs in Cr detoxification (Shanker et al., 2005; Diwan et al., 2010), two direct products of sulfur assimilation pathway, other than PCs or MTs, can be involved in chromium detoxification. The metal can indeed be sequestered through the formation of thiolate and cysteinthiolate complexes with glutathione and various derivatives of cysteine (Brauer and Wetterhahn, 1991; Brauer et al., 1996).

The chromate/sulfate interaction is further evidenced by the observation that chromium exposure induces the same effects as sulfur starvation through competition both at the transporter level and at some step of the subsequent assimilation pathway (Pereira et al., 2008). In accordance with a sulfur-starvation state, all metabolite pools produced through the sulfur pathway, including methionine, cystathionine, GSH and GSSG decreased in the presence of chromium, as well as during S starvation. A similar decrease in internal sulfur levels has been observed in S-starved *Z. mays* plants and in and S-supplied plants treated for 2 days with 0.2 mM chromate (Schiavon et al., 2007).

## 1.3 - Sulfur pathway in algae

Sulfur (S) is an essential element for all the organisms. The importance of S is not simply quantitative, since it is also associated with its presence in numerous pivotal structural and functional compounds such as the amino acids cysteine and methionine, non-proteic thiols (glutathione), sulfolipids, vitamins, cofactors and cell wall constituents (Takahashi et al. 2011). Algae acquire S as sulfate ($SO_4^{2-}$), the most abundant form of inorganic S in nature, in which S appears with its highest oxidation number (+VI). S assimilation, both in algae and plants, mostly takes place in chloroplasts with the exception of *E. gracilis* that reduces sulfate in mitochondria (Brunold and Schiff 1976).

### 1.3.1 - Sulfur Acquisition

#### *1.3.1.1 - Arylsulfatase*

Sulfate can be in the form of inorganic anion circulating in soil solutions or in aquatic environments. Sulfur can also be extracted from organic molecules dispersed in the environment. Although there is no evidence for the direct use of such molecules as a source of S for algae, microalgae produce some sulfatases in order to use sulfate esters as carbon and/or sulfur source. One of these is the arylsulfatases (ARS; mostly eukaryotic), enzymes that cleave organic $SO_4^{2-}$ and release the residual phenol (Gonzalez-Ballester and Grossman, 2009 and references therein) and alkylsulphatases, which catalysed and produce $SO_4^{2-}$ and an aldehyde (Kahnert and Kertesz 2000; Hagelueken et al. 2006). ARSs are released in the extracellular medium and facilitate the supplying of exogenous, esterified sulfate by their ability to cleave ester bonds between sulfate and organic substances (de Hostos et al. 1988, Ravina et al. 2002).

In *C. reinhardtii* ARS expression is regulated by $SO_4^{2-}$ availability. In low $SO_4^{2-}$ availability, this alga exhibits a suite of responses including the synthesis of extracellular ARS. The analysis of the *C. reinhardtii* genome revealed the possible presence of 18 hypothetical copies of ARS, organized in clusters. Two of which, namely *ARS1* and *ARS2*, are over-expressed during sulfur deprivation. The organization and the high similarity of these sequences suggests a possible common evolutionary origin and a similar regulatory mechanism. It is not yet known if the different ARS genes encode proteins related to different substrate specificity, different cellular localization or catalytic properties (deHostos et al., 1989; Ravina et al., 2002; Gonzalez-Ballester and Grossman, 2009).

#### *1.3.1.2 - Sulfur transporters*

The process of sulfur assimilation in algae starts from the active uptake by means of specific transporters. Algae plasma membrane transporters can couple the influx of sulfate with co-transport of positively charged counterions such as proton ($H^+$) and sodium ($Na^+$). For these mechanisms, the counterion concentration gradients serve as driving force for the influx of sulfate across the membranes (Takahashi et al., 2012). The $H^+/SO_4^{2-}$ transporters, namely *SULTR* gene family (SULfate TRansporter) have been identified in all photosynthetic organisms studied so far (Gonzalez-Ballester and Grossman, 2009; Takahashi et al., 2012; Bromke et al., 2013). Differently from the

SULTR, SLT transporters (Sac1 Like Transporters), catalyse a $Na^+/SO_4^{2-}$ antiport and have high similarity with animal sulfate transporters (Fig. 1.8) (Gonzalez-Ballester and Grossman, 2009).

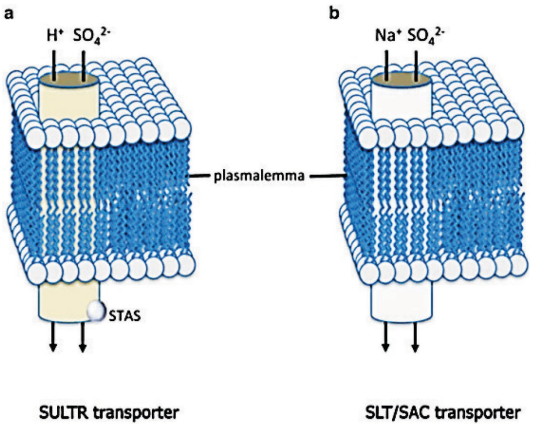


**Figure 1.8 – Plasmalemma sulfate transporters.** Two main kinds of plasmalemma sulfate transporters have been identified in algae: **(a)** $H^+/SO_4^{2-}$ (SULTR) or **(b)** $Na^+/SO_4^{2-}$ (SLT) cotransporters (Giordano and Prioretti, 2016, modified).

Plant sulfate transporters belonging to the SULTR family were identified for the first time by functional complementation in yeast strains containing mutations in the sulfate genes (Smith et al., 1995). The SULTR transporters possess from 10 to 14 predicted transmembrane domains and often contain, at the cytosolic carboxy-terminal end, a STAS (Sulfate Transporter and Anti-Sigma factor antagonist) domain, which is common in anion transporters and is believed to have regulatory functions (Gonzalez-Ballester and Grossman, 2009). STAS domain is connected to the transmembrane portion through a poorly conserved region of variable length known as the linker domain (Gonzalez-Ballester and Grossman, 2009). In *A. thaliana* mutations of the STAS domain prevent the accumulation of SULTR1;2, while a change in some amino acids situated in the linker domain drastically reduces the efficiency of sulfate import channel (Shibagaki and Grossman, 2006).

SULTR-like sequences have been found in the diatoms *Thalassiosira pseudonana* and *Phaeodactylum tricornutum*; in the pelagophyte *Aureococcus anophagefferens*; in the Rhodophyte *C. merolae*; in the Prasinophyte *Ostreococcus sp.* as well as in the chlorophycean green alga *C. reinhardtii*. Some of them contain STAS domains; however, the exact function of the products of these genes needs to be confirmed (Giordano and Prioretti, 2016).

$Na^+/SO_4^{2-}$ antiporters, namely SLTs (Sac1 Like Transporters), were identified in *C. reinhardtii* using the sequencing data of the alga genome (Merchant et al., 2007) and looking for homologies with sequences of sulfate transporters between plants, animals and bacteria (Pootakham et al., 2010). These transporters are very similar to $Na^+/SO_4^{2-}$ transporter of the SLC13 family. All the three members of the SLT family in *Chlamydomonas* (SLT1, SLT2 and SLT3) contain 10-12 predicted transmembrane domains and an intracellular loop containing a TrkA-C domain. The TrkA-C domain function is not completely known but it is thought to be involved in the regulation of the sulfate transporter activity (Pootakham et al., 2010).

In green algae the number of the SLT and SULTR transporters is heterogeneous. In *C. reinhardtii*, were identified seven putative sulfate transporters located on the plasmalemma: four $H^+/SO_4^{2-}$ co-transporters, named SULTR1, SULTR2, SULTR3 and SULTR4 (the latter, then turned out to be a molybdenum transporter located on the tonoplast and was renamed MOT1), and three animal-type $Na^+/SO_4^{2-}$ co-transporters (SLT1 to SLT3) (Pootakham et al., 2010). *V. carteri* appears to have an $H^+/SO_4^{2-}$ and two $Na^+/SO_4^{2-}$ exchanger, while *Ostreococcus tauri* possesses only two $Na^+/SO_4^{2-}$ and no $H^+/SO_4^{2-}$ transporters. Interestingly, no transporters that catalyze an anion exchange with $Cl^-$, $HCO_3^-$ or $I^-$ have been found in algae, although they exist in yeasts, fungi and animals (Takahashi et al., 2012). The presence of $H^+$ or $Na^+$ co-transporters in algae is probably dependent on environmental conditions, specifically on pH and $Na^+$ availability. Unfortunately, the information for marine algal sulfate transporters is very poor to hypothesize the clear functions of these two different types of transporters in the ocean environments. At least, in genome of *E. huxleyi* both types of transporters were found (Giordano and Prioretti, 2016).

In *C. reinhardtii*, the transcripts of *SULTR2*, *SLT1* and *SLT2* increased upon S deprivation, while the transcript of *SULTR1* suffers a drastic decrease; whereas *SULTR3* and *SLT3* remain unchanged. The increase of transcripts for *SULTR2*, *SLT1* and *SLT2* was followed by the increase of the respective polypeptide in the subsequent 24h; however, when $SO_4^{2-}$ was reintroduced in the culture medium, a decline was detected. Therefore, *SULTR2*, *SLT1* and *SLT2* transporters behave as inducible high-affinity transporters (Pootakham et al., 2010).

In cyanobacteria and in the inner chloroplast envelopment of green algae, exists a completely different kind of sulfate transporters. In these membranes, sulfate transport is indeed catalyzed by ATP-binding cassette (ABC) transporters (Melis and Chen, 2005;

Takahashi et al., 2012). ABC transporters are transmembrane permease holocomplexes formed by two heterodimers; the transmembrane channel is formed by the proteins SulP and SulP2 (SULP stands for sulphate permeases) and each of them is bound to a sulfate-binding protein (Sbp) on the cytosolic side and to an ATP-binding protein (Sabc) on the stromal side (Fig. 1.9) (Melis and Chen 2005). These proteins are encoded by genes similar to the *cysT*, *cysW*, *SBPA* and *cysA* genes of prokaryotes. This transport is energized by ATP hydrolysis (Sirko et al. 1990; Laudenbach and Grossman 1991).

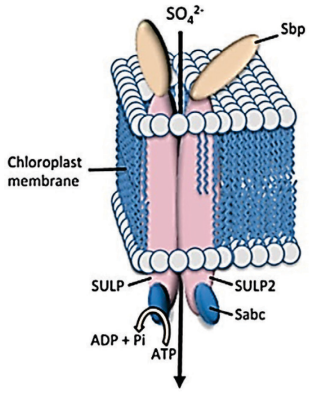


**Figure 1.9 - ATP-binding-cassette transporter (ABC)** in green algae chloroplast inner membrane and in the plasmalemma of cyanobacteria. (Giordano and Prioretti, 2016, modified).

SulP possess an unusual large hydrophilic loop close to its N-terminus that appears missing in the SulP2 protein. Thus, the heterodimer SulP–SulP2 transmembrane complex own 14 transmembrane helices and 3 large hydrophilic loops facing toward the outside of the chloroplast. These SulP–SulP2 heterodimer folding properties are directly related to the function of this transmembrane complex. This transport system is presumably responsible for sulfate import into the plastid, where primary assimilation of sulfate and biosynthesis of cysteine and methionine takes place (Melis and Chen, 2005). In *C. reinhardtii* both the transcript and SULP1 protein increased upon sulfur deprivation in a strain in which *sulP* gene has been silenced by RNA antisense a reduced sulfate assimilation capacity, although the nutrient is provided in standard concentrations inside the culture medium. The impossibility to isolate a mutant missing SULP1 gene, suggested that its complete absence is lethal for *C. reinhardtii* (Melis and Chen, 2005). No such transporters have been identified in other organisms (Takahashi et al., 2012) and the mechanism of plastidial sulfate transport in vascular plants is still not known (Lindberg and Melis, 2008). Unfortunately, the relatively detailed understanding of sulfate uptake in *Chlamydomonas* cannot be transferred *sic et simpliciter* to other microalgae. Different

behaviours should be expected between freshwater and marine algae since sulfate concentration in the oceans is quite high and constant and the presence of a finely regulated system may thus be unnecessary (Giordano et al., 2005).

### 1.3.2 - Sulfur Assimilation

Sulfate acquired from the environment must be activated to a useful form since production of sulfite from sulfate is energetically unfavorable and essentially impossible unless the redox potential of sulfate is lowered.

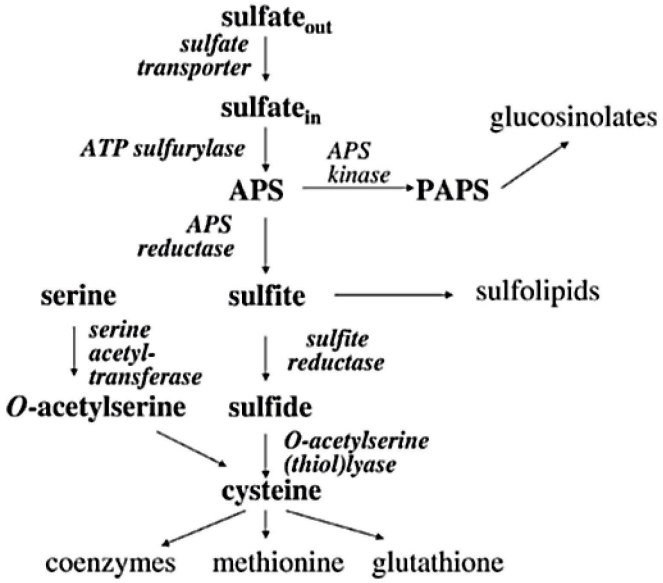


**Figure 1.10 - Overview of Plant Sulfur Metabolism.** Metabolites (**bold**) and enzymes (italic) involved in the sulfur assimilation pathway are shown.

ATP sulfurylase (ATP: sulfate adenylyl transferase; EC 2.7.7.4) catalyses the first (and energetically committed) step in the plant sulfur assimilation pathway generating adenosine-5'-phosphosulfate (APS) and inorganic pyrophosphate ($PP_i$) from sulfate and adenosine 5′-triphosphate (ATP) (Takahashi et al., 2011; Koprivova & Kopriva, 2016) (Fig. 1.10).

As other nucleotidyl transferases, ATS requires $Mg^{2+}$ for sulfate binding at the active site (Farley et al. 1976); subsequently, the two terminal phosphate groups of ATP are cleaved as pyrophosphate, and the residual adenosine 5′-monophosphate (AMP) is transferred onto the sulfate; finally, pyrophosphate is released with Mg (Shaw and Anderson 1974).

In diatoms, dinoflagellates and haptophytes, the reaction of ATS is coupled with the hydrolysis of pyrophosphate catalysed by a pyrophosphatase.

ATSs, in plants, are coded by a variable number of genes. Higher plants possess at least two genes, with the exception of *Selaginella moellendorffi* in which only one was detected (Kopriva et al., 2009). Literature data initially indicated the presence of a unique ATS coding gene in green algae, with the exception of *C. reinhardtii* with two isoforms chloroplastic localizazed (Yildiz et al. 1996; Allmer et al. 2006; Patron et al. 2008; Prioretti et al. 2014). At least two aminoacidic accessions, sharing homology with ATS in various groups of green algae, have however been more recently found in data banks (Sardella et al. 2019).

Studies conducted on the two *C. reinhardtii* isoforms indicated that they were under control of the *SAC1* gene (Sulfur ACclimation protein 1) and their expression increased following sulfur deficiency in the culture medium (Yildiz et al., 1996; Zhang et al., 2004).

The algae with chlorophyll *a+c* possess two ATPS, one in the chloroplast and the other in the cytosol; the plastidial enzyme is responsible for the production of APS for primary S assimilation. The cytosolic ATPS is fused to an APK at the N-terminus and is rather similar to the metazoan enzyme (Patron et al. 2008).

The APS produced by the action of the ATP sulfurylases can be reduced by APS reductase (APR) or phosphorylated by APS kinase (APK) to form 3'-phosphoadesonsine-5'-phosphosulfate (PAPS), which will be used in sulfation processes or can be re-conveyed to assimilation process through the activity of PAPS reductase. The APS partition between the two reactions depends on an oxide-reductive state regulation: oxidative conditions, that facilitate disulfides formation, increase APR activity while decrease the production of PAPS by APSK (Jez et al., 2019).

The sulfate moiety of APS is reduced to sulfite by APR (EC 1.8.99.2) that catalyzes the reduction of APS to sulfite and AMP, using reduced glutathione as the electron donor (Kopriva, 2004).

In *C. reinhardtii* there is a single gene encoding APR: both the transcript and the APR protein increase following sulfur deprivation (Zhang et al., 2004). Several papers suggest that APR is the main enzyme that regulates the assimilation pathway, since it is influenced by several treatments that have no effect on other pathway enzymes (Hatzfeld et al., 1998; Westerman et al., 2001; Koprivova et al., 2000; Hesse et al., 2003).

The distinction between ATS, APR and APSK is not always so clear: in dinoflagellates ATS and APR are merged into a single protein and the analogue arrangement was found

for ATS and APSK in metazoans and diatoms (Prioretti et al., 2014). In *Physcomitrella patens* a pivotal role in sulfate assimilation pathway regulation seems to be attributable to sulfite reductase (SIR), since none of the two APR isoforms present in this bryophyte is influenced by the treatments that regulate this enzyme in higher plants (Wiedemann et al., 2007).

The APR generated sulfite ($SO_3^{2-}$) is then reduced to sulfide by sulfite reductase (SIR). SIR is a plastid enzyme that uses siroeme and FeS clusters as cofactors and ferrodoxin as an electron donor. In *C. reinhardtii* three SIR genes are present: two of them are ferredoxine type (*SIR1* and *SIR2*) and one of bacterial type (*SIR3*), which uses NADPH as cofactor. The expression of *SIR1* and *SIR2* increases upon sulfur deficiency (Zhang et al., 2004). Bacterial-type SIRs have also been found in the nuclear genomes of the diatom *T. pseudonana* and the red alga *C. merolae* (Shibagaki and Grossman 2008); the functions of the products of these genes remain yet elusive.

The fixation of reduced S into organic matter occurs through the insertion of sulfide onto the amino acid O-acetylserine (OAS) to produce cysteine; this reaction is catalyzed by OAS (*thiol*)lyase (OASTL; EC 2.5.1.47). Serine acetyltransferase (SAT; EC 2.3.1.30) catalyzes OAS production from serine and acetyl-coenzyme A (Takahashi et al. 2011).

OASTL and SAT are encoded by a number of genes: *C. reinhardtii* has four genes (*ASL1* to *ASL4*) coding for putative OASTL proteins, of which only *ASL4* has been characterized and shows an increase in expression during sulfur deprivation (Zhang et al., 2004). *P. tricornutum*, *T. pseudonana* possess three genes encoding OASTL whereas in *Emiliania huxleyi* 11 putative OASTL sequences have been identified. Three genes have been annotated as *SAT* in *P. tricornutum*, *T. pseudonana* and *E. huxleyi*, and two genes in *C. reinhardtii* (Kopriva et al. 2009).

## 1.4 - The model organism *Scenedesmus acutus* (Meyen, 1829)

*Scenedesmus* Meyen is a pleomorphic green algal genus. It is single celled or colonial with 2, (usually 4 or 8), 16 to 32 celled coenobia. In colonial form, cells rearranged linearly in one row (4 cells) or alternately in 2 to 3 rows (8 or more cells), attaching with lateral walls or in sub-polar region only. The single cells of this genus are spherical, ellipsoidal, elongated or fusiform shaped; 3-78µm long, 2-10 µm broad; apices capitate,

obtuse, acute or tapering; cell wall ribbed, granulated or dented without spines. The cells show a single nucleus and a single parietal chloroplast with single pyrenoid (Rai, 2013).

### 1.4.1 - *Scenedesmus* genus: an historical overview

Currently, the green microalgae classification is continuously relocating these taxa, since it only considers the morphological characteristics due to few molecular sequences available (Leliaert et al., 2012). Albeit *Scenedesmus* taxonomy does not include cryptic species (taxon in which only differences in the nucleotide sequence can be observed) its classification is still unclear (Toledo-Cervantes et al., 2018). Early, all autosporic coccal green algae characterized by flat and/or curved coenobia were described by Meyen (1829), as *Scenedesmus* (Hegewald and Wolf, 2003). Turpin (1828) described some species of the genus *Scenedesmus* and transferred them into diatoms. Then later, Ehrenberg (1834) placed them into the Desmidiaceae family. Nevertheless, Nageli (1849) collocated the genus *Scenedesmus*, and its relative species, into the Chlorococcales order and Hydrodictyaceae family. In 1926, Chodat split the genus *Scenedesmus* into several subgenera, later reduced by Hegewald and Silva (1988) to just three subgenera: *Scenedesmus*, *Desmodesmus* and *Acutodesmus* (Akgül et al., 2017). More recently, Tsarenko and John (2011) discussed the taxonomic relationships among *Acutodesmus*, *Desmodesmus* and *Scenedesmus*. Both *Desmodesmus* and *Acutodesmus* were initially described as subgenera of *Scendesmus*. Subsequently, the ITS-2 rDNA sequence analysis, raised *Desmodesmus* to generic level (An et al., 1999). Similarly, the name *Acutodesmus* was first validated by Hegewald (1978) as a subgenus and section of *Scenedesmus* Meyen (1829), with *Scenedesmus acutus* Meyen as the type but Tsarenko (2001) elevated also subgenus *Acutodesmus* to generic level. *Scendesmus acutus* remains the type species. A total of 19 species and infraspecific taxa are currently recognized within *Acutodesmus* (Wynne and Hallan, 2015).

Wynne and Hallan (2015) have recently reinstated *Tetradesmus* genus. Hegewald et al. (2010) characterized some taxa of Scenedesmaceae both morphologically and molecularly, nevertheless, native *Scenedesmus* strains still need to be characterized (Toledo-Cervantes et al., 2018).

*Tetradesmus* genus was described by Smith (1913), based upon the single species *T. wisconsinensis* G. M. Smith. Although Chodat (1913) soon merged the genus into *Scenedesmus*, West (1915) defended *Tetradesmus* as a distinct genus and also stated that

Woloszynska's (1914) genus *Victoriella* was identical to *Tetradesmus*. West (1915) transferred *Victoriella ostenfeldii* Woloszynska to *Tetradesmus* and described the new species *T. cumbricus* from the plankton of Ennerdale Water, England. Fott and Komárek (1973) recognized *Tetradesmus* and provided a key to the species and infraspecific taxa that they then included in the genus. *Tetradesmus* was established as a monotypic genus by G. M. Smith (1913). The problem is that the generic name *Tetradesmus* G. M. Smith (1913) has priority over *Acutodesmus* (E. Hegewald) P. M. Tsarenko, and with the present taxonomic treatment of these species, several taxa need to be transferred to *Tetradesmus*.

### 1.4.2 - *Scenedesmus acutus* wild-type

*Scenedesmus acutus* (Meyen, 1829), currently regarded as a synonym of *Tetradesmus obliquus* (Turpin) M. J. Wynne, belongs to the *Chlorophyceae* class (ord. Sphaeropleales).

*S. acutus* is a unicellular freshwater alga (Fig 1.11) with a cosmopolitan distribution. It is a model organism within Sphaeropleales for organellar genetics and it is recognized as an industrially relevant strain for food and fuel production (Breuer et al., 2012; Remmers et al., 2017). In nature, *S. acutus* has fusiform or elliptic haploid cells that can be isolated or organized in cenobia, formed by 4 (or more rarely 2 or 8) cells placed close to each other with parallel main axes. Nevertheless, it generally grows as isolated cells without forming cell aggregates in the culture media. *S. acutus* has a single nucleus and a single chloroplast in a parietal position with a single pyrenoid inside. Its reproduction is mainly vegetative in which each cell gives rise to a daughter colony. In each colony the number of cells is generally multiple of 2. Sexual reproduction, through the formation of flagellated gametes, has been reported occasionally often following unfavourable and or stress conditions (Corradi et al., 1995).

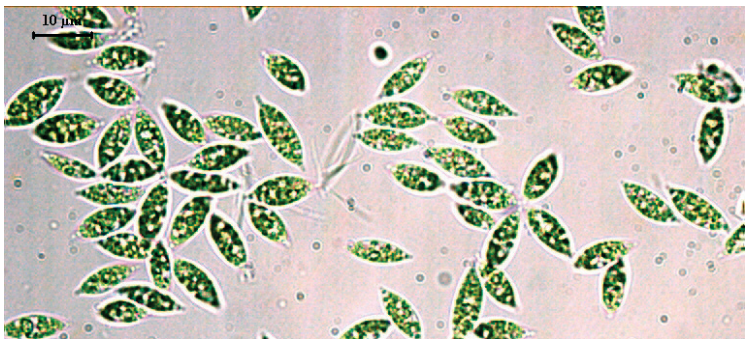


**Figure 1.11 – LM photomicrograph of *S. acutus***

*S. acutus* nuclear genome is distributed on four chromosomes (Dzhambazov et al., 2002) and it has recently been sequenced, but the detailed genome structure (i.e. gene models and annotations) has not yet been described. In particular, a draft assembly of the nuclear genome was reported for *T. obliquus* strain UTEX393 with a size of approximately 109 Mbp (Carreres et al., 2017). In contrast, the draft assembly of the nuclear genome of *T. obliquus* Strain DOE0152z is almost twice the size (>210 Mbp). Furthermore, DOE0152z strain contains a plastid chromosome of 167,272 bp and the mitochondrial genome 41,704 bp assembled too (Starkenburg et al., 2017).

### 1.4.3 - *Scenedesmus acutus* chromium-tolerant strain

In our laboratory, a chromium-tolerant strain (Cr-t) of *S. acutus* was selected by treating the wild type population (wt) with a sublethal concentration (1 mg/l) of hexavalent chromium for a long period (3 months). The Cr(VI)-tolerance was heritable since the Cr-t strain was able to grow in the presence of high Cr(VI) concentrations even after prolonged culturing in Cr(VI)-free medium (Corradi et al., 1995a,b). The Cr-t strain showed to be co-tolerant to Cu and, moderately, Zn (Abd-El-Monem et al., 1998), as well as to Cd (Torricelli et al., 2004).

The morphological features showed that both wt and Cr-t cells grown in standard conditions had a similar cell diameter but the exposure to 1 mg Cr(VI)/l and 2 mg Cr(VI)/l induced a block in the cell division in wt and Cr-t respectively, with the consequence of a significant size increase. These modifications were accompanied by an increase of vacuolization, number of starch grains, pyrenoid size and an accumulation of high-density precipitates inside the cytoplasm Also a significant increase of the nuclear size, more pronounced in the wt than in Cr-t cells was observed (Cozza et al., 2016).

The Cr-t was able to grow in the presence of a Cr(VI) concentration (1 mg Cr(VI)/l) which completely inhibited the growth in the wt and maintain higher chlorophyll content and photosynthesis rates than the wt when exposed to Cr(VI). The constitutive level of reduced glutathione (GSH) was similar in the two strains, while the level of free Cys was significantly higher in the Cr-t strain. The constitutive level of GSH was similar in the two strains, while the level of free Cys was significantly higher in the Cr-t strain respect to the wt (Torricelli et al., 2004).

The Cr(VI) treatment induced a variation in the euchromatin/heterochromatin ratio in both strains suggesting that chromatin remodelling could be at the basis of differential

gene expression and metal tolerance. To gain additional information on the remodelling of the nuclear chromatin, Cozza et al. (2016) analysed DNA methylation by immunolocalization of 5-mC, before and after Cr exposure. Altogether the results suggested a low level of methylation in the genome of *S. acutus*. The Authors found that the nucleus of wt cells showed a basal higher amount of methylated cytosines compared with the Cr-t ones. After Cr treatments, the wt cells showed a strong decrease in methylation, mainly in the heterochromatic fraction, while the Cr-t strain (with an initial lower methylation level respect with wt) increased its methylation level after Cr exposure. These results suggested the existence of a strict link between the methylation pattern and the metal tolerance in the *S. acutus* Cr-t strain (Cozza et al., 2016).

Although sulfur availability is at the basis of resistance to many biotic and abiotic stresses, a study by Gorbi et al. (2007) indicates that the S-deprivation for 7 days induced a transient increase in chromium tolerance in both wt and Cr-t strains. Both strains grown in sulfur deprived medium did not divide and only an enlargement of the cells was observed; once transferred into standard medium, both the strains resumed their growth and were able to acquire a transient Cr(VI)-tolerance. In fact, in both the strains the cells grew and divided at Cr(VI) concentrations which, in standard conditions, completely inhibited cell divisions (Gorbi et al. 2006). However, this tolerance increase was transient as it was lost after 2 days of growth in standard medium. Moreover, after S- deprivation the two strains increased their capacity for sulfur uptake and were able to rapidly restore GSH pool and increase free Cys to levels almost twice as those of unstarved cells. These responses suggested that the higher tolerance to Cr(VI) after S-starvation was linked to the up-regulation of the sulfate uptake/assimilatory process (Gorbi et al., 2007).

Afterwards, Marieschi et al. (2015) demonstrated that even a 3-day sulfur deprivation induced in both strains an increase in chromium tolerance. The Authors proposed that under S starvation, the activation of sulfur uptake/assimilation pathways may have two direct consequences related to Cr-tolerance/detoxification: (i) inhibition in Cr uptake due to the activation of sulfate transporter; (ii) enhanced sulfate accumulation and availability to the cells for the production of sulfur-containing Cr detoxification molecules. The end-products of sulfur assimilation pathway can indeed be involved in metal detoxification either *via* an increased antioxidant response (using S-containing molecules such as GSH), or by chelation (using PCs or MTs) and compartmentalization in vacuoles. These mechanisms could be differently prevalent in the two strains: in the wt the reduction in Cr uptake was hypothesized to occur through the induction of high affinity sulfate

transporters (presumably constitutively expressed in the Cr-t strain), while in Cr-t apparently the main defence strategy was the enhancement of detoxifying capacity (Marieschi et al., 2015).

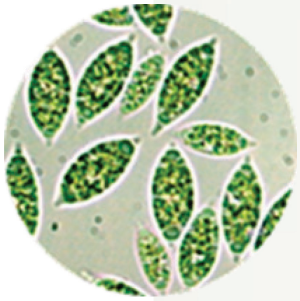

# *Aim of the work*

In the last decades, accelerated industrialization, intensive agricultural activities, extensive mining and rapid urbanization caused widespread diffusion, throughout different environmental compartments, of many contaminants, including metals (Emamverdian et al., 2015). For these reasons, understanding the mechanisms by which plants sense and respond to environmental stress is becoming even more necessary in order to improve both their resistance and tolerance and preserve environmental sustainability. The knowledge of these mechanisms in algal organisms means understanding how the biodiversity of primary producers reacts to these challenging conditions and how these mechanisms evolved and get transmissed in photosynthetic organisms.

Within this scenario, there is increasing awareness that the epigenetic control of gene expression, assuring a rapid and extensive modulation of genome, represents a dynamic mechanism which allow the plants to adapt and withstand stressful situations. Despite this information, the complex mechanisms by which DNA methylation modulates plant stress responses is yet largely unresolved, mainly with respect to heavy metal stress, for which a metal- and species-specific response was evidenced. Moreover, very few data about the epigenetic features exist in algae.

In this context, the aim of the present work is to gain further insight into the mechanisms and molecular processes that act in and are regulated by DNA methylation under stress condition, by comparing two *Scenedesmus acutus* strains with different chromium sensitivity (wt *vs* Cr-t strain). Attention is focused on stress induced by heavy metals, which are dangerous environmental pollutants, and Cr has been selected as one of the most toxic and widespread in environment.

In *S. acutus* a relation between sulfur deprivation and Cr-tolerance in wt *vs* Cr-t strain has been demonstrated (Gorbi et al., 2007; Marieschi et al., 2015). Moreover, recent data about the localization of 5-mC in the Cr-t *vs* wt strain of this alga, performed by an immunocytochemical approach, before and after Cr(VI) exposure, showed some changes in the level of 5-mC (Cozza et al., 2016). These data suggest that epigenetic mechanisms could have been at the basis of the Cr-tolerance acquisition in *S. acutus* during the selection in Cr supplemented medium (Corradi et al., 1995), then fixed in the algal population, inherited and maintained through the progeny even in absence of the metal. Thus, *S. acutus* represents a good model in order to define the reprogramming of epigenetic events leading to the tolerance to external stimuli (e.g. Cr exposure and/or S-

starvation) and to assess if the transgenerational transfer of the tolerance is due to this epigenetic information.

In order to get a general overview of genetic networks and metabolic pathway affected by a state of DNA methylation, an -Omics approach can be applied. In particular, the methylome of Cr-t *vs* wt strain was analysed by WGBS-seq to assess whether epigenetic changes, inherited by the progeny, could be at the basis of the Cr-tolerance.

In our study we furthermore investigated the link between sulfur avaibilty and Cr sensitivity. It is known that sulfur availability can modulate the ability to cope with environmental stresses, a phenomenon known as SIR/SED (Sulfur Induced Resistance or Sulfur Enhanced Defence) and that chromate may compete for sulfate transport into the cells (Perez-Castineira et al., 1998; Pereira et al., 2008). Previous data reported that in *S. acutus* sulfur deprivation induced the activation of sulfate absorption and assimilation, leading to significant consequences on the Cr-tolerance (Gorbi et al., 2007). Hence, in order to clarify the relationship between sulfur and Cr-tolerance and to better elucidate the mechanisms underlying the adaptation by natural selection to different sensitivity to Cr in this microalga, we investigated the expression of some putative genes involved both in the sulfur uptake as well as in sulfur assimilation.

CHAPTER

2

# *Materials and methods*

## 2.1 - *In vitro* culture of *Scenedesmus acutus*

Two strains of the freshwater green alga of *Scenedesmus acutus* (M.), wild-type (wt) and chromium tolerant (Cr-t) respectively, were used as experimental material. The Cr-t strain was isolated by treating wt population with a sublethal concentration (1 mg/l) hexavalent chromium (Cr(VI)) for 3 months (Corradi et al., 1995). These strains were collected at Laboratory of Plant Biology of Department of Chemistry, Life Sciences and Environmental Sustainability of University of Parma since 1990s.

Synchronized axenic cultures of the wt and Cr-t strains of *S. acutus* were grown, as descript by Marieschi et al. (2015), in US EPA (1978) liquid culture medium at pH=7.2 ± 0.1, modified by dissolving both micro- and macro-nutrients in distilled water to obtain a final concentration double of that indicated. No organic matter was present in the medium at the beginning of the culture (Tab. 2.1). The algae were maintained in a climate-controlled chamber (23 ± 1 °C) at 16:8 h light/dark regime with 230 µmol/($m^2$ s) light intensity irradiance. The cultures were continuously aerated (sterile filtered air). To perform the experiments with algae in exponential growth phase, culture medium was always renewed 3 days before starting each experiment by adding 1800 ml of fresh medium to 200 ml of algal suspension in 2 l Erlenmeyer flasks (Stock Culture).

All materials and culture media had been previously autoclaved for 15 min at 121°C and 1 atm.

| Element | Final concentration |
|---|---|
| $NaNO_3$ | 51,0 mg/l |
| $K_2HPO_4$ | 2,088 mg/l |
| $MgCl_2 \cdot 6\ H_2O$ | 24,34 mg/l |
| $MgSO_4 \cdot 7\ H_2O$ | 29,4 mg/l |
| $CaCl_2\ 2\ H_2O$ | 8,82 mg/l |
| $NaHCO_3$ | 30,0 mg/l |
| $FeCl_3$ | 192,0 µg/l |
| $Na_2$ EDTA $\cdot$ 2 $H_2O$ | 600,0 µg/l |
| $H_3BO_3$ | 371,04 µg/l |
| $MnCl_2$ | 528,52 µg/l |
| $ZnCl_2$ | 6,542 µg/l |
| $CoCl_2$ | 1,56 µg/l |
| $CuCl_2 \cdot 2\ H_2O$ | 0,022 µg/l |
| $Na_2MoO_4 \cdot 2\ H_2O$ | 14,52 µg/l |

**Table 2.1 - Composition of modified US EPA (1978) liquid culture medium used for *S. acutus* culture.**

## 2.2 - Sulfur starvation and chromium treatments

Aliquots of the Stock Cultures, in exponential growth phase, were centrifuged for 10 min at 2200 × *g* and washed with distilled water. The pellets were resuspended at $3\times10^6$ cells/ml density in 2 l of *standard culture medium* (+S) containing $MgSO_4$ (14.36 mg/l), or in *sulfate-deprived medium* (−S). Since $MgSO_4$ is the only source of sulfur in the standard medium, the amount of $MgCl_2$ was simultaneously increased to restore standard magnesium concentration in -S medium. After a 3-day pre-culture (called T0) in +S and in −S medium, cells of both strains were washed and collected by centrifugation. Subsequently, the cell-containing pellet was resuspended in new liquid culture medium in chromium free conditions (controls) and in medium supplemented with 1 and 2 mg Cr(VI)/l, supplied as potassium dichromate ($K_2Cr_2O_7$) for 1- and 2- day(s). The selected concentrations of Cr(VI) represent the LOEC (Lowest Observed Effect Concentration) inhibiting growth, as established in previous experiments (Gorbi et al., 2006; Gorbi et al., 2007) for the wt and the Cr-t strain, respectively. Treatments and controls were conducted in triplicates. According to previous studies (Corradi et al., 1995; Gorbi and Corradi, 1993; Gorbi et al., 2007; Torricelli et al., 2004) an initial cell density of $3\times10^6$ cells/ml was employed in order to compare the different culture condition.

## 2.3 - DNA extraction

Genomic DNA (gDNA) was extracted from samples at +S T0 condition following the procedure of Doyle & Doyle (1990) with some modifications. Cells were twice washed with double distilled water, collected by centrifugation, ground in liquid nitrogen and lyophilized. About 0.05 g of frozen samples were treated with 1 ml of extraction buffer (2% hexadecyltrimethylammonium bromide (CTAB, w/v), 100 mM Tris-HCl pH 8, 1.4 M NaCl, 20 mM EDTA; 2 % β-Mercaptoethanol was added immediately before use and incubated for 50 minutes at 65 °C. After centrifuging for 10 minutes (3000 *g*) the supernatant was collected in a clear tube and RNA was removed adding 5 ng of RNase and incubating at 37 °C for 30 minutes. One volume of chloroform/isoamilic alcool (24:1 v/v) was added and mixed by vortex before centrifuging 15 minutes at 9500 *g*. In a clean tube, DNA was precipitated from the aqueous phase for 30 minutes at -80 °C using one volume of isopropanol. After centrifuging for 30 minutes (16,500 *g* at 4 °C), the pellet was washed twice with 70% ethanol and centrifuged for 30 minutes (16,500 *g* at 4 °C).

The pellets were air-dried and resuspended in water. DNA from all samples were analysed for integrity by electrophoresis (0.8% agarose gels containing 5 µg/mL ethidium bromide)

## 2.4 - Whole genome bisulfite sequencing (WGBS-seq)

### 2.4.1 - Library preparation and sequencing

Genomic DNA was extracted as described above and quantified using the Qubit 2.0 Fluorometer (Invitrogen, Carlsbad, CA). gDNA (100-200 ng) was bisulfite converted using the Ovation Ultralow Methyl-Seq with TrueMethyl oxBS (NuGEN, Redwood City, CA) following the manufacturer's instructions. The system produces directional bisulfite-converted libraries. The forward sequencing reads correspond to a bisulfite-converted version of either the original top or the original bottom strand (the C-to-T reads) and the reverse sequencing reads correspond to the complement of the original top or the complement of the original bottom strand (the G-to-A reads).

To estimate bisulfite conversion efficiency, unmethylated lambda phage DNA was spiked into the target sample DNA library and this mixture of DNA library was used for bisulfite conversion and then sequencing. Finally, the reads were mapped to the lambda phage reference genome. As lambda phage DNA has no methylated cytosines, it was possible to estimate bisulfite conversion efficiency by computing methylated C in the alignments. Final libraries were checked with both Qubit 2.0 Fluorometer (Invitrogen, Carlsbad, CA) and Agilent Bioanalyzer DNA assay. Libraries were subsequently pooled equal-molar, in six-sample pools and sequenced across a NovaSeq6000 (150bp paired-end; Illumina; CA, USA).

### 2.4.2 - Sequencing analysis

Raw data were processed for both format conversion and de-multiplexing by Bcl2Fastq 2.0.2 version of the Illumina pipeline. Adapter sequences was masked with Cutadapt v1.11 from raw fastq data using the following parameters: --anywhere (on both adapter sequences) --overlap 5, --times 2, --minimum-length 35 and --mask-adapter (Martin, 2011). Lower quality bases and adapters were removed by ERNE software (Del Fabbro et al., 2013).

Alignments of reads on *T. obliquus* UTEX 393 reference genome (accession no. GCA_900108755.1; Carreras et al., 2017) was performed with Bismark v 0.19.0 using

the parameters --bowtie2 e -N 1 (Krueger & Andrews 2011). Bismark maps bisulfite treated sequencing reads to a genome of interest and perform methylation calls in a single step, discriminating between cytosine methylation in CG, CHG and CHH context.

### 2.4.3 - Data analysis

Alignment files in Sequence Alignment Map (SAM) format output by Bismark were loaded into R v 3.6.1 (R Development Core Team) using functions implemented in methylKit v 0.9.5 Bioconductor package (Akalin et al., 2012). Different methyKit functions were used to analysed descriptive statistics on samples, correlation between samples, finding differentially methylated bases or regions and tiling windows analysis.
By sliding window approach, using 500 bp windows size and 250 bp step size, differentially methylated regions across the *T. obliquus* UTEX 393 genome were identified. In CG, CHG and CHH contexts, differentially hyper- and hypomethylated regions between strains (from the comparison Cr-t *vs* wt) were identified using *q value* < 0.01 and a percentage methylation difference larger than 25% as cutoff.
Since the detailed genome structure (i.e. gene models and annotations) of *T. obliquus* UTEX 393 has not been described, its genome was annotated using AUGUSTUS software (Stanke et al., 2008). Differentially methylated regions were mapped to various annotated features of hypothetic genic region, including protein-coding genes, and their sub-features, which promoter regions, gene body and 5'- and 3'-untranslated regions, through the genomic coordinates.
KOBAS 3.0 (http://kobas.cbi.pku.edu.cn/) software was used for the statistical analyses of the Gene Ontology (GO) data by Singular Enrichment Analysis (SEA) algorithm. GO term enrichment of hyper- and hypo- methylated hypothetic genes was performed separately using Fisher's exact test (*P value* < 0.05) and *C. reinhardtii* as referment organism. Categorization results were expressed as Molecular Functions (F), Biological Processes (P) and Cellular Components (C) like independent hierarchies. In addition, the same tool was used to test the statistical enrichment of differentially methylated genes in Kyoto Encyclopedia of Genes and Genomes (KEGG) (http://www.genome.jp/kegg/) pathways (Mao et al. 2005).

## 2.5 - Total RNA extraction

Total RNA was extracted from Cr-treated and untreated cell of both strains by using RNeasy Plant Mini Kit (QIAGEN). Since the extraction buffer of this kit was not efficient for the extraction of *S. acutus* RNA, the same buffer used for DNA extraction was employed. The first steps of manufacture indication were consequently modified. Culture aliquots were collected by centrifugation, twice washed with double distilled water, frozen in liquid nitrogen, lyophilized, mortar grinded in liquid nitrogen and stored at −80° C before RNA extraction. About 50 mg of cell powder were transferred into 2 ml tube and 1 ml of extraction buffer was added. Following an incubation for 40 min at 58°C, the tubes were centrifugated for 10 minutes (3000 *g*), afterward the supernatant was collected in a clear tube and 1 volume of chloroform/isoamilic alcool (24:1 v/v) was added. After centrifugation for 15 minutes at 9500 *g*, aqueous phase was transferred in QI shredder spin column (lilac) placed in a 2 ml collection tube and centrifuged at 20,000 *g* (full speed) for 2 minutes. The flow-through was transferred in a new microcentrifuge tube and precipitated by adding 0,5 volume of ethanol (96–100%) and mixing immediately by pipetting. The sample (usually 650 µl), including any precipitate that may have formed, was transferred to a RNeasy spin column (pink) placed in a 2 ml collection tube (supplied in the kit) and centrifuged at 16,000 *g* for 15 seconds. Washings of the spin column membrane were performed by adding 350 µl Buffer RW1 and centrifuging the sample at 16,000 *g* for 15 seconds. To eliminate DNA contamination on column DNase digestion (RQ1 RNase-Free Dnase) was performed. A mix containing 8 µl of RQ1 buffer, 8 µl DNase (8 unit) and 64 µl of RNase free water previously prepared, was added directly on the membrane of the RNeasy spin column (pink) and incubate at room temperature for 15 minutes. Washing was performed as described above. Purification of RNA was obtained by adding 500 µl Buffer RPE and then centrifuging the sample at 16,000 *g* for 15 seconds. Two additional washing with 500 µl and 350 µl Buffer RPE were carried out. In order to remove residual ethanol which may interfere with downstream reactions a centrifugation at full speed for 1 minute was applied. The RNeasy spin column was transferred into a new 1,5 ml collection tube and 30 µl RNase-free water were added directly on the spin column membrane and the sample was centrifuged at 16,000 *g* for 1 minute to elute the RNA. RNA was quantified by Nanodrop (ND-1000) and integrity was checked through an Agilent 2100 Bioanalyzer (Agilent Technologies). Only RNA samples with an RNA integrity number ≥ 7 were used to cDNA synthesis.

## 2.6 - Single Strand cDNA synthesis

First-strand cDNA synthesis was performed by SuperScript™ III Invitrogen USA, according to the manufacturer's instructions, as described above. A reaction mix containing 1 µg of DNaseI (Roche)-treated total RNA, 1 µl of oligo(dT)$_{20}$ (50 µM), 1 µl of 10 mM dNTPmix and DEPC-treated water up to 10 µl was incubated at 65 °C for 5 minutes and then on ice for at least 1 minute. The following cDNA Synthesis mix containing 2 µl RT buffer (10x), 4 µl $MgCl_2$ (25 mM), 2 µl DDT (0,1 M), 40 U RNaseOUT and 200 U SuperScript™ III RT was added to the previous reaction mix and incubated at 50 °C for 50 minutes. The reaction was terminated at 85 °C for 5 minutes then the sample was chilled on ice. Any residual RNA was digested by adding 1 µl of RNase H (2 U/µl) and incubate at 37 °C for 20 minutes.

## 2.7 - Identification of candidate genes

The identification of candidate genes, belonging to sulfur uptake/assimilation pathway, was carried out by peculiar approach. First, for each gene, a consensus sequence was built by using the gene sequences present in the database (NCBI) of the other green algae phylogenetically close to *S. acutus*. Subsequently, the obtained consensus sequence was aligned on *T. obliquus* UTEX 393 genome. On the identified region of *T. obliquus* genome, primers (Tab 2.2) were designed and used to amplify the corresponding fragments both in gDNA and cDNA through PCR (Polymerase Chain Reaction). Finally, PCR products were loaded on agarose gel (prepared in 1X TAE buffer (40mM Tris, 20mM acetic acid, 1 mM EDTA), eluted, purified (§ 2.7.1) and sequenced (§ 2.7.2).

For amplification of fragments with sequencing purposes, polymerase with 3'-5' exonuclease (proofreading) activity was used. PCRs where performed using *Platinum® Pfx DNA Polymerase* (Invitrogen). Each rection was prepared mixing the following components: 1µl of 50mM $MgSO_4$, 1.5µl of 10mM dNTP mix, 1.5 µl (150 ng each) of gene-specific primers (10µM each), 5 –10 µl of 10X Pfx Amplification Buffer, 1 µl of template (10 pg – 200 ng), 1.25 U Platinum® Pfx DNA and sterile water was added to reach a final volume of 50µl. PCR was performed on MWG Biotech Inc Primus 96 Thermal Cycler using the cycling parameters as follows: 94 °C for 5 min followed by 34 cycles of 94°C for 15 seconds, 58-60 °C for 30 seconds and 68 °C for 1-3 minute.

| Gene | Primer | | Tm (°C) |
|---|---|---|---|
| *SaARS* | FW1 | 5'- ATGGGTGCTCGAGCAGTGG - 3' | 62 |
| | FW2 | 5'- TTCTACATCCAAGTTGCGCC - 3' | 60 |
| | FW3 | 5'- AAAAGCAGGGCAGCTCACC - 3' | 62 |
| | BW1 | 5'- CCTCCTCATTATGGTTTGGC - 3' | 60 |
| | BW2 | 5'- ACTGTTGTCAGGGTGAATGG - 3' | 60 |
| | BW3 | 5'- GAGTACTTAGCCTCATCAACC - 3' | 62 |
| *SaSULTR1* | FW1 | 5'- AAGGCCAAGAAGTCGACCC - 3' | 62 |
| | FW2 | 5'- TGTGCCCAGCGTGTGGGG - 3' | 62 |
| | BW1 | 5'- AAACAGCCACACGTGGTAGG - 3' | 62 |
| | BW2 | 5'- ATGATGATGGCCCCAATCGC - 3' | 62 |
| *SaSULTR2* | FW1 | 5'- CCCTCCGTGTATGGGCTG - 3' | 60 |
| | FW2 | 5'- CGTTTGACTGGGCGGCGC - 3' | 62 |
| | BW1 | 5'- GTAGGCCACCAGCTTGTCC - 3' | 62 |
| | BW2 | 5'- GTGCACTCTCACGAAGATCC - 3' | 62 |
| *SaSLT1(?)* | FW1 | 5'- ATGGCTGTTGCTGCAGTAGC - 3' | 62 |
| | FW2 | 5'- TCATCCATGAGGGTGACACC - 3' | 62 |
| | FW3 | 5'- ACGCTGGAGCACATGCAGG - 3' | 62 |
| | BW1 | 5'- CTTCACGGACTGCTCCACG - 3' | 62 |
| | BW2 | 5'- ATTGTATGCACCGTTGTTTGC - 3' | 60 |
| *SaSLT2(?)* | FW1 | 5'- GTATCATTGGGCTGGGATGG - 3' | 62 |
| | FW2 | 5'- ATCACTCCATACGGCCTGC - 3' | 60 |
| | FW3 | 5'- CTCACCAATGCACAAGACGC - 3' | 62 |
| | FW4 | 5'- CTTTACGCAGATCTTCGAGC - 3' | 60 |
| | FW5 | 5'- CTTCAAGAAGCGCTTCAAGG - 3' | 60 |
| | BW1 | 5'- CAGCAGCCATGAGTAAGTCC - 3' | 62 |
| | BW2 | 5'- CACATGGTGATCACGTGTGG - 3' | 62 |
| | BW3 | 5'- TTTGCTGCGATGTCTTTGCC - 3' | 60 |
| | BW4 | 5'- TGTGTTGCCACCATTGCTGC - 3' | 62 |
| | BW5 | 5'- GAAGATGCCACTGCATACGC - 3' | 62 |
| *SaATS1* | FW1 | 5'- ATGGTGCCAGCTGAGCAGC - 3' | 62 |
| | BW1 | 5'- CTGTGTGGGCCCGCAGGT - 3' | 62 |
| *SaATS2* | FW1 | 5'- ATGGTGCCAGCTGAGCAG - 3' | 62 |
| | BW1 | 5'- GTGCTGCGCGAGCACGCA - 3' | 62 |
| *SaSulP1* | FW1 | 5'- GCCTGTTCCTGTAGCATTG -3' | 58 |
| | FW2 | 5'- GGCACCCACAAAGTCGTACT -3' | 56 |
| *SaSulP2* | FW1 | 5'- GGTATTCTGGCATGTGACGC -3' | 62 |
| | FW2 | 5'- GCCAACCCTCTGCAGGTATT -3' | 62 |
| | BW1 | 5'- TCCACTTTGTCCTTGACCCA -3' | 60 |
| | BW2 | 5'- CAGCCTGCTCCACTTTGTC -3' | 60 |
| *SaSabc* | FW | 5'- TGGTGAAGCATTTCAACACCG -3' | 62 |
| | BW | 5'- CTCGTCAAACTCCATCATGG -3' | 60 |
| *SaAPK* | FW | 5'- CTATGCTTGCTCAGGTGGC -3' | 60 |
| | BW | 5'- AGGATCTTTGCGGCTGAAAC -3' | 60 |
| *SaAPR* | FW | 5'- ATGCAGCTGCAGGCTAGC - 3' | 58 |
| | BW | 5'- TCAAGACGCTGGCTGGCA - 3' | 58 |

| | | | |
|---|---|---|---|
| *SaSIR1* | FW1 | 5'- CAGCTGCTGCAGCAGAGG - 3' | 60 |
| | FW2 | 5'- CATGCAGCTGATGAAGTTCC - 3' | 60 |
| | BW1 | 5'- CAGCGGCTTGAAGTCCTGG - 3' | 62 |
| | BW2 | 5'- CCCATTCAGCTTCTGCAGC - 3' | 60 |
| *SaSIR3* | FW1 | 5'- TGGGAAACAGCATGAGCACG - 3' | 62 |
| | FW2 | 5'- GATGACAAGGACACGGTGC - 3' | 60 |
| | BW1 | 5'- GTTGCTGGGCCATATGCCC - 3' | 62 |
| | BW2 | 5'- ACCACACACGTAGAAGTGG - 3' | 60 |
| | BW3 | 5'- CACACGTCCCTCTCGTAGC - 3' | 62 |
| *SaOASTL1* | FW | 5'- TGTACCTGAACAGCGTGACG - 3' | 62 |
| | BW | 5'- AGCGTCGAAGCTCCACAGC - 3' | 62 |
| *SaOASTL2* | FW1 | 5'- TGGTTGACAAAGAAGGGCAG - 3' | 60 |
| | FW2 | 5'- TGAAGAGACATTGGCAAGCG - 3' | 62 |
| | BW1 | 5'- TTCAACAGCTGCATCATCCG - 3' | 60 |
| | BW2 | 5'- ACAAAAGCAAGCCCCCTGC - 3' | 60 |
| *SaOASTL3* | FW | 5'- GTTGCAATCCAGGCTACACC - 3' | 60 |
| | BW | 5'- CGTCCCGCATCTTGATGCG - 3' | 62 |
| *SaOASTL4* | FW1 | 5'- CCAACAAGAAGATCAAGGGC - 3' | 60 |
| | FW2 | 5'- CACTCCAGACTCCTTCATCC - 3' | 62 |
| | BW1 | 5'- GTGGTCTCGTAGTGCACGC - 3' | 62 |
| | BW2 | 5'- CGTCGAAGGTCATCTTCTCC - 3' | 62 |
| *SaSAT1* | FW | 5'- ATGCAGCTGGCACAGCAGC - 3' | 62 |
| | BW | 5'- CATAGTCCAGGATGAAGTCC - 3' | 60 |
| *SaSAT2* | FW1 | 5'- GTGAATGTCAGTTTGGGAGC - 3' | 60 |
| | FW2 | 5'- CTGGCTGTTGACCTGCACC - 3' | 62 |
| | BW1 | 5'- CAGCAGTGACACATTGTTGC - 3' | 60 |
| | BW2 | 5'- CATACTCCGGGTCCTCTGC - 3' | 62 |
| *SaCGS1* | FW1 | 5'- CCGCAGCAATGGAGTGTCG - 3' | 62 |
| | FW2 | 5'- GGAGCAGAACAAGGTCTCG - 3' | 60 |
| | BW1 | 5'- TAGTGGCCGAATGAATCACC - 3' | 60 |
| | BW2 | 5'- GATCTGGTCCAACGCCTGC - 3' | 62 |
| *SaMETC* | FW1 | 5'- CCTCACCAGTGGTAGCAGC - 3' | 62 |
| | FW2 | 5'- CCATCCGCGTGTTTGACCG - 3' | 62 |
| | FW3 | 5'- TGTGAAGGCTGCCATCATCC - 3' | 62 |
| | BW1 | 5'- AGGTTGCTGCCCTTGTGGC - 3' | 62 |
| | BW2 | 5'- GTGTGAGGAACGAGTTGTCC - 3' | 62 |
| | BW3 | 5'- GACTCCAGCTGCTGTATCC - 3' | 60 |
| *SaTHS* | FW1 | 5'- CAGCTGCACATGTTGCTGG - 3' | 60 |
| | FW2 | 5'- GTGCAGCCCATCGCAAACG - 3' | 62 |
| | BW1 | 5'- AGTCTGTGTCTATGCTCAGC - 3' | 60 |
| | BW2 | 5'- ATGTTGAAGGTCTTCTTGAGC - 3' | 60 |

| | | | |
|---|---|---|---|
| *SaMETH1* | FW | 5'- GTGATGGCCTTCGACAAGAC - 3' | 62 |
| | BW1 | 5'- CTTGACCGTGGCAATGACAA - 3' | 60 |
| | BW2 | 5'- TCCTTGCCGTCCATCTTCTT - 3' | 60 |
| *SaMETH2* | FW | 5'- CACAATTGACGCCTCTGGAG - 3' | 62 |
| | BW | 5'- AAGAACTTCTCCAGCGCGTA - 3' | 60 |
| *SaGSH1* | FW | 5'- CGAGCATATCAAAGGCGTGT -3' | 60 |
| | BW1 | 5'- CAGAGCGTTGATGTACTGCC -3' | 58 |
| | BW2 | 5'- AGTGCCCTTCATCGTAGCC -3' | 62 |
| *SaGSH2* | FW1 | 5'- GTCAAATACAGACGCAGAGCT -3' | 60 |
| | FW2 | 5'- TGGCTCAGATACCAGACGC -3' | 60 |
| | FW3 | 5'-TCTCTCGACAACATCAGCGA -3' | 60 |
| | BW1 | 5'- AGTGGGGTAGTCATTGGGTG -3' | 62 |
| | BW2 | 5'- GTTTTGGATGGCGTCTTGGA -3' | 60 |
| | BW3 | 5'- TAGATGCCCAGTTCGCTCAA -3' | 60 |
| *SaSAC3* | FW | 5'- TGGTGAAGCATTTCAACACC - 3' | 58 |
| | BW | 5'- CTCGTCAAACTCCATCATGG - 3' | 60 |

**Table 2.2 – List of primers used to characterize genes involved in sulfur uptake/assimilation pathway**

### 2.7.1 - Extraction of DNA from Agarose Gel

After a successful amplification of cDNA or gDNA using PCR, the electrophoretic band was gel eluted and cleaned up using a QIAquick Gel Extraction Kit (QIAGENE). Using a sharp scalpel, the band was quikly excised from gel with the aid of a UV transilluminator. The size of the slice was minimised by removing any excess agarose. The slice was transferred to a tube and weighed. Three volumes of Buffer QG were added and the gel incubates for 10 minutes at 50 °C vortexing every 2 minutes until dissolved. One volume of isopropanol was added to increase the yield. The sample was transferred into a QIAquick spin column, which was then placed in a 2 ml collection tube and centrifugated for 1 minute. The flow-through was discarded, 0.75 ml PE buffer added and let stand for 5 minutes before centrifuging for 1 minute. The flow-through was discarded again and the column spun for a further minute. To elute the DNA the QIAquick spin column was inserted into a clean 1.5 ml microcentrifuge tube, 30 ul Buffer EB added and allowed to stand for 1 minute. The column was then centrifuged for 1 minute.

### 2.7.1 - Sequencing of DNA fragment

PCRs were performed by using primers complementary to the region of interest. After extraction from agarose gel, PCR product was sequenced by BRM Genomics (Via Redipuglia 21A, Padua,) using Sanger method.

## 2.8 - RT-qPCR

Primers used for quantitative real-time PCR analysis (RT-qPCR) were designed using Primer Express™ Software v3.0.1 (Applied Biosystems). Primers pairs where selected according to their: (a) robustness: successful amplification over a range of annealing temperatures, (b) specificity: generation of a single significant peak in the melting curve, and (c) consistency: highly reproducible Ct values within the reactions of a triplicate. Only the pairs with an average efficiency between 0.90 and 1.0 were used.
RT-qPCR was performed using a STEP ONE instrument (Applied Biosystems). Amplification reactions were prepared in a final volume of 20 µl containing: 2.5 µl Select SYBR® Green PCR Master Mix (Applied Biosystems), 1 µl each primer (0.2 µM final concentration) and 50 ng cDNA. All the reactions were run in triplicate in 48-well reaction plates and negative controls were included. The cycling parameters were as follows: 50°C for 2 min. 95°C for 2 min, followed by 40 cycles of 95°C for 10 seconds and 60°C for 30 seconds. Melting curve analysis was also performed to confirm the existence of a unique PCR product and evaluated by an increase of 0.5 °C every 10 s, from 60 °C to 95 °C.

### 2.8.1 - Relative quantification RT-qPCR

The expression of differentially methylated genes between Cr-t and wt was statistical analysed through the "Comparative Ct method" also known as the ΔΔCt method, where $\Delta\Delta Ct = \Delta Ct_{[sample]} - \Delta Ct_{[reference]}$. Relative expression of each target gene was calculated using the Relative Expression Software Tool REST 2009, version 2.0.13 (Pfaffl et al., 2002). *SaARS, SaSULTR1, SaOASTL3, SaSABC, SaSAT1* and *SaGSH1* genes were analysed by using primers designed on the specific sequences and reported in Table 2.3. The RT-qPCR data were normalized using *SaCBLP* (encoding a G protein beta subuni-like polypeptide) as housekeeping gene. *SaCBLP* gene was characterized in this work

with the aims of being used as a control gene and was tested to verify the stability of its expression between the strains.

| Gene | Primer | | Tm (°C) |
|---|---|---|---|
| *SaARS* | FW | 5'- TTCACCCTGACAACAGTGTAACC - 3' | 58 |
| | BW | 5'- GCCTGTAGAAGTCATCGTGCTT - 3' | 57 |
| *SaSULTR1* | FW | 5'- TGGCTACCCTTCCAGTATGTTG - 3' | 58 |
| | BW | 5'- GGACGTGGACTCAAGCATGT - 3' | 57 |
| *SaSabc* | FW | 5'- AGTCAGGCAGCCCCAATG - 3' | 58 |
| | BW | 5'- CCGACGAAGCCCATAACAA - 3' | 58 |
| *SaOASTL3* | FW | 5'- GATGGCCGCATCAAGATG - 3' | 57 |
| | BW | 5'- CAGTGCCCAGCAAACAACTC - 3' | 58 |
| *SaSAT1* | FW | 5'- AGCGTGGAAGCCGTGTT - 3' | 56 |
| | BW | 5'- ACTGTCAGGCGGGTTGTG - 3' | 57 |
| *SaGSH1* | FW | 5'- ATGACAGGGACTACCTCAGAAACG - 3' | 60 |
| | BW | 5'- ACGGTGCCTCCCTTGAAAG - 3' | 59 |
| *SaCBLP* | FW | 5'- GTGCTGTCCGTGGCCTTCT - 3' | 60 |
| | BW | 5'- TGTTCCACAGCTTAATGGACTTGT - 3' | 59 |

**Table 2.3 – List of primers used for relative quantification RT-qPCR of differently methylated gene in Cr-t *vs* wt**

### 2.8.2 - Absolute quantification RT-qPCR

From our analyses it emerged that *SaCBLP* gene is constitutively expressed in both strains also in cells grown in S-deprived medium (as in *C. reinhardtii* (Gonzales-Ballester et al., 2010)) but no after Cr(VI)-treatment. For this reason, absolute quantification RT-qPCR was used to analyse expression genes in Cr(VI)-treated cells.

External calibration curves for target genes were prepared with double-stranded cDNA fragments. The DNA fragments, used to generate the calibration curves, were produced by PCR with the same primers used for subsequent quantification. Double stranded DNA fragments were gel purified as descripted in the section 2.7.1 and quantified by Qubit 2.0 Fluorometer (Invitrogen, Carlsbad, CA). The curve was generated by using serially diluted standards of know concentrations and produced a linear relationship between Ct and the logarithm of the initial amount of total template DNA (Heid et al., 1996).

Initial copy number for generating calibration curve was calculated using the following equation (Whelan et al., 2003):

$$Copy\ number = \frac{6.022 * 10^{23} * dsDNA\ amount\ (ng)}{dsDNA\ length\ (bp) * 650 * 10^{9}}$$

The amount of target gene was calculated by interpolation of the Ct value obtained with the built calibration curve.

Target gene level of was reported as the numbers of molecules per nanogram cDNA. For each target gene, cDNA amplicons obtainable with the specific primers, listed in Table 2.4, were approximately up to 300bp long. Statistical analysis was performed by using one-way ANOVA with Tukey *post hoc* test ($p < 0.05$) after Shapiro-Wilk normality test and Levene's test homoscedasticity test.

| Gene | Primer | | Tm (°C) |
|---|---|---|---|
| *SaSULTR1* | FW | 5'- TGGCTACCCTTCCAGTATGTTG - 3' | 58 |
| | BW | 5'- GGACGTGGACTCAAGCATGT - 3' | 57 |
| *SaSULTR2* | FW | 5'- AAGGTGATCCAGGTGGCATT - 3' | 58 |
| | BW | 5'- CGCCCCGCTGGTGAA - 3' | 60 |
| *SaSulP1* | FW | 5'- CGAGTTTGGCAGCATTGTCA - 3' | 59 |
| | BW | 5'- ACTGCTCAAGGCACTGGAAGA - 3' | 59 |
| *SaSulP2* | FW | 5' - GCCAACCCTCTGCAGGTATT - 3' | 58 |
| | BW | 5'- TTGGTCAGGATGACGCCATA - 3' | 59 |

**Table 2.4 – List of primers used for absolute quantification RT-qPCR of studied genes encoding sulfur transporters.**

## 2.9 - Bioinformatic tools and software

Sequence homology analyses were performed by using BlastX and Blastp (www.ncbi.nlm.nih.gov/BLAST/), ClustalOmega (www.ebi.ac.uk/Tools/msa/clustalo/) and ClustalX (www.clustal.org/clustal2/). Nucleotide sequences have been translated into amino acids sequences using the TranslateTool program (web.expasy.org/translate/). Prediction and analyses of protein structures were performed by Phyre2 web (Kelley et al., 2015) and the 3D models were visualized through EzMol web tool (Reynolds et al., 2018). The presence of chloroplast transit peptides (cTP) in protein sequences and the location of potential cTP cleavage sites were predict using ChloroP 1.1 Server (Emanuelsson et al., 1999). Prediction of membrane-spanning regions and their orientation were analysed by using TMpred (Hofmann and Stoffel, 1993). Phylogenetic analyses were performed through MEGA X software (Kumar et al., 2018). The heat maps were created by ClusVis web tool (Metsalu and Vilo, 2015). Statistical analyses were performed using SPSS software (http://www-03.ibm.com/software/products/it/spss-statsstandard).

CHAPTER

3

# *Results*

## 3.1 - Quality Evaluation of single-base resolution methylomes (WGBS-seq, Whole Genome Bisulfite Sequencing)

In order to profile DNA methylation patterns at single-nucleotide resolution both in wt and Cr-t strain, six whole-genome bisulfite-treated DNA libraries (three libraries for wt and three libraries for the Cr-t strain respectively) were prepared as reported in materials and methods (§ 2.4.1.). Single-base DNA methylation BS-Seq of the six libraries generated a total of raw reads (150 bp) listed in the table 3.1.

For each sample, the bisulfite conversion rate (%) determined using the unmethylated λ phage genome, was higher than 98% (Tab.3.1). After quality filtering, the reads for all the samples resulted of high quality and so they uniquely mapped to the *Tetradesmus obliquus* UTEX 393 genome (Carreres et al., 2017) (Fig. 3.1). The choice of the genome of *T. obliquus* strain UTEX 393 for this alignment was determined by its greater sequence homology with respect to *T. obliquus* strain DOE0152z, also found in NCBI database.

| Sample name | Reads (M) | Bisulfite conversion rate (%) | | |
|---|---|---|---|---|
| | | R1 | R2 | R1_R2 |
| 1-wt_1 | 35.466 | 98.93 | 98.82 | 98.88 |
| 2-wt_2 | 38.876 | 98.99 | 98.9 | 98.95 |
| 3-wt_3 | 36.413 | 98.91 | 98.8 | 98.86 |
| 4-Cr-t_1 | 38.434 | 98.81 | 98.6 | 98.71 |
| 5-Cr-t_2 | 42.104 | 98.87 | 98.78 | 98.83 |
| 6-Cr-t_3 | 36.902 | 98.85 | 98.76 | 98.81 |

**Table 3.1 - Total of raw reads generated by WGBS and bisulfite conversion rate (in percentage) calculated for each sample.**

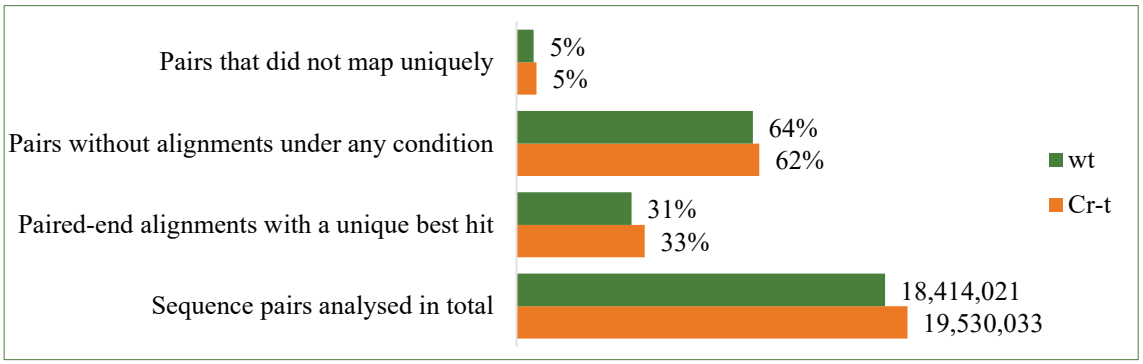


**Figure 3.1 - Alignment of the reads against to T. obliquus UTEX 393 genome.**

These high-quality sequence reads represented about 13X genome coverage.

The percentage of methylated cytosines in CG, CHG and CHH sites was very similar across the three biological replicates, both in Cr-t as well as in wt strain. In particular, roughly 68% of the cytosine positions in the CG context of genome were methylated, around 25% of the positions were completely unmethylated and the remaining positions were partially methylated to various degrees in both the strains (Fig.3.2). On the contrary, the CHG and CHH forms showed roughly 68% of the cytosine positions unmethylated; however no fully methylated positions were observed (Fig. 3.2).

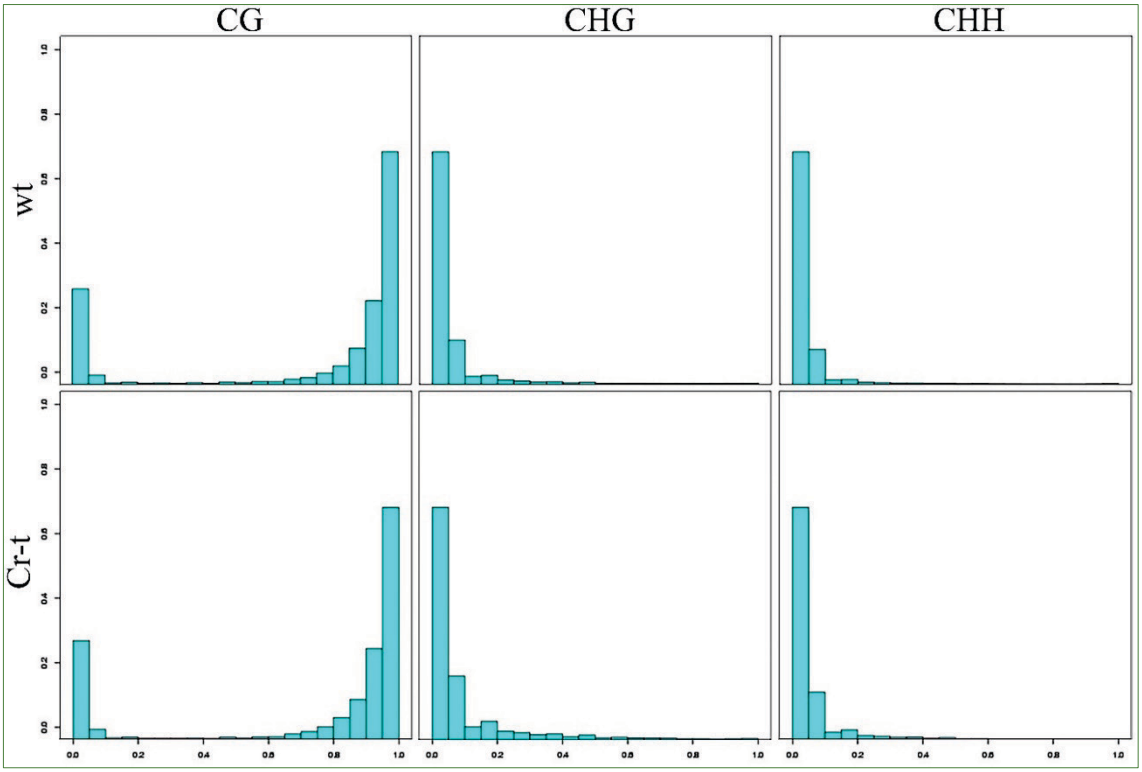


**Figure 3.2 - Percentage of DNA methylation of wt and Cr-t strain in the CG, CHG and CHH sites.**

Pearson's correlation analyses clearly showed that samples of the same strain cluster together independently (Fig. 3.3). As regard the CG methylation, the Pearson's correlation coefficient was constantly 0.98 within each strain and 0.97 in comparisons between samples of different strains. For CHG methylation context, Pearson's correlation coefficient was in the range of 0.85 to 0.86 when we compared Cr-t samples and 0.87 in the wt ones; whereas, comparing the samples of different strain, the coefficient ranged from 0.79 to 0.84. In the same way, Pearson's correlation coefficient of methylation in CHH context, was higher within each strain and lower between samples of different strain (Fig. 3.3).

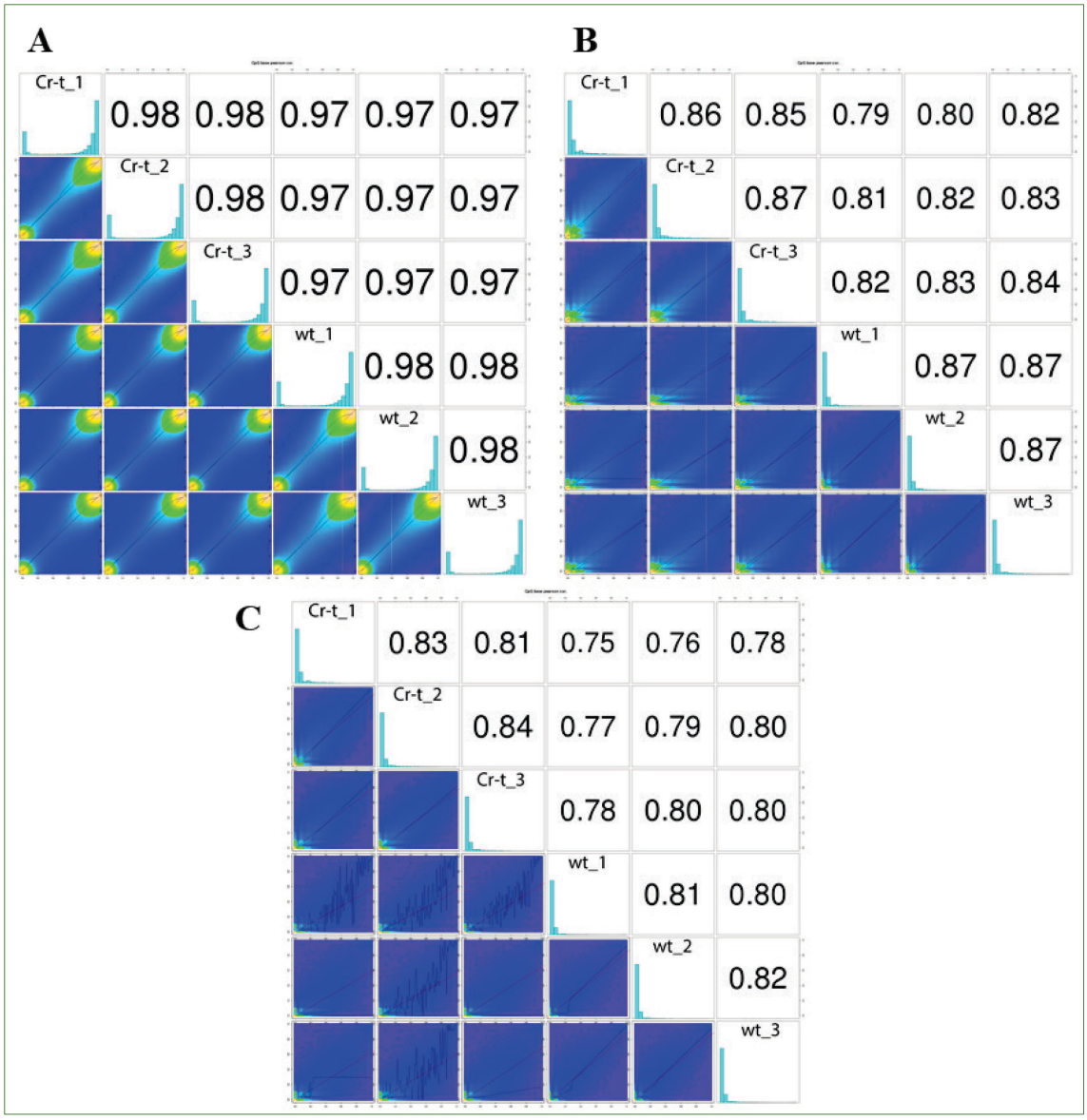


**Figure 3.3 – Pearson's correlation between different strains in CG (A), CHG (B) and CHH context (C).**

## 3.2 - DNA methylation landscape in wild-type and Cr-tolerant strain

In *S. acutus* strains, a total of 61776448 and 74258686 methylated cytosine (mC) were respectively identified in the wt and in Cr-t. The overall methylation degree in the CHG and CHH contexts were significantly higher in the Cr-t samples (*P value* < 0.05) compared to wt ones (Fig. 3.4). In particular, CHG methylation levels were 4.4 % in the Cr-t and 2.6 % in wt strain; whereas in CHH context, values of 2.7 % and 1.6 % were observed in the Cr-t and in the wt respectively. On the contrary, in CG context no

significatively differences in methylation level were observed between the strains (Cr-t 76.3 % *vs* wt 76.9 %, *P value* = 0.65) (Figure 3.4).

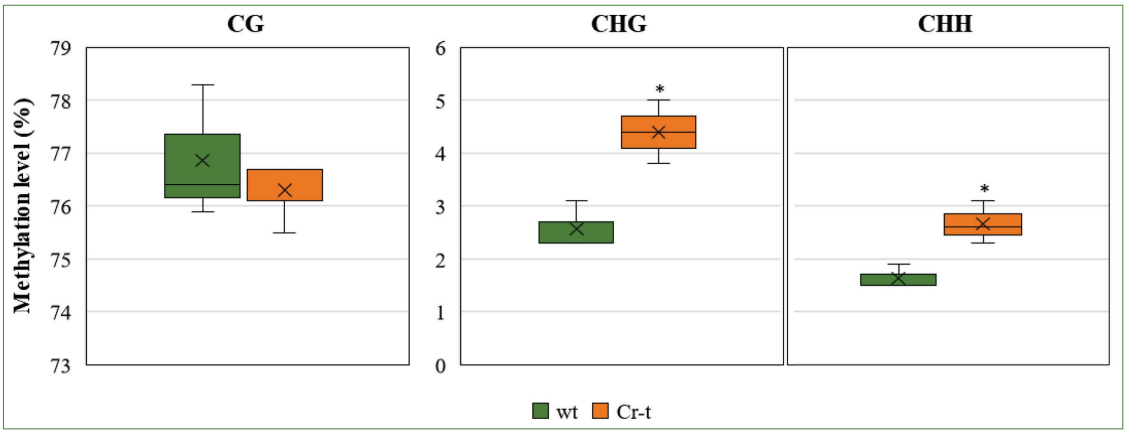


**Figure 3.4 - Methylation level in CG, CHG and CHH context in wt and Cr-t strain. *: significative for P < 0.05**

## 3.3 - Identification of Differential Methylation Regions (DMRs) and associate genes

Methylation normally occurs at clusters of cytosines in discrete regions of the genome; however, within these regions the exact cytosines methylation varies from cell to cell and between biological samples. At the single cytosine level, the methylation appears to be largely stochastic but it is correlated with the methylation levels of other cytosines around it. For this reason, instead of looking for differences in methylation of individual cytosines, it is often more biologically informative to define which methylated regions vary between the samples (*Differentially Methylated Regions*, or DMRs). A sliding window approach, using 500 bp windows size and 250 bp step size, was employed across the *T. obliquus* genome (just used for the previous alignment WGBS-seq reads) in order to identify differentially methylated regions. Differentially hyper- and hypomethylated regions between the Cr-t and the wt strain were identified in CG, CHG and CHH contexts, using *q value* < 0.01 and a percentage methylation difference larger than 25%. These DRMs were characterized and the results reported in Fig.3.5.

Interestingly, 244 hypomethylated and 210 hypermethylated regions were identified in CG context; on the contrary, 106 hypermethylated and only 9 hypomethylated regions were identified in CHG context; whereas only 56 hypermethylated and 2 hypomethylated regions were identified in CHH context (Fig. 3.5A).

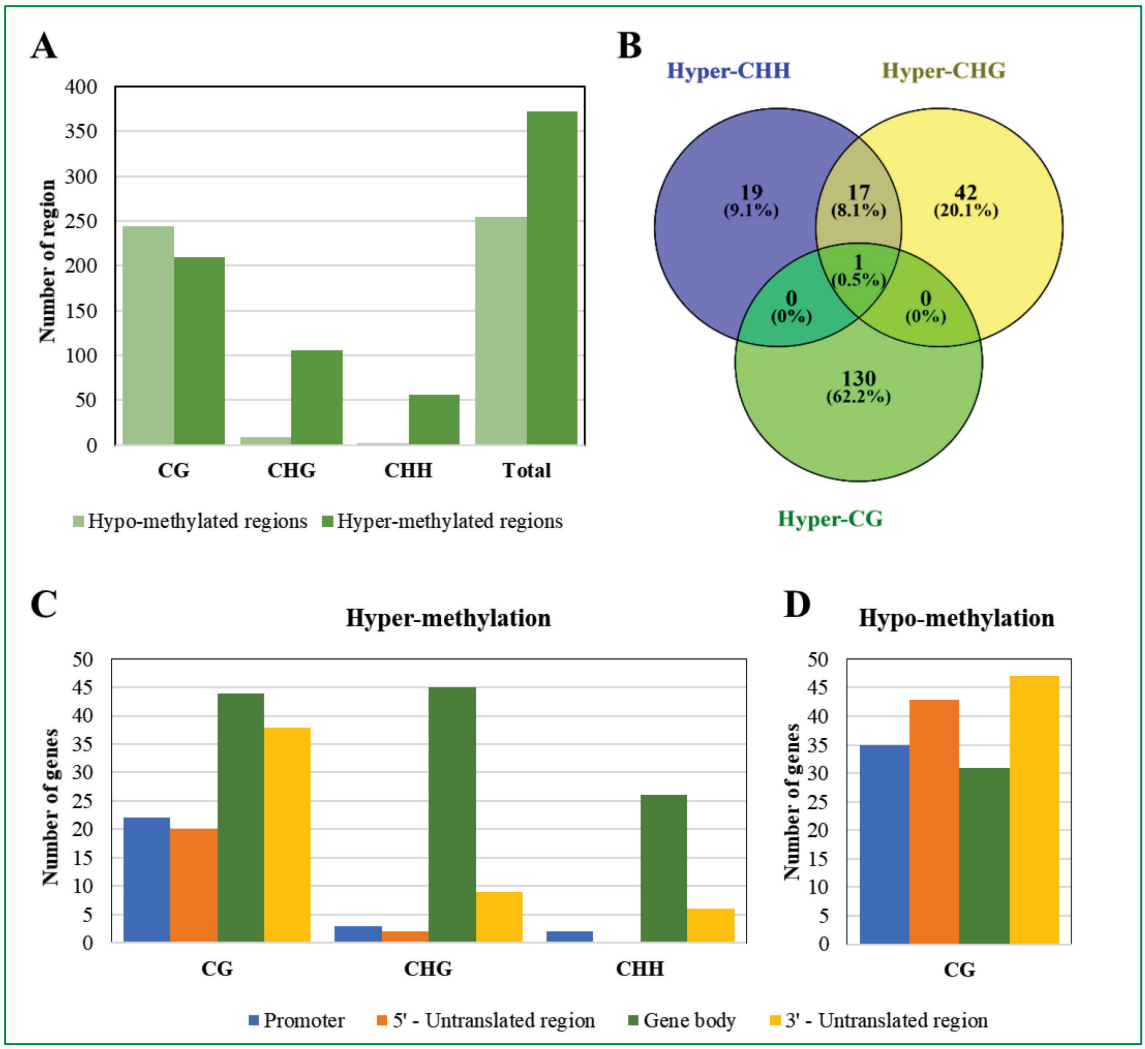


**Figure 3.5 - Characterization of differentially methylated regions detected in Cr-t strain *vs* wt. A**, Number of differentially hyper- and hypo-methylated regions in CG, CHG and CHH contexts. **B**, Number of protein-coding genes overlapping with differentially hypermethylated regions in CG, CHG and CHH contexts. The total number of differentially methylated genes in each context is shown in parentheses. **C** and **D**, Distribution of differentially hypermethylated regions (C) and hypomethylated regions (D) to various annotated features of hypothetic protein-coding genes.

In order to identify the genes differentially methylated between Cr-t and wt strains, *T. obliquus* UTEX 393 was annotated using AUGUSTUS (software for gene prediction in eukaryotic genomic sequences); identifying 12886 putative genes. Each differentially methylated region detected in Cr-t strain *vs* wt was assigned to proximal hypothetic protein-coding genes based on the genomic coordinates. The results showed that 62.9% (131 genes), 56.6% (60 genes) and 64.9% (37 genes) of the hypermethylated regions in CG, CHG and CHH contexts respectively, overlapped with protein-coding genes (Fig. 3.5, B). Similarly, 68.85% (168 genes), 11.1% (1 gene) and 0% (no gene) of the hypomethylated regions in CG, CHG and CHH contexts respectively, overlapped with protein-coding genes (Fig. 3.5B). As a result, a total number of 229 and 168 genes were

identified as hyper- and hypomethylated respectively in Cr-t strain *vs* wt. Interestingly, among these genes, 18 were hypermethylated in more than one context; 17 genes were hypermethylated in both CHH and CHG contexts and only 1 gene was hypermethylated in all contexts (Fig. 3.5B).

In order to define which genic regions were associated with a specific methylation context, we examined the distribution of differentially hyper- and hypomethylated genes in various annotated features of genic regions, including promoter regions, 2000 bp upstream of the transcription start site, gene body up to 5'- and 3'- untranslated regions. The hypermethylation in CHG and CHH contexts occurred predominantly in the gene body and less extent in the flanking regions, whereas CG hypermethylation was mainly located in the gene body and to a less extent in the 5' untranslated region (Fig. 3.5C).

The CG hypomethylation occurred in the same way among the different genic regions although to a greater extent in both 5'- and 3'- untranslated regions (Fig. 3.5D).

The Singular Enrichment Analysis (SEA) algorithm was used *via* KOBAS 3.0 to analyse Gene Ontology (GO) term enrichment of hyper- and hypo- methylated hypothetic genes, using *C. reinhardtii* as reference organism and Fisher's exact test ($P$ *value* $< 0.05$). Results of the GO categorization were expressed as three independent hierarchies: Molecular Functions, F (gene product at biochemical level), Biological Processes, P (cellular events to which the gene product contributes) and Cellular Components, C (location or complex of gene/protein). Among the 209 hypermethylated hypothetical genes, 129 genes were successfully blasted in KOBAS 3.0. Regarding Molecular Function, the higher significant term corresponded to helicase activity (GO:0004386) followed by several binding activity (ATP (GO:0005524), adenyl ribonucleotide (GO:0032559), adenyl nucleotide (GO:0030554), nucleoside (GO:0001882), ribonucleotide (GO:0032553), nucleotide (GO:0000166) and purine (GO:0017076)) as well as activity of ATPase (GO:0016887), lyase (GO:0016829) and transcription regulator (GO:0030528). As regard as Biological Processes, 37 differentially hypermethylated genes were significantly enriched: i.e metabolic process (GO:0008152), regulation of transcription (GO:0006351), RNA metabolic process (GO:0051252), protein metabolic process (GO:0019538) and regulation of several process (GO:0050794, GO:0051171, GO:0031326, GO:0009889, GO:0010556, GO:0010468, GO:0050789). No significant Cellular Components were found in hypermethylated gene fraction (Fig. 3.6).


**Figure 3.6 - Gene Ontology (GO) term enrichment of hypermethylated hypothetic genes.** Fisher's exact test for the significant enrichment analysis of GO terms of the biological process (P) and molecular function (F) categories of the hypermethylated hypothetic genes ($P < 0.05$).

Among the hypomethylated hypothetical genes, 103 were successfully blasted in KOBAS 3.0. For these genes, all functional groups have been identified, although the Biological Process consisted only of GO:0008152 metabolic process. Molecular function was costituited by ATPase activity, coupled (GO:0042623), transporter activity (GO:0005215), active transmembrane transporter activity (GO:0022804), nucleoside-

triphosphatase activity (GO:0017111), hydrolase activity, acting on acid anhydrides, in phosphorus-containing anhydrides (GO:0016818), pyrophosphatase activity (GO:0016462), hydrolase activity, acting on acid anhydrides (GO:0016817), substrate-specific transmembrane transporter activity (GO:0022891), ATPase activity (GO:0016887), hydrolase activity (GO:0016787) and substrate-specific transporter activity (GO:0022892). Finally, Cellular Component GO included: cell (GO:0005623), cell part (GO:0044464), membrane (GO:0016020), intracellular (GO:0005622) and intracellular part (GO:0044424) categories (Fig.3.7).

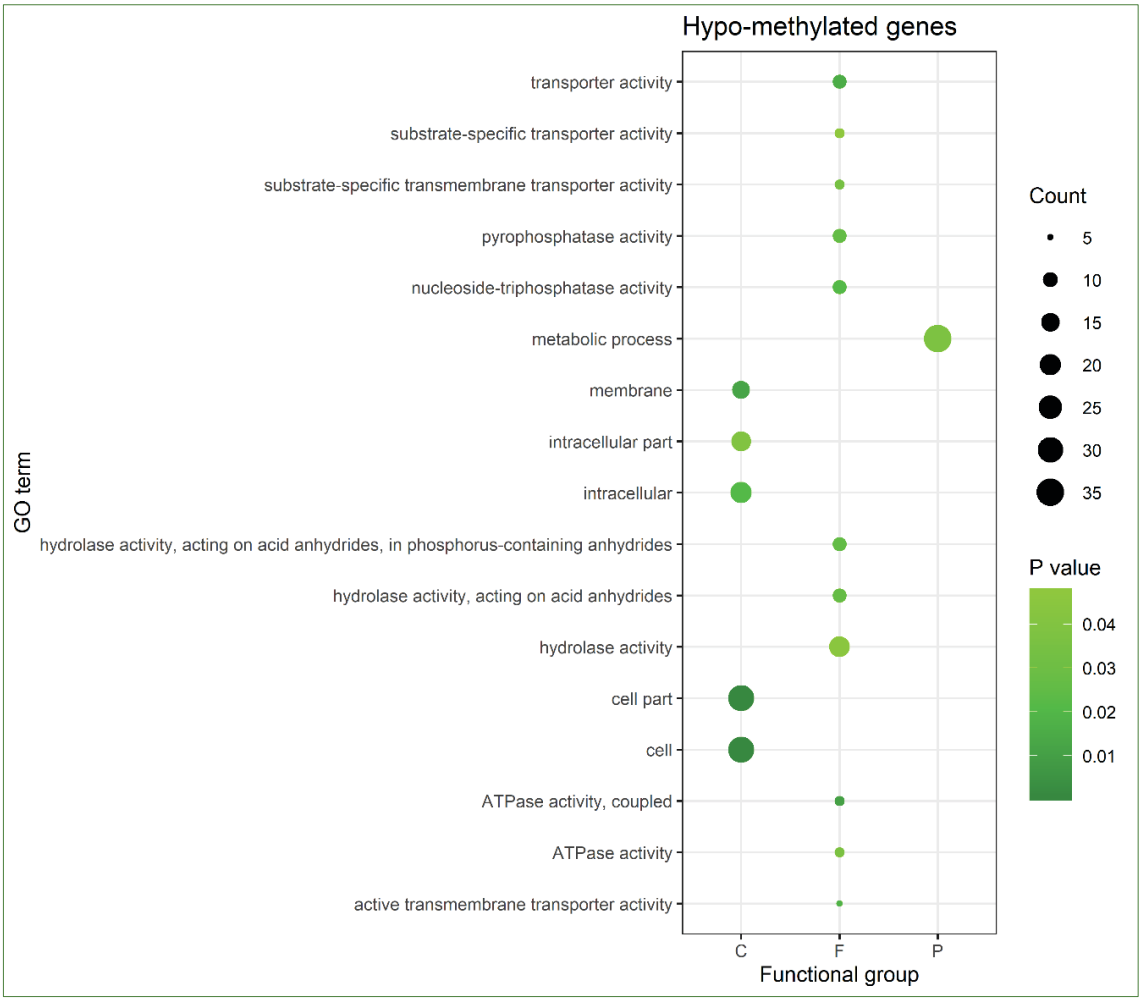


**Figure 3.7 - Gene Ontology (GO) term enrichment of hypomethylated hypothetic genes.** All GO terms in bubble chart were significant ($P < 0.05$).

Kyoto Encyclopedia of Genes and Genomes (KEGG) pathway analysis is a useful bioinformatics software that directed the associations of the genes with the organism and environment. In order to unveil the different life processes or metabolisms between strains, hyper- and hypo- fractions of differentially methylated genes were blasted with

KEGG data base by using KOBAS 3.0 software. Data analyses showed that Cr-t hypermethylated genes were involved in important pathways as Biosynthesis of secondary metabolites, Metabolic pathways, Biosynthesis of amino acids, Pentose phosphate pathway, Glycerophospholipid metabolism, RNA transport, Cysteine and methionine metabolism, mRNA surveillance pathway, Glycolysis/Gluconeogenesis, Ubiquitin mediated proteolysis, Spliceosome, Sulfur metabolism, Glycerolipid metabolism, 2-Oxocarboxylic acid metabolism, Carbon metabolism, Glutathione metabolism and Glycine, serine and threonine metabolism (Fig. 3.8). The significantly enriched KEGG pathways of hypomethylated fraction were Riboflavin metabolism, Metabolic pathways, Pantothenate and CoA biosynthesis, Photosynthesis - antenna proteins, Phagosome, DNA replication, Pyrimidine metabolism and Carbon fixation in photosynthetic organisms (Fig. 3.9).

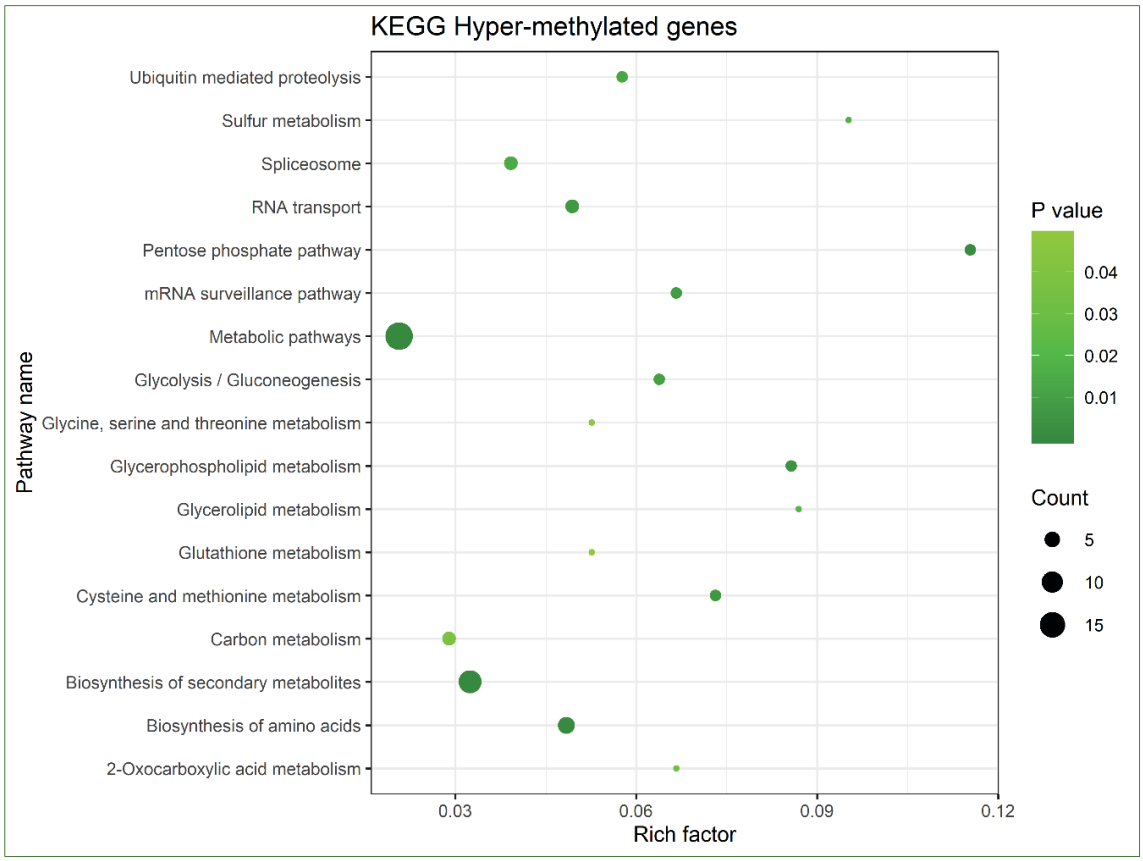


**Figure 3.8 - Pathway analysis of hypermethylated genes.** KEGG pathway enrichment analysis of differentially hypermethylated genes in the Cr-t was performed. The size of the circle represents the gene numbers and the colour represents the P value. Only significant pathways are present in the chart ($P < 0.05$).

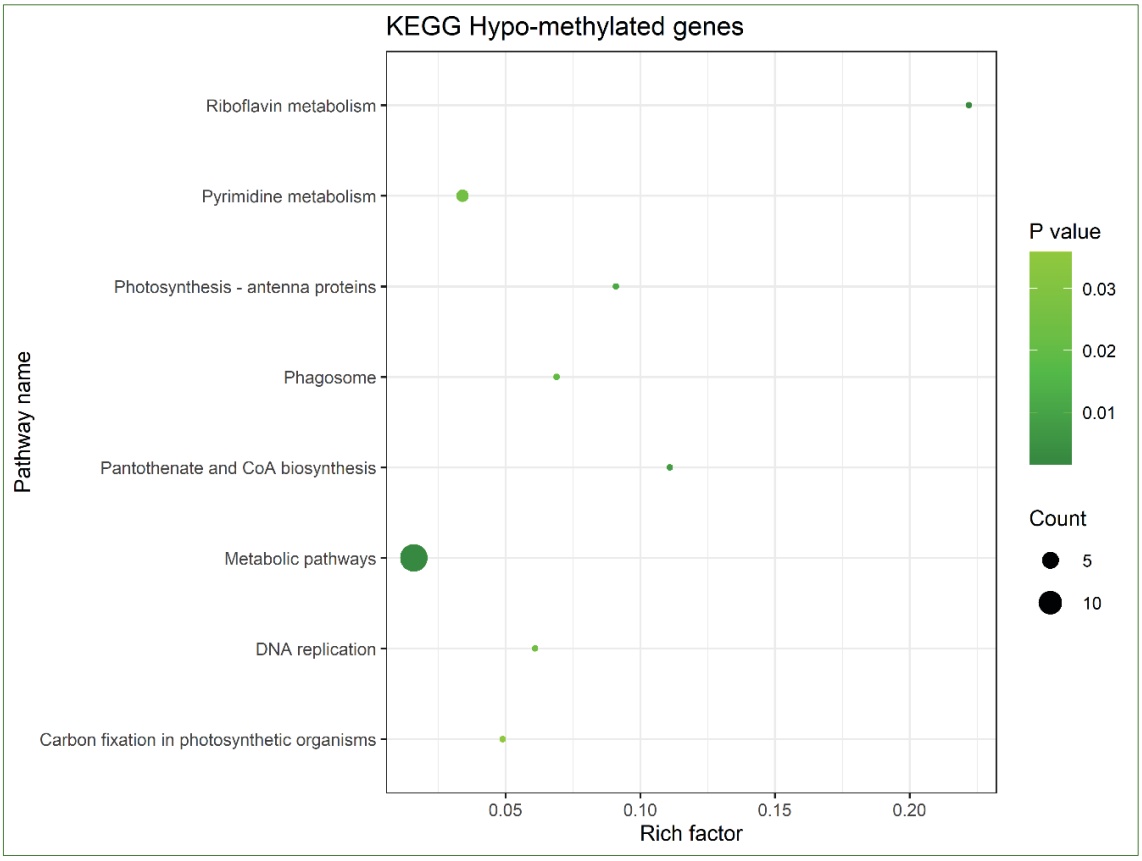


**Figure 3.9 - Pathway analysis of hypomethylated genes.** KEGG pathway enrichment analysis of differentially hypomethylated genes in the Cr-t strain was performed. The size of the circle represents the gene numbers and the colour represents the P value. Only significant pathways are present in the chart ($P < 0.05$).

## 3.4 - DNA methylation in Sulfur pathway

Sulfur pathway, as mentioned in the previous chapter, is strongly related with chromium-tolerance and sulfur uptake/assimilation; the same pathway resulted also enriched in the KEGG analysis. Therefore, in order to better understand the relationship between Cr-tolerance and differential methylation of the sulfur pathway genes, we identified and characterized, by cDNA amplification, 29 genes involved in sulfur metabolism including transporters, assimilation enzymes and enzymes involved in downstream cysteine metabolism (Tab. 3.2). Among these, for *SaATS1, SaATS2, SaSULP1, SaSabc, SaAPR, SaOASTL1, SaOASTL3, SAC3,* partially identified in previous works, we attained their full-lengt. Besides we completely identified and characterized *SaARS, SaSULTR1, SaSULTR2, SaSIR1, SaSIR3, SaOASTL2, SaOASTL4, SaSAT1, SaSAT2, SaCGS1, SaCBS, SaTHS, SaMETE* and *SaGSH1* genes; finally we partially identified *SaSULP2,*

*SaMETH1, SaMETH2* and *SaGSH2* genes whereas *SaSLT* characterization still remained uncertain.

The features and the functional activity of all identified genes are reported in table 3.2.

| Activity | Genes | Length (bp) | Length CDS (bp) | Number of exons |
|---|---|---|---|---|
| Arylsulfatase | ***SaARS*** | 9309 | 2190 | 17 |
| Sulfate transporter ($H^+/SO_4^{2-}$ family) | ***SaSULTR1*** | 7036 | 2133 | 12 |
| | *SaSULTR2* | 7431 | 1903 | 15 |
| Sulfate transporter ($Na^+/SO_4^{2-}$ family) | *SaSLT1?** | 1692 | 971 | 3 |
| | *SaSLT2?** | 2135 | 847 | 5 |
| ATP sulfurylase | *SaATS1* | 2255 | 1125 | 6 |
| | *SaATS2* | 3422 | 1254 | 7 |
| Chloroplast sulfate transporter (subunits) | *SaSULP1* | 2453 | 1152 | 5 |
| | *SaSULP2** | 4191 | 840 | 7 |
| | ***SaSabc*** | 4814 | 1419 | 11 |
| APS kinase | *SaAPK** | 2888 | 750 | 8 |
| APS reductase | *SaAPR* | 2979 | 1242 | 8 |
| Sulfite reductase | *SaSIR1* | 7539 | 1953 | 14 |
| | *SaSIR3* | 3450 | 2286 | 5 |
| O-acetylserine(thiol)-lyase | *SaOASTL1* | 3641 | 978 | 10 |
| | *SaOASTL2* | 3484 | 1188 | 7 |
| | ***SaOASTL3*** | 4368 | 1233 | 9 |
| | *SaOASTL4* | 3349 | 1026 | 10 |
| Serine acetyltransferase | ***SaSAT1*** | 2004 | 1098 | 4 |
| | *SaSAT2* | 4147 | 1830 | 8 |
| Cystathionine γ-synthase | *SaCGS1* | 3579 | 1416 | 6 |
| Cystathionine β-lyase | *SaCBS* | 6788 | 2478 | 11 |
| Threonine synthase | *SaTHS* | 5962 | 1545 | 12 |
| Methionine synthase | *METH1** | 5829 | 2586 | 10 |
| | *METH2** | 4628 | 1299 | 6 |
| | *SaMETE* | 11210 | 2532 | 10 |
| γ-Glutamylcysteine synthetase | ***SaGSH1*** | 4170 | 1455 | 7 |
| GSH synthetase | *SaGSH2** | 5581 | 2136 | 11 |
| Negative regulatory protein | *SAC3* | 3726 | 1044 | 9 |

**Table 3.2 – Features of characterized genes.** *: partially identified genes; **Bold fonts**: differently methylated genes; **?**: uncertain characterization

The identified genes were mapped on *T. obliquus* genome, and then, each differentially methylated region, was assigned to proximal identified genes based on the genomic coordinates. The gene methylation levels were investigated from upstream, gene body up to the downstream regions.

Among the identified genes of the sulfur pathway, six genes were differently methylated in Cr-t *vs* wt. In particular, *SaSULTR1, SaARS* and *SaOASTL3* were hypomethylated in

CG context and more precisely, *SaSULTR1* on the promoter region whereas the remainder on gene body. *SaSabc* and *SaSAT1* were hypermethylated in CG context on gene body; *SaGSH1* was hypermethylated in CHG context on gene body (Fig. 3.10).

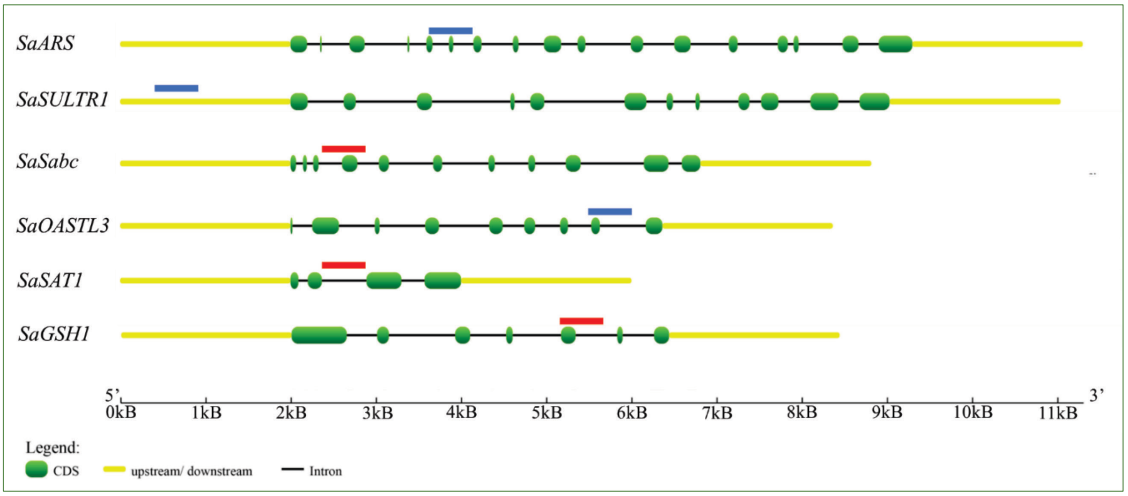


**Figure 3.10 – Features of genes of sulfur pathway differently methylated in Cr-t *vs* wt.** Hypomethylated regions (blue); hypermethylated region (red).

To understand if the different DNA methylation of these genes could modulate their expression, a RT-qPCR was carried out using ΔΔCt method. Expression results showed that *SaARS* and *SaSULTR1* were significantly ($p < 0.001$) up-regulated, whereas the other genes were significantly ($p < 0.001$) down-regulated in Cr-t strain. Overall, all the analysed genes, except for *SaOASTL3,* showed a negative association between DNA methylation and their expression level (Fig. 3.11).

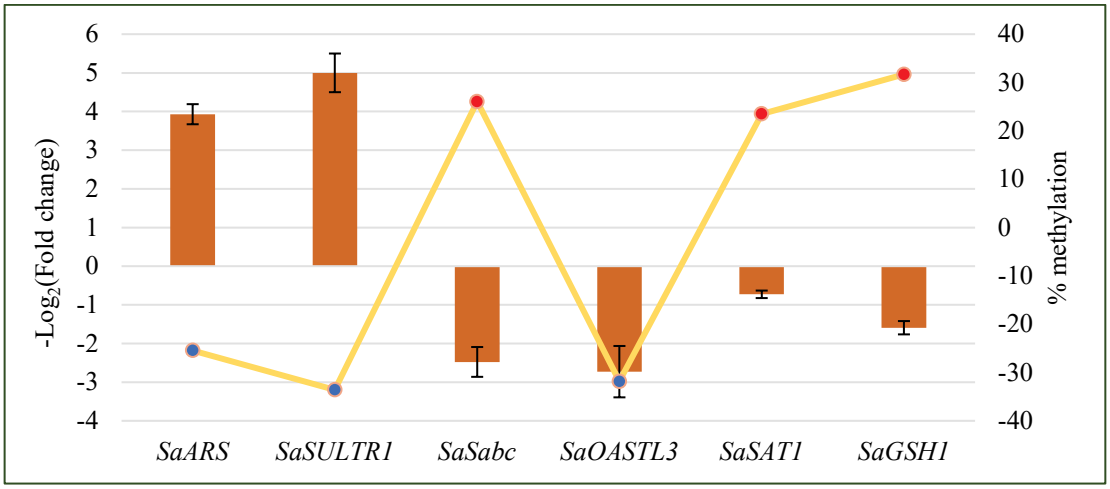


**Figure 3.11 – Expression analysis by RT-qPCR of Differentially methylated genes (Cr-t strain *vs* wt)** The RT-qPCR data were normalized using *SaCBLP* as housekeeping gene. The results represent the mean value (± standard deviation) of three replicates. All genes analysed were significant different between strains ($p > 0{,}0001$). The bars represent -$Log_2$(fold change expression); the lines represent the methylation level (%).

## 3.5 - Sulfur uptake

### 3.5.1 - Plasma-membrane transporters

The influx of sulfate into the cell can be coupled with co-transport of positively charged counter ions such as proton ($H^+$) and sodium ($Na^+$) operated respectively by SULTRs and SLTs transporters located on the plasma membrane.

#### *3.5.1.1 - SULTRs*

Attention was focused on SULTRs transporters, namely $H^+/SO_4^{2-}$ type transports. Two genes encoding putative SULTR (SULfate TRansporter) were identified and named *SaSULTR1* and *SaSULTR2*. The full-length coding DNA sequence (CDS) of the *SaSULTR1* gene from *S. acutus* was isolated employing RT-PCR method and subjected to sequence based in silico analysis.

Sequence analysis of the *T. obliquus* UTEX393 genome (available in public database), using this newly cloned cDNA sequences indicated the presence of two distinct loci, one on scaffold 1191 corresponding to the sequence designated as *SaSULTR1* (Accession no: MG969380), and the other, corresponding to *SaSULTR2* (Accession no: MF457897), located on scaffold 86. Albeit theirs deduced amino acid sequences are highly similar (48 % identity and 63 % similarity sequence), gene structure of *SaSULTR1* and *SaSULTR2* is different (Fig. 3.12). The CDSs of *SaSULTR1* and *SaSULTR2* are 2133 and 1903 bp long and code for predicted polypeptides of 711 and 641 amino acids, respectively. The genomic organization of *SaSULTR1* is constituted by 12 exons separated by 11 introns, whereas that of *SaSULTR2* indicated the presence of 15 exons interrupted by 14 introns (Fig. 3.12). Moreover, the two *SaSULTR1* and *SaSULTR2* CDSs showed 57 % identity and similarity at the nucleotide sequence but both the intron sizes and nucleotide sequences were highly differing between the two genes. Furthermore, differences in the regulative STAS domain in the protein 3' was evidenced between SaSULTR1 and SaSULTR2.

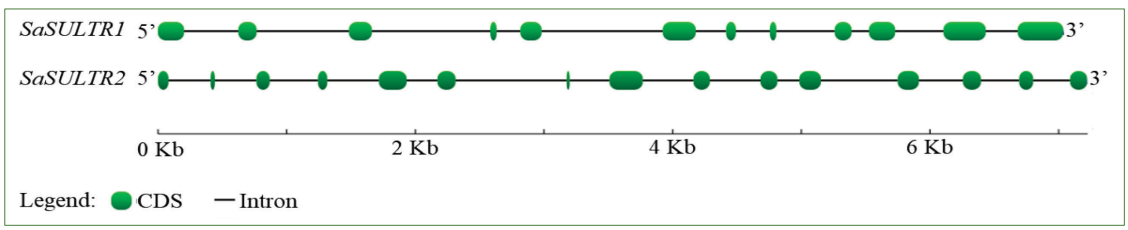


**Figure 3.12 – Structures of two *SaSULTRs* genes.**

### *3.5.1.2 - SLT*

*SLT* genes have been as well subject of this work. Three fragments were identified and sequenced which putatively codified for $Na^+/SO_4^{2-}$ transporters (SLC13 family). Despite the use of AUGUSTUS software allowed us to identify putative SLT sequences in four different scaffolds of *T. obliquus* UTEX393 genome, the *SLT* sequences on scaffold 1182 and 113 are identic, is thus not clear if three or four gene are present in of *T. obliquus* genome. The organization of these gene seems quite complex, since also in *C. reinhardtii* genome three genes are present and two of them are placed head-to-tail and partially overlapped. Due to this complex organization the isolation and characterization of *SaSLT* genes, employing RT-PCR and sequencing method, has not yet be completed. One of the identified fragments matched on scaffold 1182 and 113, the others on scaffold 1318, and their deduced amino acid sequences had similar identity with the different SLTs in *R. subcapitata* and *C. reinhardtii* (Tab 3.3 and 3.4). In the deduced amino acid sequences of respective sequenced fragments were identified TrkA-C domains and Anion ArsB/NhaD permease domains.

Moreover, the two obtained fragments matching on scaffold 1318 likely belong to the same gene, but their correct characterization, interpreted from ortholog proteins in other organisms, is still uncertain. For these reasons, their expression analysis was yet not possible.

| | Max Score | Total Score | Query Cover | E value | % Identity | Accession |
|---|---|---|---|---|---|---|
| sodium sulfate co-transporter *Raphidocelis subcapitata* | 308 | 308 | 0.98 | 7E-95 | 60.81 | GBF91816.1 |
| sodium sulfate co-transporter *R. subcapitata* | 285 | 285 | 0.74 | 6E-87 | 73.58 | GBF89760.1 |
| sodium/sulfate co-transporter *C. reinhardtii* (SLT1) | 234 | 234 | 0.99 | 1E-67 | 49.06 | XP_001690975.1 |
| sodium/sulfate co-transporter *C. reinhardtii* (SLT2) | 207 | 207 | 0.99 | 2E-57 | 42.96 | XP_001690491.1 |
| sodium/sulfate co-transporter *C. reinhardtii* (SLT3) | 229 | 229 | 0.99 | 8E-66 | 48.12 | XP_001690490.1 |
| hypothetical protein CHLRE_10g445050v5 *C. reinhardtii* | 229 | 229 | 0.99 | 7E-66 | 47.94 | PNW77628.1 |

**Table 3.3 – BlastX result of the fragment matching on scaffolds 1182 and 113 (SaSLT1) with sodium/sulfate co-transporter of *R. subcapitata* and *C. reinhardtii*.**

| | Max Score | Total Score | Query Cover | E value | % Identity | Accession |
|---|---|---|---|---|---|---|
| sodium sulfate co-transporter *R. subcapitata* | 374 | 374 | 0.97 | 1E-119 | 64.86 | GBF91816.1 |
| sodium sulfate co-transporter *R. subcapitata* | 241 | 241 | 0.99 | 2.00E-69 | 49.47 | GBF94386.1 |
| sodium/sulfate co-transporter *C. reinhardtii* (SLT1) | 278 | 323 | 0.98 | 1E-83 | 51.07 | XP_001690975.1 |
| sodium/sulfate co-transporter *C. reinhardtii* (SLT2) | 283 | 328 | 0.98 | 4E-85 | 50.00 | XP_001690491.1 |
| sodium/sulfate co-transporter *C. reinhardtii* (SLT3) | 285 | 335 | 0.98 | 4E-86 | 50.71 | XP_001690490.1 |
| hypothetical protein CHLRE_10g445050v5 *C. reinhardtii* | 285 | 335 | 0.98 | 2E-86 | 50.71 | PNW77628.1 |

**Table 3.4 - BlastX result of the fragments matching on scaffolds 1318 with sodium/sulfate co-transporter of *R. subcapitata* and *C. reinhardtii***

### 3.5.2 - Chloroplast sulfate transporter

We have also completely identified *SaSabc* and *SaSulP1* and partially *SaSulP2* genes, coding for 3 of the 4 subunits of the chloroplast ABC transporter holocomplex responsible of the routing of sulfate into the plastid for reductive assimilation. SulP1 and SulP2 forms the channel whereas Sabc is the ATP-binding protein on the stromal side of the transporter.

#### *3.5.2.1 - SaSulp1*

*SaSulP1* and *SaSulP2*, mapped on *T. obliquus* UTEX393 genome, respectively on scaffold 990 and scaffold 341. Their gene structures are shown in the figure below.

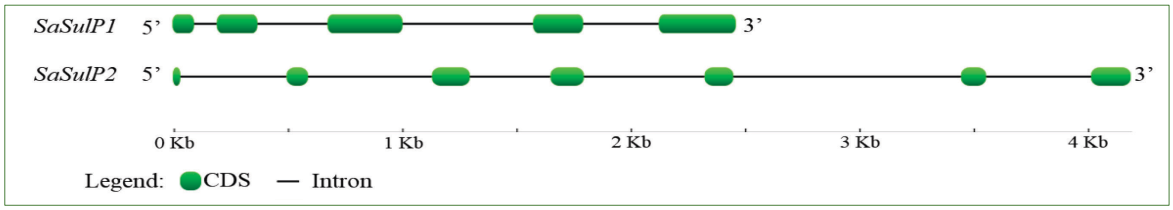


**Figure 3.13 - Structures of the two *SaSulPs* genes.**

Sequence analysis of the deduced amino acid sequence of *SaSulP1* gene, which putatively encoded a membrane-bound protein, showed homology with *C. reinhardtii* SulP, sharing a 53.9% identity and 64.8% similarity. Analysis of the amino acid sequence of SulP1 using the ChloroP tool indicated the presence of a chloroplast transit peptide consisting

of the first 81 amino acids of the precursor protein (Fig. 3.14A). The predicted molecular mass of the precursor and mature form of SulP1 was 40.8 and 32.6 kDa, respectively. Furthermore, amino acid sequence was analysed to predict membrane-spanning regions, by using TMpred and Phyre2 tools associated with sequences alignment of *C. reinhardtii* SulP with SaSulP1and seven transmembrane helices have been identified (Fig. 3.14, C and D).

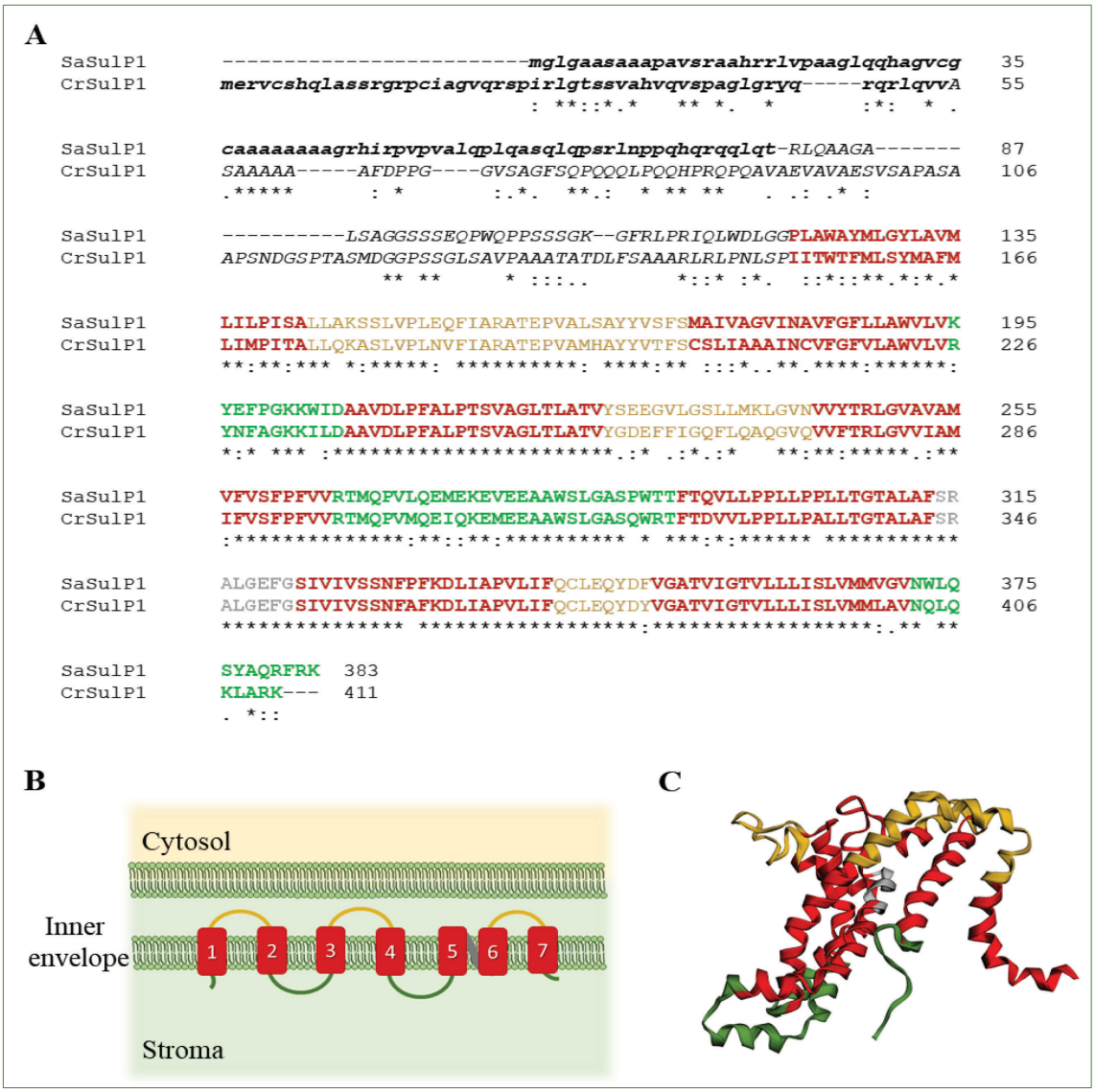


**Figure 3.14 - SaSulp1 amino acid sequence, conserved motif transit peptide and membrane folding model. A)** SaSulp1 protein sequence compared to SulP1 C. reinhardtii. ***Lowercase italic and bold*:** predicted chloroplast transit peptide. **B)** Putative membrane folding model. **C)** tridimensional structure built on *Molybdate/tungstate ABC transporter, permease protein model* (Hollenstein et al., 2007). **red**: transmembrane domains; **green**: regions of protein lie in the chloroplast stroma; **yellow**: regions of protein lie in the intermembrane space; **grey**: alpha-helix motif between fifth and sixth transmembrane helices.

### *3.5.2.2 - SaSulp2*

*SaSulP2* gene was homologous to *C. reinhardtii SulP2*, with a 60.2 % identity and 67.2% similarity in the amino acid sequence and to SulP2 (26 % amino acid identity, 45 % similarity). The chloroplast transit peptide sequence of SulP2 has not yet been identified and the sequence so far obtained reached the first segment of *C. reinhardtii* SulP located on stromal side of the envelope membrane (Fig. 3.15). SaSulP2 sequence was analysed as described for SulP1 to predict membrane-spanning regions. In the deduced aminoacidic sequence were identified five transmembrane helices (Fig. 3.15, B) and an alpha-helix motif between fourth and fifth transmembrane helices putatively located in the pocket when the two subunits are associated to form the channel.

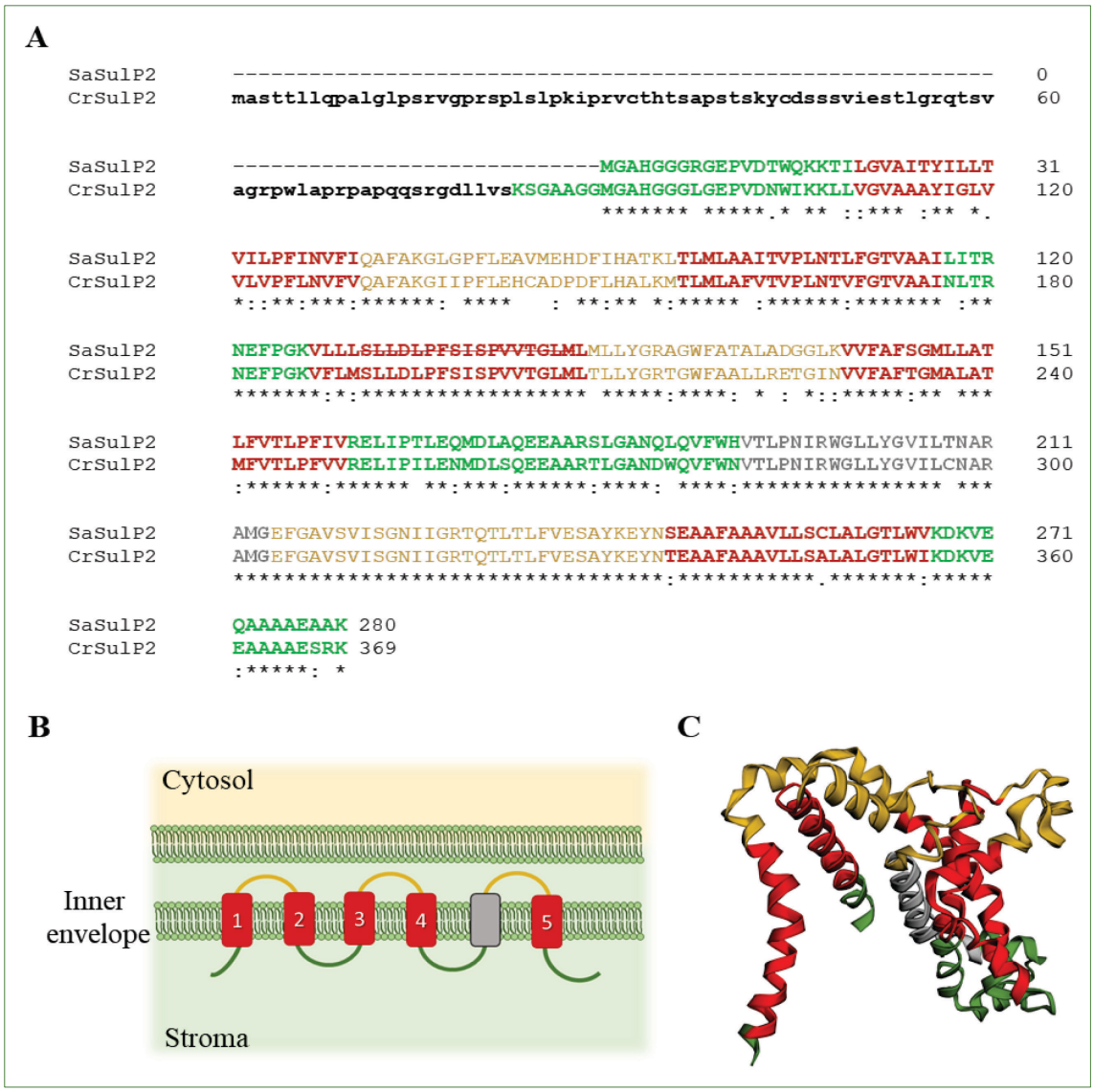


**Figure 3.15 - SaSulp2 amino acid sequence, conserved motif transit peptide and membrane folding model. A)** SaSulp2 protein sequence compared to SulP2 *C. reinhardtii*. **Lowercase italic and bold:** predicted chloroplast transit peptide. **B)** Putative membrane folding model. **C)** tridimensional structure built on *Molybdate/tungstate ABC transporter, permease protein model* (Hollenstein et al., 2007). **red**:

transmembrane domains; **green**: regions of protein lie in the chloroplast stroma; **yellow**: regions of protein lie in the intermembrane space; **grey**: alpha-helix motif between fourth and fifth transmembrane helices.

### *3.5.2.3 - SaSabc*

The full-length of *SaSabc* sequence, partially identified and sequenced before, was attained and characterized in this work. The sequence was mapped on of *T. obliquus* UTEX393 genome and its structure are reported in figure 3.16.

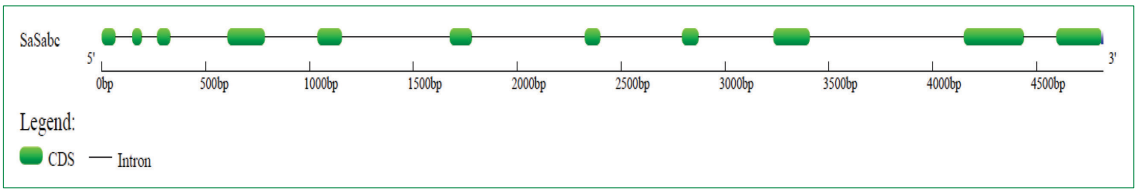


**Figure 3.16 – Structure of *SaSabc* gene**

The deduced amino acid sequence codified by *SaSabc* gene showed 55.9 % of identity and 66.1 % of similarity with *C. reinhardtii Sabc*. Using the ChloroP tool a chloroplast transit peptide sequence (the first 49 amino acids) was identified. Moreover, six conserved motifs, common to ABC transporter ATP hydrolyzing subunits, were identified by alignment between *C. reinhardtii* Sabc and SaSabc. Four of them were involved in binding and hydrolysis of ATP whereas the remaining two were probably involved in ATP hydrolysis and/or interaction with the membrane-spanning subunits (Fig. 3.17). These motifs are highly conserved ad are identical to those of *C. reinhardtii* Sabc.

**A**

```
SaSabc      mlpagraqalrssrdstacaakpgprs----vgsssrssfprrwvavqaldtsALEEQQQ    56
CrSabc      ma---sllaqttsrlgarpaaqagpvaqmapmasrvqpampsallplharatttsv----    53
            *       *  :** .:  **: ** :    :.*  : ::*   : ::*  *::

SaSabc      QQQAAQLNGNGSSTAHQHRAAAAAGVSRPSGPTATLTDEDVNGMQLDGIQLEQQQQPTGL    116
CrSabc      acrAASIDKPVVYT---PRDSSQQSSNGAGEVSMSISSMDEVGPSYEGIITDAPTRPTGL    110
              :**.::     *    * ::  . .  .  : :::. *  * . :**  :   :****

SaSabc      YVRVRGMVKHFNTAKGVFKAVDGVDVDIPPSSICALLGPSGSGKTTLLRLVAGLELPTGG    176
CrSabc      YVRVRNMVKHFSTAKGLFRAVDGVDVDIEPSSIVALLGPSGSGKTTLLRLIAGLEQPTGG    170
            *****.*****.****:*:********* **** ****************:**** ****

SaSabc      KIYFDDLDATDLAVQDRQVGMVFQSYALFNHMTVSENIKFGLQVRKLPVDHDKRAADLLE    236
CrSabc      NIYFDDTDATNLSVQDRQIGFVFQSYALFNHKTVAENIKFGLEVRKLNIDHDKRVAELLA    230
            :***** ***:*:*****:*:********** **:*******:**** :*****.*:**

SaSabc      LVQLTGLGDRYPRQLSGGQRQRVALARALASNPRLLLLDEPFGALDAVVRKQLRAGLKEI    296
CrSabc      LVQLTGLGDRYPRQLSGGQRQRVALARALASNPRLLLLDEPFGALDAVVRKQLRTGLREI    290
            ************************************************:**:**

SaSabc      VRSVGVTTIIVTHDQEEAFDLADQVVIFNRGLIEQSGSPNEIIKRPATPFVMGFVGDTNS    356
CrSabc      VRSVGVTTIIVTHDQEEAFDLADKVVVFNRGLVEQQGSPTEIIKRPRTPFIMKFVGETNV    350
            **********************:**:*****:**.***.****** ***:* ***:**

SaSabc      VPAGCMLVRRSGFNPRLGKARVMFRPSDIRLSKEYVATL-DGQQVVTPATVNEAANMGWT    415
CrSabc      VPATSLLAKRMRFNT--SKTSVMFRPHDIKLFKTVPPESGEGALTTVGANVADKANLGWV    408
            *** .:*.:*  **   .*: ***** **:* *       :*  ... *.* : **:**.

SaSabc      MKYTLKFDDDVEVEFSVTRAQADKEFKLDVGQRIYVVVPPSAMMEFDETELGSAPII      472
CrSabc      VKYTLRFDDDVECELQLSRDQDEREYNLVVGSRVFVHVPHRTMMGFNASDVDSTPIV      465
            :****:****** *:.::* * ::*::* **.*::* **  :** *: :::.*:**:
```

**B**

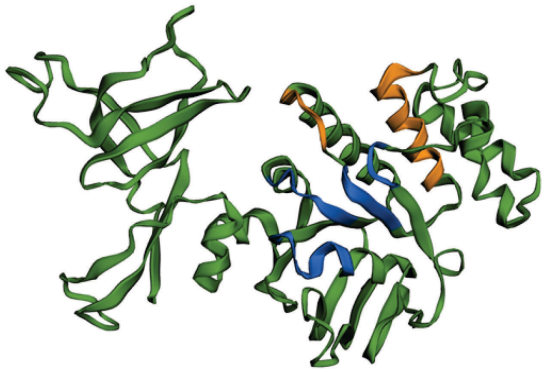

**Figure 3.17 - SaSabc amino acid sequence, conserved motif peptide and membrane folding model. A)** SaSabc protein sequence compared to Sabc *C. reinhardtii*. **B)** tridimensional structure built on Molybdate/tungstate ABC transporter, permease protein model (Hollenstein et al., 2007). **Lowercase bold** predicted transit peptide. **Bold fonts** conserved motifs common to ATP hydrolyzing subunits of ABC transporters: **Blue bold,** motifs involved in binding and hydrolysis of ATP; **Orange bold,** motifs postulated to be involved in ATP hydrolysis and/or interaction with the membrane-spanning subunits.

## Phylogenetic analysis of identified sulfur transporters

Phylogenetic analysis was performed to examine the relationship of the sulfur transporters proteins identified in *S. acutus* with those from other algae.

Algal SULTRs transporters are present in a subgroup from which diverged plant SULTR4 subfamily (Pootakham et al. 2010; Takahashi et al. 2012). The most studied *C. reinhardtii* transport system indicate that SULTR1 and SULTR2 are more closely related to plant SULTR transporter family whereas SULTR3 is closer to bacterial sequences (Pootakham et al. 2010).

Albeit the reduced number of algal SULTR sequences limits the data interpretation, the phylogenetic analysis of SaSULTRs and other Chlorophyceaen green algae homologous proteins shows that these transporters cluster according algal taxa, independently from the transporter type (Fig. I.1). SaSULTR1 and SaSULTR2 indeed clustered together with proteins of *Monoraphidium* and *Raphidocelis* and splitting between SULTR1 and SULTR2 were observed only within the same order (as occur for CrSULTR1 and CrSULTR2).

This result suggested that a recent gene duplication, or in any case subsequent to the separation of the different evolutionary algae groups, occurred between the two transporters. Probably the members of SULTRs subfamily underwent subsequent duplication and specialization to play different roles in sulfate transport process.

By contrast, evolutionary trajectories were completely different from members of chloroplast-localized sulfate transporter.

Dendrogram regarding SaSulP1 and SaSulP2 has highlighted as the two proteins cluster in two different groups corresponding to CysTs and CysWs subunits of the prokaryotic holocomplex of the ABC transporter (Fig. II). The first group included SulP1 and CysT whereas the second group included SulP2 and CysW. Moreover, SulP1s (subunit of eukaryotic ABC-transporter) and CysTs (prokaryotic ABC-transporter subunit) were further separated into two sub-group. In the same way, eukaryotic ABC-transporter SulP2s and prokaryotic ABC-transporter subunit CysWs were further splitted into two sub-groups.

The analysis of SaSabc (Fig. III) showed the same divergence between eukaryotic and prokaryotic subunits of sulfur ABC-transporter.

The phylogenetic analysis indicated distinct evolutionary origin of the sulfate transporters studied in this work. It would seem that while a recent gene duplication occurred in plasma membrane sulfur transporter, a more ancestral and horizontal transfer has occurred in genes codifying for the chloroplast ABC-transporter subunits.

Despite being conserved in many algal groups, the four genes coding for the ABC chloroplast sulfate transporter show a no uniform distribution between nuclear and chloroplastic genomes of different organisms (Lindberg and Melis 2008). The three identified genes *SaSulP1* and *SaSulP2* as well as *SaSabc* are present on *S. acutus* nuclear genome. Although *Sbp* has not yet been identified in the *S. acutus* genome, this gene is not present in the chloroplastic genome of *S. obliquus* (de Cambiaire et al., 2006), thus, as reported for *C. reinhardtii* (Lindberg and Melis, 2008), also in *S. acutus* all the four genes seem nuclear-encoded.

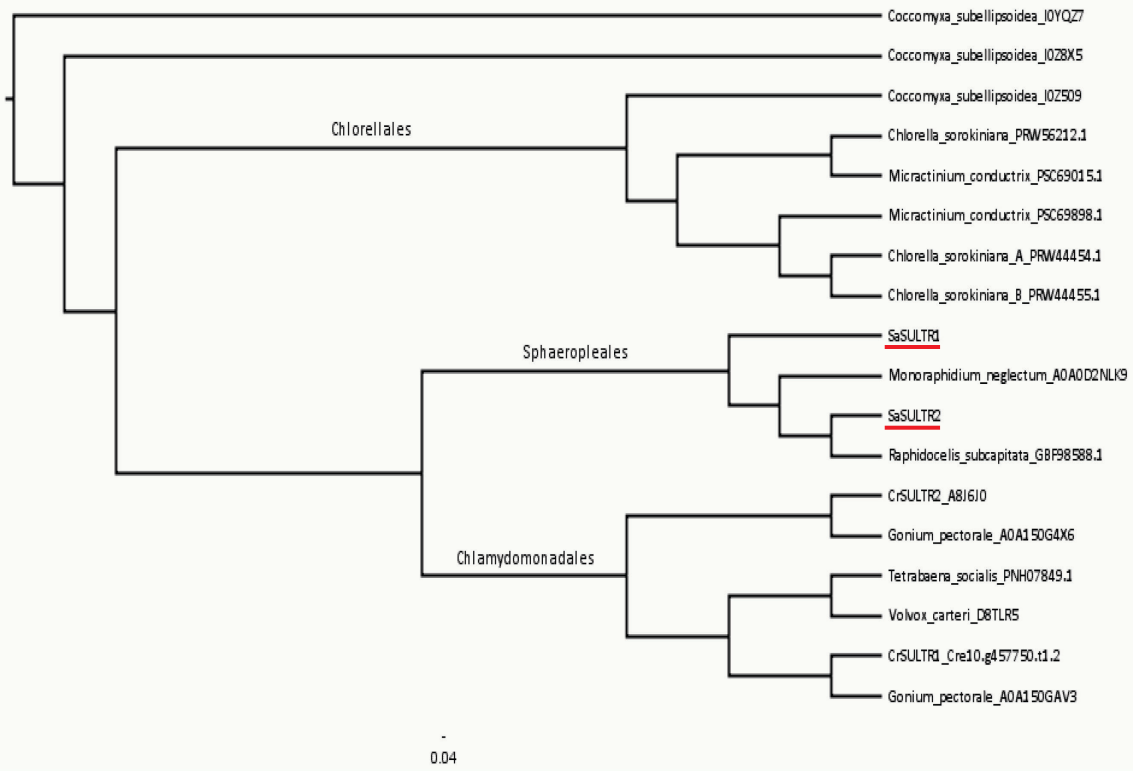


**Figure I - Phylogenetic tree of SaSULTR1 and SaSULTR2.** The evolutionary history was inferred by using the Neighbor-Join method. The tree is drawn to scale, with branch lengths in the same units as those of the evolutionary distances used to infer the phylogenetic tree. The analysis involved SaSULTR1 and SaSULTR2 of *S. acutus* and other green algae amino acid sequences. Evolutionary analyses were conducted in MEGA X. *S. acutus* sequences are underlined in red.

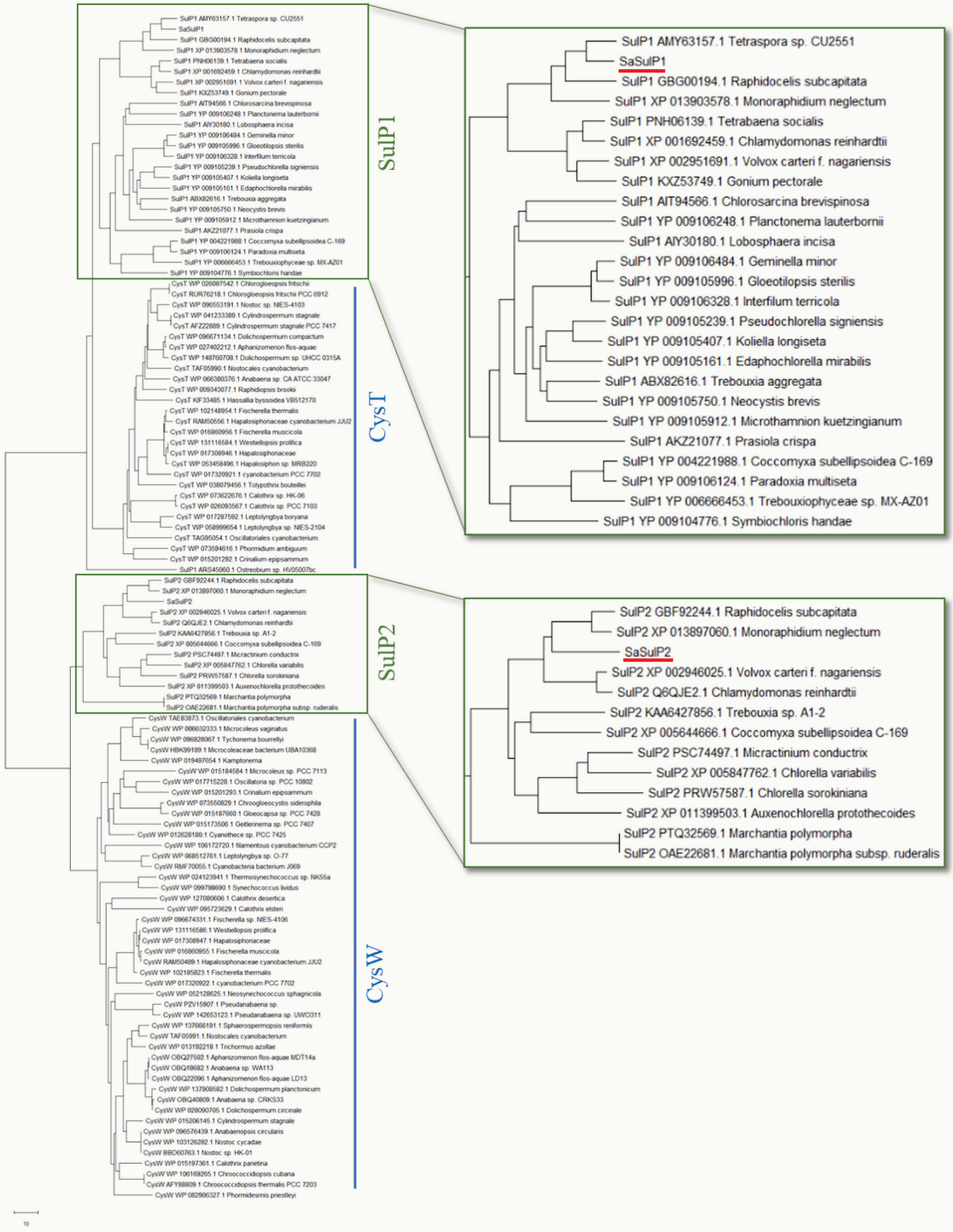


**Figure II** - **Phylogenetic tree of SaSulP1 and SaSulP2.** The evolutionary history was inferred through the Neighbor-Join method by using MEGA X. The tree is drawn to scale, with branch lengths in the same units as those of the evolutionary distances used to infer the phylogenetic tree. The analysis involved SulP1 and SulP2 amino acid sequences of *S. acutus* and those of other eukaryotic as well as prokaryotic CysT and CysW. *S. acutus* sequences are underlined in red.

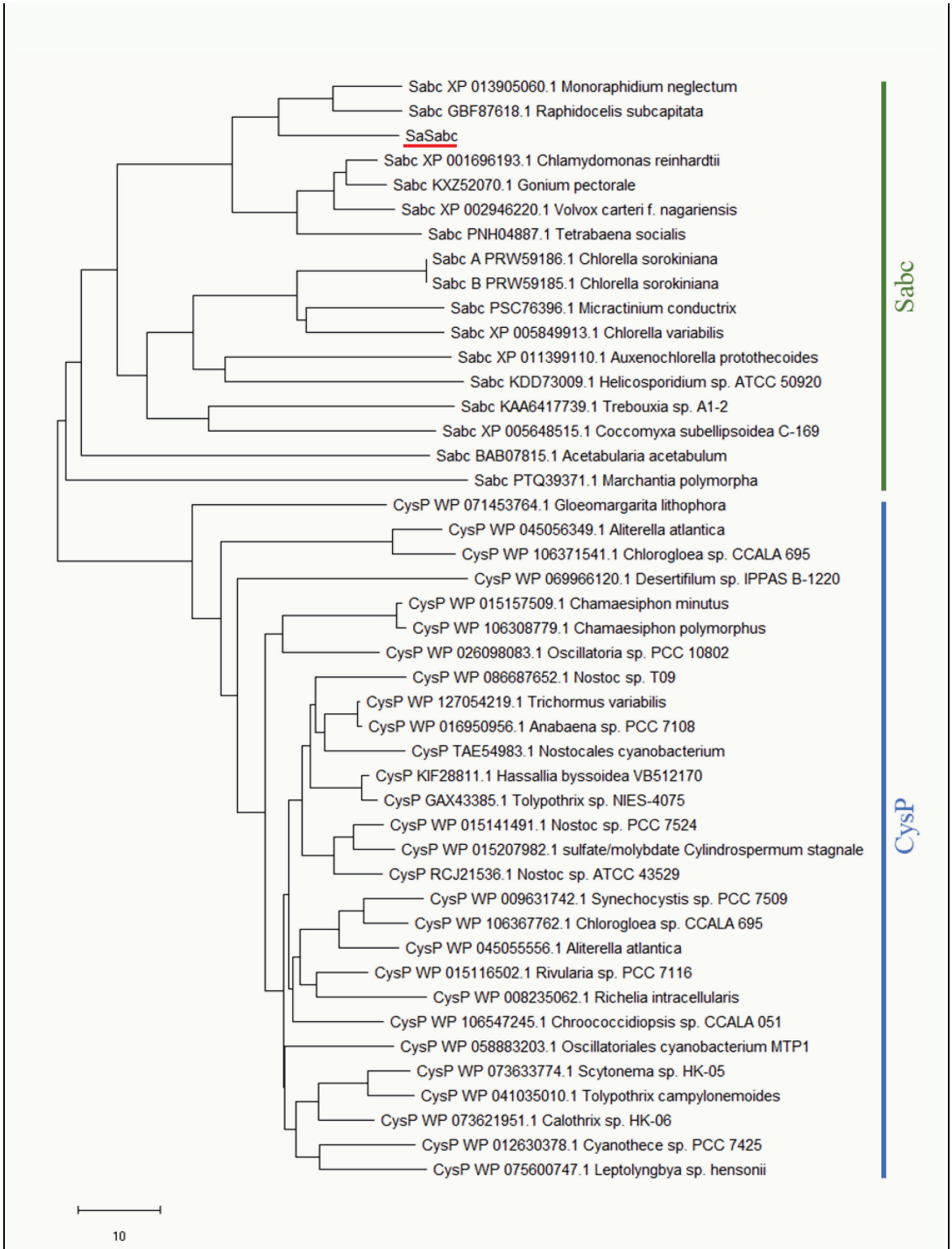


**Figure III - Phylogenetic tree of SaSabc.** The evolutionary history was inferred by using the Neighbor-Join method. The tree is drawn to scale, with branch lengths in the same units as those of the evolutionary distances used to infer the phylogenetic tree. The analysis involved eukaryotic Sabc, including SaSabc *S. acutus* and prokaryotic CysP amino acid sequences. Evolutionary analyses were conducted in MEGA X. *S. acutus* sequence is underlined in red.

### 3.5.4 - *SULTRs* gene expression

To understand the role of sulfur uptake in Cr-tolerance as well as in the transient Cr-tolerance increase induced by S-deprivation, *SULTRs* expression was quantified at transcriptional level by RT-qPCR in both strains after the different treatments.

Differences were observed in *SULTRs* gene expression between strains.

In control S-sufficient conditions (Fig. 3.18) *SaSULTR1* was expressed only by Cr-t cells. Similar expression levels were observed in the wt only after chromium exposure which induced a significant increase ($p$<0.001) in the expression of this gene at both the tested concentrations (even with different time courses). Also, in Cr-t strain no difference was observed between the control cells and those exposed to 1 mg Cr(VI)/l, whereas a dramatic up regulation (9- 13-fold the control) was induced when this strain was exposed its LOEC, namely 2 mg Cr(VI)/l.

S-starvation induced a strong *SaSULTR1* expression inasmuch the transcript level was extremely high in both strain after pre-culture in S deprived medium (Fig. 3.19). Moreover, in these conditions nutritional stress was clearly predominant masking chromium effects in S-replete cells during the first 24h culture. Also, in this condition different behaviour was observed between strains since after nutrient resupply wt downregulated *SaSULTR1* more rapidly than Cr-t cells, and Cr-t strain maintained high level of *SaSULTR1* expression upon 48 h of 2 mg Cr(VI)/l exposure.

After 48 h renewal medium, in both strains *SaSULTR1* expression still maintained significantly ($p$ < 0.0001) higher than their counterparts grown in S-sufficient conditions.

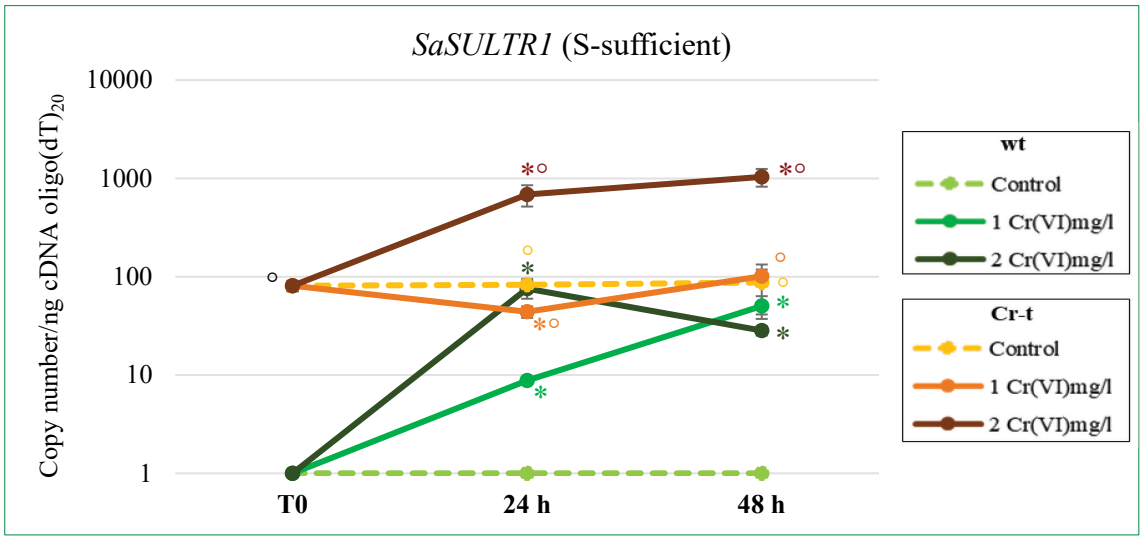


**Figure 3.18** - **Absolute quantification of *SaSULTR1* expression in S-sufficient condition.** Statistical analysis was performed by using one-way ANOVA with Tukey post hoc test (p < 0.05) after Shapiro-Wilk normality test. *: significantly difference between Cr-treated (with 1 or 2 mg Cr(VI)/l) and untreated cells within strain. °: significantly difference between the two strains in similar conditions.

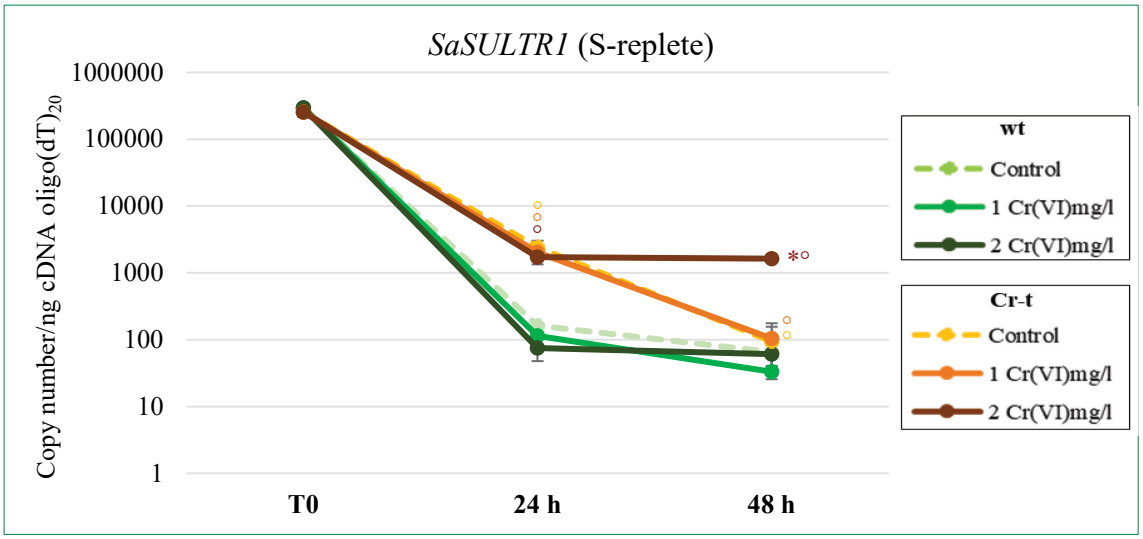


**Figure 3.19 - Absolute quantification of *SaSULTR1* expression in S-replete condition.** Statistical analysis was performed by using one-way ANOVA with Tukey post hoc test ($p < 0.05$) after Shapiro-Wilk normality test. *: significantly difference between Cr-treated (with 1 or 2 mg Cr(VI)/l) and untreated cells within strain. °: significantly difference between the two strains in similar conditions.

In contrast, *SaSULTR2* expression was higher in the wt at the end of pre-culture in +S medium and increased in both strains after 24h from medium renewal, both in control and in 2mg Cr(VI)/l exposed cells. On the contrary, in the presence of 1 mg Cr(VI)/l it decreased in wt and exactly followed control time course in the Cr-t strain (Fig. 3.20).

Even *SaSULTR2* expression was enhanced by S starvation and both strains, at the end of pre-culture in -S medium, showed transcript levels higher than in S-sufficient condition (4.4- and 25-fold in wt and Cr-t, respectively).

After 24h from nutrient re-supply, in wt *SaSULTR2*expression decreased, though remaining higher than in S-sufficient condition, and Cr-exposure induced a further significantly decrease. *SaSULTR2* transcription levels were restored thereafter.

In Cr-t strain, *SaSULTR2* expression remained stable at 24 h and decreased to basal level after 48 h with the only exception of 2 mg Cr(VI)/l exposed cells as already observed for *SaSULTR1* (Fig. 3.21).

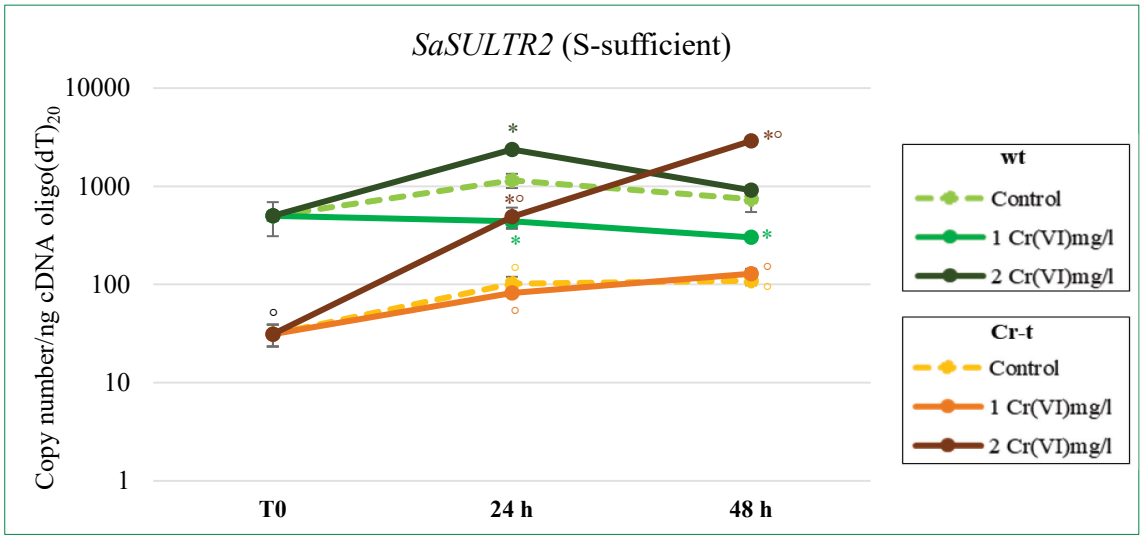


**Figure 3.20 - Absolute quantification of *SaSULTR2* expression in S-sufficient condition.** Statistical analysis was performed by using one-way ANOVA with Tukey post hoc test ($p < 0.05$) after Shapiro-Wilk normality test. *: significantly difference between Cr-treated (with 1 or 2 mg Cr(VI)/l) and untreated cells within strain. °: significantly difference between the two strains in similar conditions.

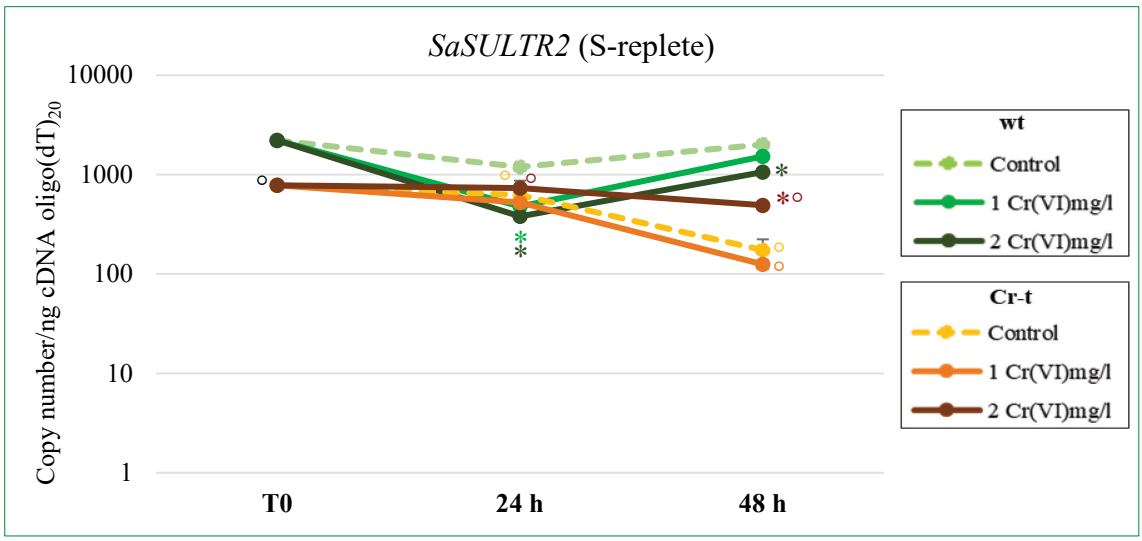


**Figure 3.21 - Absolute quantification of *SaSULTR2* expression in S-replete condition.** Statistical analysis was performed by using one-way ANOVA with Tukey post hoc test ($p < 0.05$) after Shapiro-Wilk normality test. *: significantly difference between Cr-treated (with 1 or 2 mg Cr(VI)/l) and untreated cells within strain. °: significantly difference between the two strains in similar conditions.

The comparison between *SaSULTR1* and *SaSULTR2* copy number (Tab. 3.5) showed that the wt expresses a higher total number of transporters than the Cr-t strain in S-sufficient condition, whereas Cr-t compensates the low transporter number with the expression of the putatively high affinity transporter *SaSULTR1* (not expressed by the wt). After 24 h from nutrient renewal both strains increased transporters number mainly increasing *SaSULTR2* transcription whereas *SaSULTR1* copy number remained unchanged.

In S-deprived condition both strains significantly enhanced S-uptake, both by changing the affinity and increasing the transporters number. The more evident response was indeed the strong induction of *SaSULTR1* transcription (which reach levels not significantly different in the two strains). Meantime an increase in *SaSULTR2* copy number was also observed, being the copy number in the wt however significantly higher than in the Cr-t strain. After 24h from nutrient re-supply in S-replete condition, due to the slower silencing of both gene expression in this strain, the total copy number of *SULTRs* was higher in Cr-t than wt, yet, with an inverted ratio between the two transporter levels, being *SaSULTR1* lower and *SaSULTR2* higher in the wt and vice-versa in the Cr-t.

| | | | ***SaSULTR1*** | ***SaSULTR2*** | **SUM of *SaSULTR1* and *SaSULTR2*** |
|---|---|---|---|---|---|
| **S-sufficient** | T0 | wt | $0 \pm 0^{e}$ | $500 \pm 54^{d}$ | $500 \pm 54^{e}$ |
| | | Cr-t | $81 \pm 9^{d}$ | $31 \pm 8^{f}$ | $112 \pm 7^{g}$ |
| | 24 h | wt | $0 \pm 0^{e}$ | $1150 \pm 64^{b}$ | $1150 \pm 64^{d}$ |
| | | Cr-t | $82 \pm 13^{d}$ | $102 \pm 18^{e}$ | $184 \pm 28^{f}$ |
| **S-replete** | T0 | wt | $294000 \pm 2777^{a}$ | $2200 \pm 60^{a}$ | $296200 \pm 2834^{a}$ |
| | | Cr-t | $256000 \pm 39939^{a}$ | $780 \pm 72^{c}$ | $256780 \pm 39981^{a}$ |
| | 24 h | wt | $161 \pm 14^{c}$ | $1195 \pm 17^{b}$ | $1356 \pm 27^{c}$ |
| | | Cr-t | $2409 \pm 614^{b}$ | $619 \pm 71^{cd}$ | $3029 \pm 680^{b}$ |

**Table 3.5 - Copy number/ng cDNA oligo(dT)$_{20}$ encoding SaSULTR2 and SaSULTR1 transporter in untreated cells in T0 and after 24 h of medium renewal.** Statistical analysis was performed within column by using one-way ANOVA with Tukey post hoc test after Shapiro-Wilk normality test. Data are reported as mean value ± standard deviation. Different letters label significantly different values ($p<0.05$).

### 3.5.5 - *SulPs* genes expression

In order to investigate if sulfate intake in the chloroplast is differently regulated in the two strains, we quantified the transcription of the genes encoding the channel of chloroplast sulfate transporter (*SaSulP1* and *SaSulP2*) under the different growth conditions through RT-qPCR.

In wt cells *SaSulP1* expression was 2-fold higher than in the Cr-t strain and chromium exposure induced opposite response in the two strains. A decrease of expression occurred in the wt and vice-versa an increase in the Cr-t strain (Fig. 3.22).

S-starvation induced a marked accumulation of transcript also for *SaSulP1* in both strains (7.3-fold in wt and 8-fold in Cr-t) although wt strain showed significantly higher levels than Cr-t. In the wt *SaSulP1* expression decreased more slowly than the Cr-t strain after nutrient resupply and a downregulation occurred after 24 hours Cr-exposure.

In the Cr-t strain instead a similar decrease was observed only in control cells while in chromium exposed cells *SaSulP1* transcription remained higher than in control and even a further increase was observed after 24 hours at 1 mg Cr(VI)/l (Fig. 3.23).

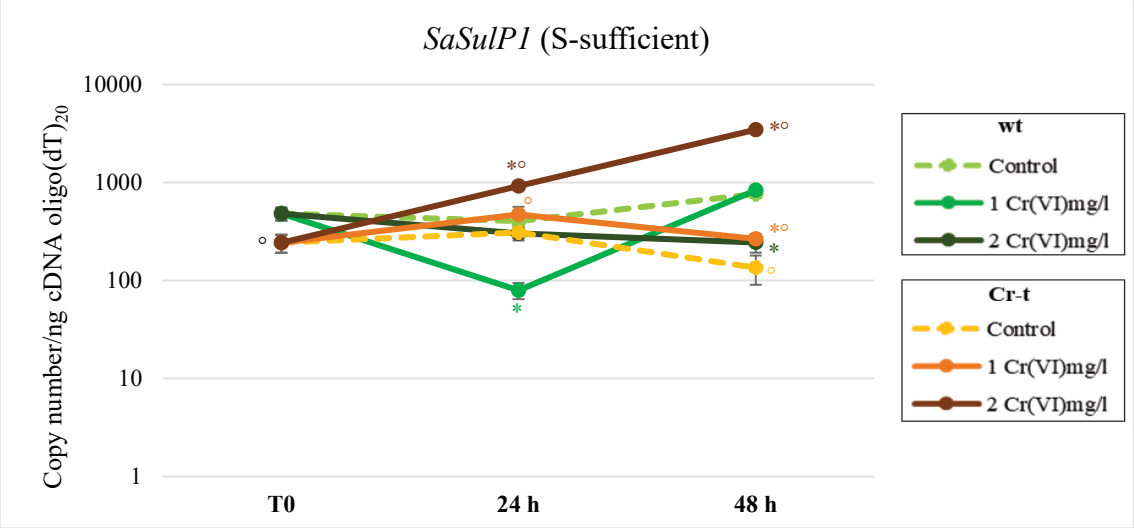


**Figure 3.22 - Absolute quantification of *SaSulP1* expression in S-sufficient condition.** Statistical analysis was performed by using one-way ANOVA with Tukey post hoc test ($p < 0.05$) after Shapiro-Wilk normality test. *: significantly difference between Cr-treated (with 1 or 2 mg Cr(VI)/l) and untreated cells within strain. °: significantly difference between the two strains in similar conditions.

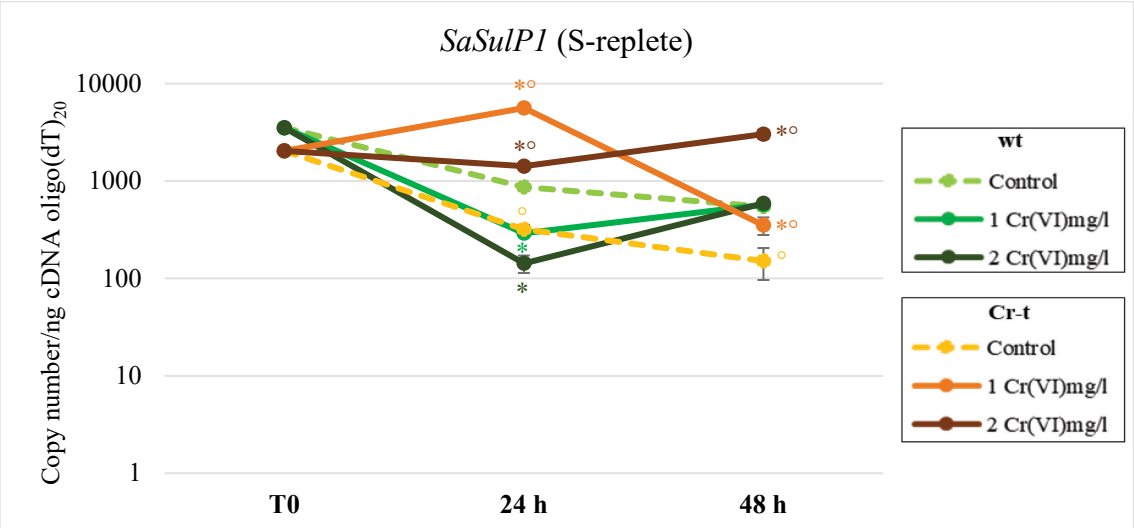


**Figure 3.23 - Absolute quantification of *SaSulP1* expression in S-replete condition.** Statistical analysis was performed by using one-way ANOVA with Tukey post hoc test ($p < 0.05$) after Shapiro-Wilk normality test. *: significantly difference between Cr-treated (with 1 or 2 mg Cr(VI)/l) and untreated cells within strain. °: significantly difference between the two strains in similar conditions.

Weaker variations were observed as regard as *SaSulP2* expression in S-sufficient conditions, however also for this gene a reduced transcription was observed in wt cells exposed to chromium (both at 24 and 48 hours). Cr-t instead behaves as wt at 24h while

a significant increase (albeit lower of that observed for *SaSulp1*) was observed after 48h of chromium exposure (Fig. 3.24).

*SaSulP2* expression was strongly enhanced by S-starvation most of all in the wt in which a 4.2-fold increase in copy number was observed. Notwithstanding *SaSulP2* expression decreased in both strains after medium renewal and Cr-t rapidly restored basal level for this gene, *SaSulp2* transcription remained significantly elevated (above basal level) in the wt till 48h. Also in S-replete condition *SaSulP2* expression was negatively affected by chromium exposure in the wt and positively in the Cr-t (Fig. 3.25).

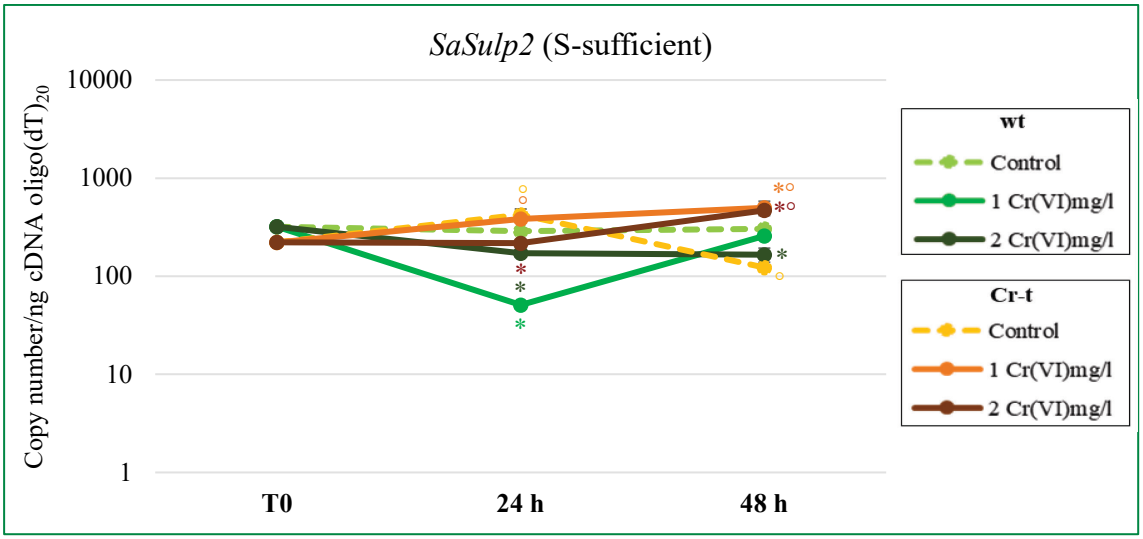


**Figure 3.24 - Absolute quantification of *SaSulP2* expression in S-sufficient condition.** Statistical analysis was performed by using one-way ANOVA with Tukey post hoc test ($p < 0.05$) after Shapiro-Wilk normality test. *: significantly difference between Cr-treated (with 1 or 2 mg Cr(VI)/l) and untreated cells within strain. °: significantly difference between the two strains in similar conditions.

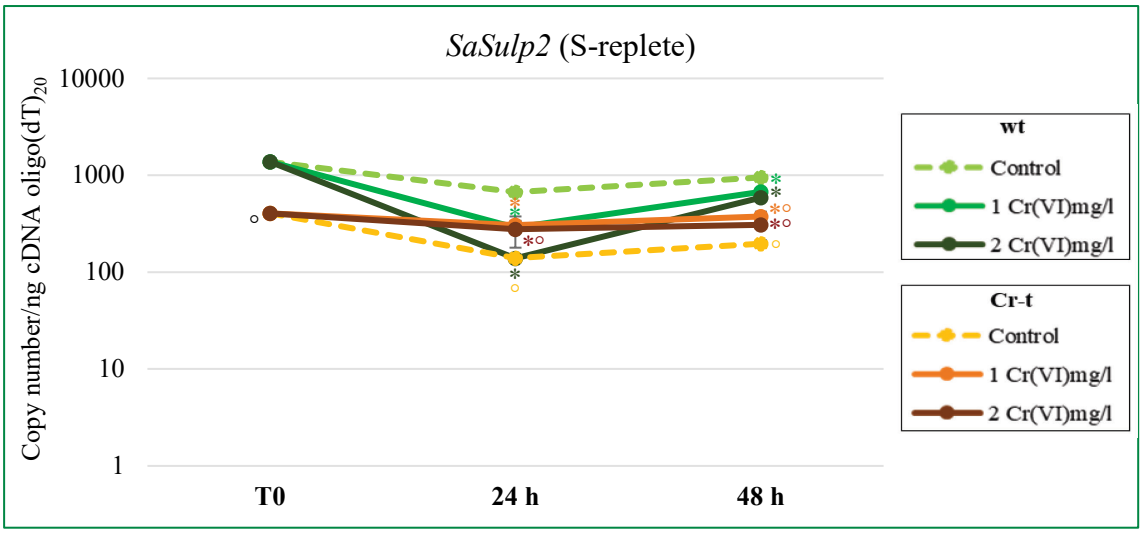


**Figure 3.25 - Absolute quantification of *SaSulP2* expression in S-replete condition.** Statistical analysis was performed by using one-way ANOVA with Tukey post hoc test ($p < 0.05$) after Shapiro-Wilk normality test. *: significantly difference between Cr-treated (with 1 or 2 mg Cr(VI)/l) and untreated cells within strain. °: significantly difference between the two strains in similar conditions.

### 3.5.6 - Correlation between *SaSULTRs* and *SaSulPs* gene expression and growth condition

Correlations were found in the expression changes of the studied genes in relation to different grown condition. Heat maps were created for an analysis of correlations amongst changes observed in both S-sufficient and S-replete conditions. The results are exposed in Fig 3.26 where genes with higher expression levels are shown in dark green, and genes with lower expression levels are shown in light green.

In S-sufficient condition, samples are clearly divided in two groups (Fig. 3.26, A). The first group included control and Cr(VI)-treated wt samples. In particular, the Cr(VI) treated samples generate a sub-cluster separate from controls, regardless of the treatment duration. In a specular way, the second group was composed by Cr-t samples with the exception of wt strain treated with 1 mg Cr(VI)/l for 24 hours which also clustered in this group. Also in S-replete condition (Fig. 3.26, B), the heatmap clearly indicate the presence of two groups globally representing the two strains. Very intriguingly, upon 2 mg Cr(VI)-treatment, wt clustered together Cr-t.

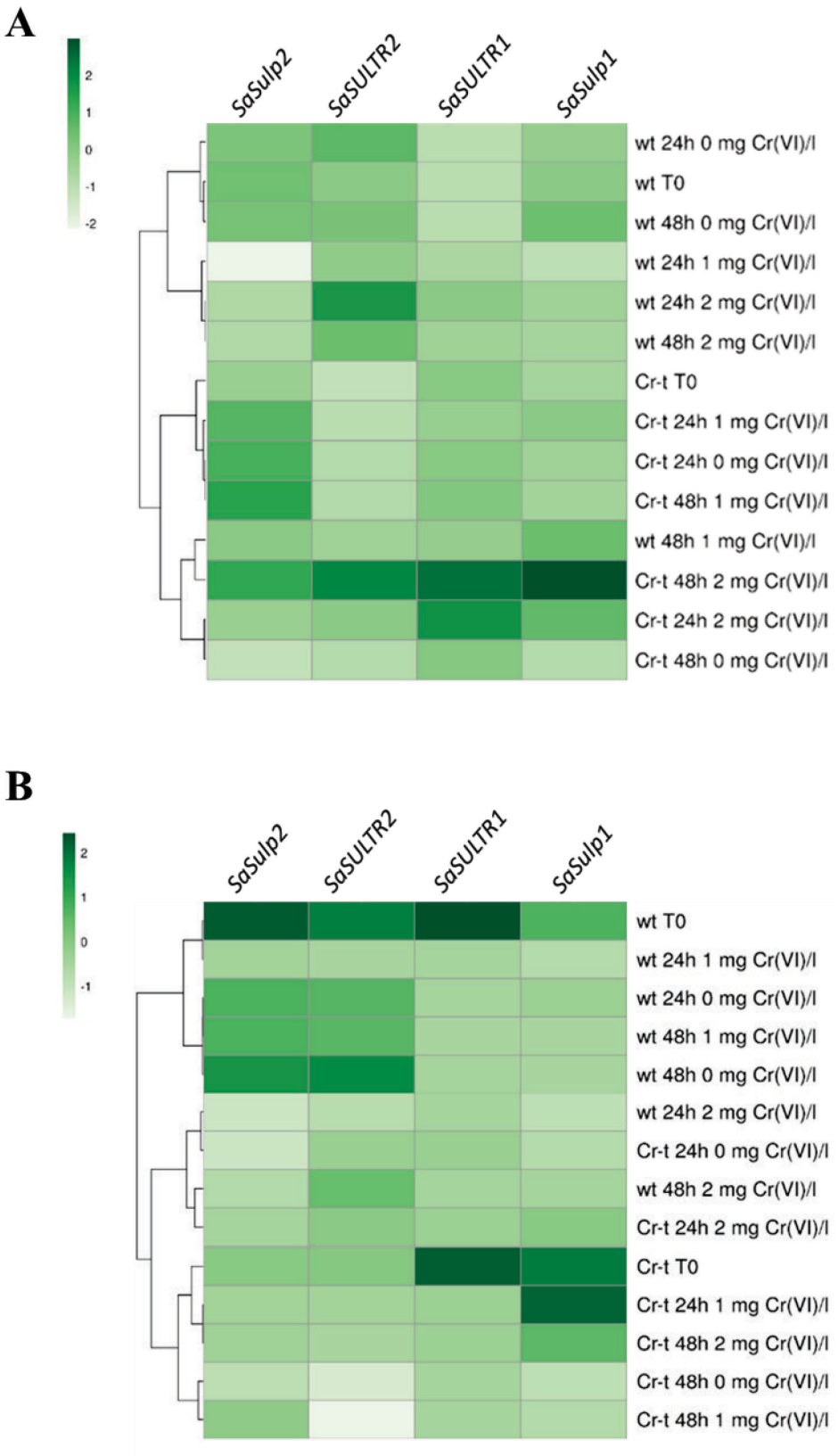


**Figure 3.26 - Heatmap of *SaSULTRs* and *SaSulPs* expression in cells growth in S-sufficient (A) and S-replete (B) condition**. Genes with higher expression levels are shown in dark red, whereas genes with lower expression levels are shown in light green.

CHAPTER

4

# *Discussion*

A Whole-Genome BS-seq (WGBS) was performed in the two strains of the freshwater green alga *S. acutus* with different Cr(VI) sensitivity, namely wt and Cr-t to gain additional information on the involvement of DNA methylation mechanisms in heavy metal tolerance in unicellular microalgae. Notwithstanding the studies on stress-responsive epigenomes and transcriptomes are important to understand the evolution of mechanisms related to stress adaptation in photosynthetic organisms, very few data have indeed been reported in algae (Feng et al, 2010, Zemach et al., 2010, Veluchamy et al., 2013).

Data generated from WGBS enable the comparison of genome-wide DNA methylation profiles under the two different biological contexts, Cr-t *vs* wt. The data of DNA methylation patterns at single nucleotide resolution showed that in both strains cytosine methylation occurred principally in the symmetric CG sites rather than in CHG and CHH contexts. This data confirms the evidence reported for *C. reinhardtii* consisting in low levels of methylation overall, but with a methylation in the CG sites twice as CHG and CHH ones (Feng et al., 2010). *V. carteri* genome as well, even much less methylated than *C. reinhardtii,* shows methylation exclusively in CG context (Zemach et al., 2010).

Albeit the overall methylation degree in CG context was similar between strains, the Cr-t showed a higher number of hypomethylated regions in CG context than wt; in Cr-t a higher hypermethylation was moreover found in CHG and CHH contexts. These results indicate that chromium tolerance is related to a hypomethylation in CG context and a hypermethylation in CHG and CHH contexts. These data are in accordance with previous results on the immunolocalization of 5-mC in CG context in Cr-t and wt strain of *S. acutus* (Cozza et. al, 2016). The authors, by using a monoclonal antibody raised against 5-mC in CG context, found a labelling index higher in the wt than in Cr-t cells, after 72h of growth in standard medium.

Among the 12886 putative protein-coding genes identified on *T. obliquus* genome, our results showed that in Cr-t strain 229 were differentially hypermethylated and 168 hypomethylated respect to wt. Globally, the hypomethylation, which occurred only in CG context, affect the different gene regions in the same manner, although to a greater extent in both 5'- and 3'- untranslated regions. Conversely, hypermethylation occurred in all the three contexts, mainly in the gene bodies and, to a much lesser extent, in the 3' untranslated regions.

In contrast to what reported for other algae and plants, our results suggest that DNA methylation in *S. acutus* occurs in all the genic regions. As reported in soybean (Rambani

et al., 2015) and *Arabidopsis* (Dowen et al., 2012) plants exposed to various biotic stress methylation/demethylation occurs predominantly in the gene body. The few data found in algae indicate that in *C. reinhardtii* gene bodies are the preferential target of methylation and exons are the only features where no-CG methylation was enriched (Feng et al., 2010). Also in *Chlorella sp.*, CHG methylation was confined to repeats; in the spike moss *S. moellendorffii* very little methylation occurred in gene bodies, whereas its transposable elements were methylated in the CG and to a lesser extent in the CHG and CHH context (Zemach et al., 2010).

Our results indicate that the 32.25% of hypermethylated regions and the 34.38% of hypomethylated regions did not overlap with the hypothetical protein-coding genes, so the methylation in these regions putatively occurred into repeats and transposable elements (TEs). This finding would suggest that the effects of methylation or demethylation occur more at genes level and mainly in the gene body, but also TEs. Methylation of repeats has also been reported in the green algae *Chlamydomonas*, *Chlorella*, and *Volvox* (Feng et al., 2010; Zemach et al., 2010). In *A. thaliana* it has been observed that a distinct chromatin state was adopted by silent TEs, which due to the combination of repressive histone H3 lysine 9 dimethylation (H3K9me2) and elevated DNA methylation levels and other histone modifications (Cokus et al., 2008; Roudier et al., 2011). This repressive heterochromatin of silent TEs is one of four major chromatin states described for the *A. thaliana* genome, and distinct from chromatin of actively transcribed genes, polycomb-repressed genes, and intergenic regions (Roudier et al., 2011). Also, TEs, as well as genes, participate in environmental stress responses through epigenetic variations (Zhang et al., 2019 and references therein). In the same way, we can hypothesize that in *S. acutus* TEs could dynamically regulate the transcription of transposons and proximal genes involved in chromium tolerance, through a remodelling of the chromatin which in turn is regulated by the DNA methylation state. This hypothesis is corroborated by previous evidences that revealed a significantly lower level of heterochromatin in Cr-t than wt strain of *S. acutus* grown in standard medium (Cozza et al., 2016), and a change in the euchromatin percentage that, after 72 h Cr(VI) exposure, became similar in the two strains and significantly higher than heterochromatin (Cozza et al., 2016). Literature data report that metal exposure can induce changes in DNA gene body methylation, as indicated by the modification observed in genes of rice plants exposed to cadmium (Feng et al., 2016). The differences observed in methylation between strains, suggest that changes in DNA methylation in the gene body and promoter regions

occurred in response the long Cr(VI) exposure during the Cr-t strain selection, with the consequent variation in regulation of gene expression. These differential methylated regions (DMRs) of Cr-t vs wt, could have then played a role in the Cr(VI)-tolerance acquiring.

We carried out GO and KEGG enrichment analyses for all the genes overlapping with DRMs to clarify the functional significance of differential methylation. We found a high significant Molecular Function term in hypermethylated genes fraction corresponding to helicase activity followed by several binding activity and transcription regulators; Biological Processes were significantly abundant among the hypermethylated genes including metabolic process, regulation of transcription, and several regulation process. Among hypomethylated genes fraction, we found a higher significant Molecular Function corresponding to ATPases, transporters, hydrolases; finally, for Cellular Component we found cell, membrane and intracellular part categories. Overall, these results indicate that enriched GO terms were related to very different biological processes in *S. acutus* involving different metabolic pathways that could be related to the Cr-tolerance. Recent studies applied high-throughput genomic technologies in order to allow novel insights regarding the mechanisms permitting plants to cope with chromium stress. For example, transcriptome-based gene profiling conducted in *B. napus*, *Raphanus sativus* and rice in response to Cr(VI) stress, show that Cr-responsive genes are involved in binding activity, metabolic process, biological regulation, cellular process and catalytic activity (Gill et al., 2016; Xie et al., 2015; Dubey et al., 2010).

Since changes in DNA methylation at genes level modulate their expression and many of the functional groups identified in this study were in common with those involved in Cr(VI) stress response in other plants, it is possible to hypothesize that the heritable methylation patterns gave rise to new gene combinations that improved resistance to metal-stress in Cr-t strain. Thus, epigenome modifications occurring in stress-related genes through hypomethylation or hypermethylation at DNA specific loci, have an adaptive significance during stress responses and not only persist during exposure to stress but can also be transmitted to the progeny.

Hyper- and hypo-methylated genes were further annotated with KEGG database to deepen insight their gene products and their relationship with gene functions in cellular processes and metabolism. The results showed some enriched pathways that appeared just modulated during Cr(VI) stress in other plants. For example, Photosynthesis - antenna proteins, Carbon fixation in photosynthetic organisms, Biosynthesis of secondary

metabolites, pentose phosphate pathway, Glycolysis/Gluconeogenesis and Glycerophospholipid metabolism were hypo- or hyper-methylated in Cr-t strain; the same pathways were negatively regulated after Cr(VI) exposure in *B. napus* (Gill et al. 2016) and in rice (Dubey et al., 2010). Interestingly in Cr-t strain, photosynthesis and chlorophyll content were not altered after 1 mg/l Cr(VI) treatment, whereas wt decreased its photosynthetic activity (Gorbi et al., 1994). Besides, we observed differential methylation between strains in genes involved in riboflavin metabolism and amino acid biosynthesis, pathways that both resulted differently regulated during chromium exposure in chickpea (Yadav et al., 2019).

Moreover, genes resulting differentially methylated between Cr-t strain *vs* wt belongs to pathways, involved in RNA transport, mRNA surveillance, Spliceosome, Phagosome, Ubiquitin mediated proteolysis, Glycerolipid metabolism, and Pyrimidine metabolism, that Gill et al. (2016) found modulated in the transcriptome profile of two cultivars of *B. napus* with different Cr-tolerance response.

All these data suggest that DNA methylation may be of particular importance in defining signal specificity associated with Cr-tolerance and in reprogramming *S. acutus* primary metabolism occurred throughout prolonged chromium exposure and playing an important role in the resistance mechanism to metal stress.

In our study, particular attention was focused on one of the pathway subject to different methylation and previously indicated as possibly involved in Cr(VI)-tolerance in *S. acutus*: the sulfur uptake/assimilation pathway. Twenty-nine genes, belonging to this pathway, have been characterized and six of them resulted differentially methylated and transcribed in Cr-t strain *vs* wt. In particular, *SaSULTR1, SaARS* and *SaOASTL3* resulted hypomethylated in CG context while *SaSabc* and *SaSAT1* were hypermethylated in CG context and *SaGSH1* hypermethylated in CHG context. Differential methylation in Cr-t, seems thus to impact the basal expression (S-sufficient condition-T0) of genes associated with sulfate pathway. In Cr-t strain we indeed observed an up-regulation of *SaARS* and *SaSULTR1*, genes involved in sulfate uptake, whereas the other differently methylated analysed genes, involved in sulfate assimilation, resulted down-regulated.

The association between promoter region hypomethylation and the upregulation of *SaSULTR1* gene in Cr-t agrees with the literature data. The methylation in the promoter region of gene usually inhibits gene expression (Zilberman et al., 2007). Dynamic DNA methylation, particularly in the promoter region, has been proposed as an important mechanism for regulation of the expression of nutrient-deficiency-responsive genes

(Huang et al., 2019). DNA methylation in the promoter could indeed repress transcription in two way: i) inhibiting the binding of transcriptional activators (thus hindering the activation of gene expression); ii) recruiting the binding of transcriptional repressors to the promoter (thus repressing gene expression) (Domcke et al., 2015). Therefore, demethylation in promoter region could activate gene expression either allowing binding of a transcriptional activator or releasing a transcriptional repressor.

Our data show that also gene body methylation/demethylation affects gene expression. *SaARS, SaSABC, SaSAT1* and *SaGSH1* were hypermethylated in gene body and downregulated in Cr-t. Intriguingly, *SaOASTL3* were hypomethylated and downregulated in Cr-t. Variable gene body methylation has been demonstrated as a general feature of plant and animal genomes although the functions of this kind of methylation are not fully understood. It has been suggested that it might regulate alternative splicing efficiency, prevent aberrant transcriptional initiation from cryptic sites within genes but at the cost of impeding transcriptional elongation (Zilberman et al., 2007; Luco et al., 2010; Maunakea et al., 2010; Li et al., 2012 Regulski et al., 2013). Moreover, inducible and developmentally regulated genes generally do not have CG gene body methylation (Aceituno et al., 2008; Coleman-Derr and Zilberman 2012). On the other hand, positive correlation between gene expression and gene body methylation was also reported (Lister et al., 2008; Feng et al., 2010; Zemach et al., 2010). Analyses conducted in rice, showed that a complicated relationship occurs between gene body methylation level and gene expression. Initially gene expression increases with methylation levels, but after a certain point, heavy gene-body methylation appears to repress gene expression; and consequently, genes with moderate levels of body methylation tend to have the highest expression levels (Li et al., 2012 and references therein). Finally, the heterogeneous effect of body methylation on gene expression could be linked to the extent of methylation in the target genes. Moderate methylation tends to enhance gene expression, whereas low or high methylation tends to inhibit gene expression (Wang et al., 2013).

The different methylation and expression level of genes involved in S uptake/assimilation in the Cr-t, suggest that epigenetic mechanisms play an important role in the modulation of sulfur pathway that in its turn is involved in metal tolerance mechanism.

The high expression of *SaARS* and *SaSULTR1,* codifying for periplasmatic arylsulfatase and Sulfate transporter ($H^+/SO_4^{2-}$ family) respectively, lets hypothesize a constitutive higher sulfur uptake in Cr-t than wt. Conversely, the low expression of genes involved in sulfur assimilation such as *SaSabc* (chloroplast sulfate ABC transporter subunit),

*SaOASTL3* (O-acetylserine(thiol)-lyase), *SaSAT1* (Serine acetyltransferase) and *SaGSH1* (γ-Glutamylcysteine synthetase) would indicate a putative reduced sulfur assimilation in Cr-t. This latter hypothesis is in contrast with data already reported for the Cr-t strain showing a higher Cys content (Gorbi et al. 2007) and a higher efficiency in Cys production (Sardella et al. 2019) than wt. Moreover, in plants Cys synthesis can occur in different cell compartments, as indicated by the different isoforms of the enzymes (SAT and OASTL) involved in the formation of the Cysteine Synthase Complex (CSC), and this configure a complex regulation network of the assimilation pathway, tightly regulated through the interaction between different components which heavily affect each other activity. Many evidences indicate that Cys biosynthesis is regulated in a compartment-specific manner: the mitochondrion would be responsible for providing most of the OAS in the cell, while cytosol would represent the major site of cysteine production (Wirtz and Hell 2007, Haas et al. 2008, Heeg et al. 2008, Watanabe et al. 2008a, Watanabe et al. 2008b). Multiple isoforms of OASTL with a possible different cell localization were found in algae (Carfagna et al., 2011) and the recent paper of Sardella et al. (2019) suggests that a cytosolic mechanism, maybe involving the OASTL isoform located in this compartment, may be involved in the higher Cys production/S assimilation of the Cr-t strain. Four OASTL isoforms are present in *S. acutus* genome and the differently methylated *SaOASTL3* isoform is homologous to OASTL3 of *C. reinhardtii* (XP_001703301.1) which is ambiguously predicted to be chloroplast targeted by homology and mitochondrial targeted by target-P analysis. We are however not aware of which role the differently methylated *SaSAT1* and *SaOASTL3* play in sulfate assimilation in *S. acutus*. It is thus difficult to argue from the analysis of single isoforms the functioning and regulation of such a complex pathway and this aspect should deserve further investigation.

On the other hand the hypothesis of a higher sulfur uptake in the Cr-t strain is corroborated by detailed analysis of expression in response to Cr-exposure and/or S-starvation performed for the *SaSULTR1, SaSULTR2*, *SaSULP1* and *SaSULP2* genes (the latter two coding channel subunits of chloroplast sulfate ABC transporter).

The differences in *SULTRs* expression, enlightened by absolute quantification of these genes through RT-qPCR, in response to Cr-treatment and/or S-starvation, together with the different uptake of both S and Cr(VI) (Sardella et al., 2019), suggested a distinct sulfate affinity between *SaSULTR1* and *SaSULTR2*.

*SaSULTR2* is constitutively expressed in wt control cells in S-sufficient conditions and moderately increased its level after S starvation, while *SaSULTR1* expression was strongly induced by S-deprivation and rapidly reduced after S-resupply.

Moreover, in S-sufficient conditions, *SaSULTR1* expression was induced by both the Cr(VI) concentrations, whereas *SaSULTR2* expression was repressed by the lower Cr(VI) concentration and activated at 2 mg Cr(VI)/l.

Altogether, these informations indicate that *SaSULTR1* is expressed to cope the nutritional stress and that chromium induces a sort of S-starvation effect as suggested by many Authors (Marzluf, 1970; Paietta, 1990; Perez-Castineira et al., 1998; Pereira et al., 2008). Interestingly a different behaviour of these transporters has been observed in the Cr-t strain that, in S-sufficient conditions, expressed *SaSULTR2* at lower level than the wt but it apparently compensated its sulfur requirement trough the constitutive expression of *SaSULTR1*. Previous works indicated that sulfur uptake in +S medium is similar in the two *S. acutus* strains or even higher in the Cr-t (Gorbi et al 2007; Sardella et al.2019). However, as shown in table 3.5.3, this result is apparently obtained by Cr-t with a lesser number of transporters. The wt indeed expressed a higher copy number of *SaSULTR2* encoding the low affinity sulfate transporter than Cr-t (500 ± 54 *vs* 31 ± 8), whereas this latter provided S uptake trough the *SaSULTR1* activation encoding the putatively high affinity transporter (81 ± 9) not expressed in the wt. This different transporter ratio likely allows the Cr-t a better efficiency in S-uptake with the further advantage in sparing energy for transporter construction. After 24h medium renewal, both strains increased the transporter numbers essentially by inducing the low affinity transporter and leaving unchanged the *SaSULTR1* transcription (Tab. 3.5.3). Both genes are clearly inducible by S-starvation but *SaSULTR1* transcription definitely overwhelm *SaSULTR2* expression, thus sulfur uptake in S-replete cells is due to the overlapping of the two transporters activities.

This hypothesis is in agreement with Marieschi et al (2015) which already speculated that in the wt cells, the reduction in chromium uptake after S-deprivation may occur through the induction of high affinity sulfate transporters, which presumably are constitutively active in the Cr-t strain and can account for the different Cr(VI) sensitivities of the two strains.

It is interesting to note that in S-replete Cr-t cells the transcription of both *SaSULTR1* and *SaSULTR2* is silenced more slowly than in the wt indicating a different regulation in the two strains linked to a different inner sulfur perception and/or exploitation. The slower

silencing of *SULTRs* genes apparently ensures the Cr-t strain to take the advantage of a prolonged sulfur uptake when this element is available in the medium.

Both genes were modulated by chromium exposure in S-sufficient conditions, albeit in different manner in the two strains. At the lower chromium concentration, the Cr-t maintained similar level of expression as in control cell whereas wt slowly induced the *SaSULTR1* transcription for the putatively high affinity transporter and reduced the expression of *SaSULTR2*. At 2 mg Cr(VI)/l both strains induced the transcription of both genes. The wt responded by moderately increasing *SULTRs* expression after 24 h (2- and 10-fold respectively for *SaSULTR2* and *SaSULTR1*) and returning to basal levels thereafter. The Cr-t induced the transcription of both genes (6- and 8.3-fold respectively for *SaSULTR2* and *SaSULTR1,* at 24 h exposure*)* which continued to increase even after 48 h, reaching levels 10- and 22-fold as the control cells.

As reported by Sardella et al. (2019) Cr-t S-sufficient cells, exposed to 2 mg Cr(VI)/l, accumulated an inner chromium amount double than wt cells, whose chromium uptake capacity seemed saturated at 1 mg Cr(VI)/l. The ability to cope a more elevated inner chromium concentration, showed by the Cr-t, is thus likely related to the different transporter regulation leading to a higher sulfur availability and an enhanced cell defence capacity.

So, the two strains likely adopt two different strategies to cope Cr(VI) in S-sufficient conditions: the wt by silencing the constitutive transporter *SaSULTR2* to reduce chromium entrance, the Cr-t instead, enhancing S uptake by inducing not only the high affinity transporter *SaSULTR1,* but also *SaSULTR2*. It is important to recall that 1 mg Cr(VI)/l and 2 mg Cr(VI)/l represented the Lowest Observed Effect Concentration (LOEC) for wt and Cr-t strain, respectively (Gorbi et al., 2007). Thus, at the lowest Cr(VI) concentration analysed, wt was affected by metal exposure and at the highest concentration, also Cr-t strain was affected by metal stress. Moreover, it is well known that the toxic effects of 1 mg Cr(VI)/l treatment was more evident in the wt strain than in the Cr-t and that exposure to 2 mg Cr(VI)/l as induced marked changes at the cellular and ultrastructural level in the cells of both strains (Cozza et al., 2016).

S-deprivation induced a strong activation of *SaSULTR1* in both strains and no differences were observed between control and chromium exposed cells, while *SaSULTR2* in this nutritional condition, seemed negatively modulated by chromium in the wt and activated at the LOEC concentration in the Cr-t strain, which once again showed a better capacity in enhancing cell defence capacity.

The strong *SaSULTR1* activation after pre-culture in S-deprived medium and its silencing after medium renewal is likely related to the transient tolerance increase observed in both strains after a period of S-starvation (Gorbi et al 2007, Marieschi et al. 2015, Sardella et al., 2019). This hypothesis is strengthened by the increase in sulfur (reaching significantly higher level in the Cr-t than in the wt strain) and the contemporary decrease in chromium uptake observed in both strains following S-starvation (Sardella et al.,2019). The Authors observed that the stoichiometric ratio (S/Cr) in/out varied from two sulfur nmoles every one nmole of chromium in S-sufficient cells to six nanomoles in S-replete cells of both strains, suggesting that the higher sulfur accumulation during recovery after starvation was due to the induction of higher affinity sulfate transporters rather than to a simple increase in transporter number.

The induction of high affinity sulfate transporters (Yildiz et al., 1994; Hawkesford, 2003; Zhang et al., 2004; Pootakham et al., 2010; Gigolashvili and Kopriva, 2014 and references therein) and the increase in sulfate transporter number during acclimation to S-starvation are well documented both in vascular plant and in algae (Green and Grossman, 1988; Appenroth et al., 2008). In *C. reinhardtii* high affinity and high capacity sulfate transporters are activated by S-starvation and function with a mechanism based on secondary active transport supported by a proton gradient generated across the plasmalemma (Yildiz et al. 1994).

Sulfate uptake and assimilation are tightly regulated in a demand-driven manner through a complex network of coordinated responses which involve transcriptional and post-transcriptional mechanisms as well as protein-protein interactions. OASTL indeed interacts with SAT in the formation of the CSC and can also affect sulfate uptake and Cys synthesis via direct interaction with the STAS domains of SULTRs transporters (Shibagaki and Grossman, 2010).

The whole pathway is activated, through positive feedback induced by the accumulation of OAS (Smith et al, 1997) and repressed, through negative feedback, by GSH or Cys (Lappartient and Touraine, 1996; Bolchi et al. 1999; Davidian and Kopriva 2010). Emerging evidence suggests that also epigenetic regulation of gene expression plays an important role in the adaptive response to S deficiency and the maintenance of S homeostasis (Huang et al., 2016). As reported in literature, in the *more sulfur accumulation1* (*msa1-1*) mutant of *A. thaliana*, a large number of differentially methylated genes were found respect to wt, even though the detailed mechanism underlying the opposite effect of *msa1* on genome-wide DNA methylation between roots

and shoots is unclear. Several genes involved in glucosinolate and anthocyanin metabolisms as well as S-deficiency responsive genes are differentially methylated in *msa1*, including *SULTR1;1*, *SULTR1;2*, *APR3* and *ATPS4* (Huang et al., 2016). Moreover, Huang et al. (2016) found a genomic region upstream of the sulfur responsive element (SURE) in the promoter of SULTR1;1 (essential for the S deficiency response (Maruyama-Nakashita et al., 2005) hyper-methylated under S sufficient and hypo-methylated under S deficiency condition (Huang et al., 2016). This was correlated with the low expression level of SULTR1;1 under S sufficient condition and its strong induction by S deficiency. In the *msa1-1* mutant, the upstream region of SURE in the promoter of SULTR1;1 is hypo-methylated and is associated with the increase of its expression level and the consequent increase of S levels in shoots (Huang et al., 2016).

In *Chlamydomonas* some sulfur availability signalling proteins have been identified, including SAC1, a plasma membrane protein (similar to $SO_4^{2-}$ transporters) that appears to function as a sensor of $SO_4^{2-}$ levels. When no $SO_4^{2-}$ is bound to SAC1, the serine-threonine kinase SNRK2.1 is activated and elicits transcriptional activation of many S-deprivation responsive genes. When the environment is S-replete, the serine-threonine kinase SNRK2.2 (also known as SAC3) causes complete repression of S-responsive gene expression, possibly by phosphorylating SNRK2.1 and inhibiting its activity. Induction of High Affinity Sulfate Transporters (HASTs) during S deprivation is SAC1-dependent, although there is some increase in HAST activity in the sac1 mutant that may represent post-translational regulation. Moreover, it is known that SNRK2.2 kinases have an epistatic relationship with SNRK 2.1 kinases, and they have a negative modulation on gene expression of SNRK 2.1 kinases (Moseley et al., 2009). In higher plants, SNRK2s family members are involved in regulation of plant tolerance to abiotic stresses (Kulik et al. 2011). Previous studies demonstrated that SNRK2 family include ten members in *Arabidopsis* and rice (Boudsocq et al., 2004). All of them, except SNRK2.9 in *Arabidopsis*, play a role under different stress conditions such as cadmium, drought, and salinity (Kulik et al., 2011).

Thus, it is also possible to hypothesize a similar control mechanism of sulfur uptake pathways in *S. acutus* with a different S perception and/or a disturbed feedback mechanism in the Cr-t strain. Previous works indicated that the Cr-t strain has always a higher Cys level than the wt and higher GSH level when exposed to metals (Gorbi et al., 2007; Sardella et al., 2019). It is thus more conceivable that positive feedback is

differently regulated in the two strains, maybe through a more elevated OAS production/accumulation, as suggested by Sardella et al. (2019).

Clearly the sulfur uptake picture in *S. acutus* is not complete without the description of *SLTs* gene expression. The retention of both $Na^+/SO_4^{2-}$ and $H+/SO_4^{2-}$ transporter types has been interpreting as the capacity of algae to survive to different environmental conditions (Pootakham et al., 2010). SLT transporters catalyse a $Na^+/SO_4^{2-}$ antiport (Gonzalez-Ballester and Grossman, 2009) and may be responsible for the majority of $SO_4^{2-}$ uptake when the pH is high and when it is more efficient to use $Na^+$ as a counter ion (Pootakham et al., 2010). In *S. acutus*, after the 4-days culture an increase in pH (ranging between 8.08 and 9.4) were observed, more pronounced in S-replete than S-sufficient condition (Marieschi et al., 2015). The involvement of SLTs transporters, especially after basification of the culture medium, can thus putatively be included in the S-deprivation responses.

Three *SLTs* genes are present in *C. reinhardtii* genome, with different substrate affinity, and three accessions were found in databank also for *R. subcapitata*, specie more closely related to *Scenedesmus*. Thus, the same number of SLT transporter has likely to be identified in *S. acutus*. To date, we have partially identified three sequences codifying for putative SLT transporters: *SaSLT1* and two sequences, apparently arranged in tandem on the same *T. obliquus* scaffold, for which is not clear the correspondence with one or two proteins. This gene organization seems analogue to that found in *C. reinhardtii* genome, in which *SLT2* and *SLT3* are tandemly arranged in a head-to-tail orientation with a partial overlapping of the 3'- untranslated region of one gene with the 5'- untranslated region and the first exon of the other. These two genes show different sulfate affinity and strong interfere in one each other transcription. The difficult we encountered in the identification of these two latter *SLT* genes has unfortunately till now made impossible the expression analysis of the whole plasma membrane transporters and limited the comprehension of their involvement in maintaining the homeostasis of S uptake.

It has been reported that, after S-starvation, Cys production was strongly enhanced in both wt and Cr-t strain (Gorbi et al., 2007; Sardella et al., 2019). Albeit in plants the major amount of Cys seems to be produced in the cytosol, (Haas et al., 2008; Heeg et al., 2008; Krueger et al., 2009) sulfate reductive assimilation in green algae are apparently exclusively localized in chloroplasts (Allmer 2006; and Ravina et al., 2002). Once $SO_4^{2-}$ is transported into the cell, it must be routed into the plastids for reductive assimilation, through an ABC-type chloroplast envelope-localized holocomplex.

A peculiar expression of both *SaSulP1* and *SaSulP2* was observed in the two strains in response to Cr(VI)-exposure, strengthening the hypothesis that the two strains cope with chromium stress in a different manner and have a different basal sulfur request. Globally, in Cr-t strain, the expression of these genes increased upon Cr-treatment when probably more sulfur was required in the chloroplast for the synthesis of sulfur-containing molecules with the consequent increased capacity to cope with intracellular chromium, either through chelation and compartmentalization or through an enhanced antioxidant response. Instead, wt decreased expression upon Cr-treatment seemed directly linked to the decrease of sulfate uptake. Besides, a negative correlation would seem to exist between Cys levels and the modulation of *SulPs* expression. In fact, at the end of the preculture in +S medium (T0) and at each recovery time, Cys content in control algae was significantly higher in the Cr-t strain than in the wt. In the wt, Cys production increased only in Cr(VI)-supplemented cells whereas in Cr-t strain Cys level was high even in the control and not significantly enhanced by chromium treatment (Sardella et al., 2109).

Upon S deprivation, *SaSulP1* and *SaSulP2* expression increased significantly in both strains. These results are in agreement with literature data indicating a specifically induction of *C. reinhardtii* putative SulP1 and SulP2 subunit belonging chloroplast sulfate transporter, like those of their cyanobacterial counterpart (CysT, CysW), in response to sulfur starvation and not upon other nutrient stresses (Lindberg and Melis, 2008 and references therein).

The heat map analysis suggests correlations between changes of *SULTRs* and *SulPs* expression and different grown condition studied. In both S-sufficient and S-replete conditions, the wt strain was clearly separated from Cr-t. Moreover, the Cr(VI) treated samples generate a sub-cluster separate from controls, regardless of the treatment duration. This means the two strains had a different response in S uptake and assimilation in response to Cr exposure. Interestingly, in S-sufficient condition, wt strain treated with 1 mg Cr(VI)/l for 24 hours clustered in Cr-t group inasmuch wt cells, upon this treatment, had a similar expression trend to Cr-t, although with lower expression levels of Cr-t cells. In a specular way, in S-replete condition, upon 2 mg Cr(VI)-treatment, wt clustered together Cr-t. Probably this happens because also in this case, wt cells expressed gene S uptake/assimilation -related in same manner of Cr-t cells since in S-replete conditions both strains “shift” their LOEC and the wt has a behavior more similar to Cr-t (Marieschi et al., 2015).

CHAPTER

5

# *Conclusions*

The analyses performed in this work clearly show that, under a Cr(VI) treatment, the Cr-t strain of *S. acutus*, exhibits a different response compared to the wt, globally resulting into a better metal detoxification and ability to cope a higher Cr(VI) inner content.. The reason of such behaviour likely relies on a higher genome plasticity of Cr-t, conferred by a different DNA methylation state. Despite our data show that the level of DNA methylation of *S. acutus* is low, as found in other green algae, it allows the Cr-t strain to better respond to Cr(VI) toxicity through an early modulation of gene expression. Namely, pathways relevant for growth and interaction with environment have been found to be differentially methylated in Cr-t compared to the wt strain. However, the emerging picture suggests that, under a prolonged heavy metal exposure, algae activity is directed to enhance and/or maintain the signal levels and response that are relevant during stress to sustaining the growth, through a different DNA methylation pattern as "stress memory".

In this context, sulfate uptake/assimilation pathway plays a pivotal role resulting in an improved cell defence capacity and at the same time, decreasing chromium uptake. Moreover, the expression of genes associated with this pathway seems to be affected by differential methylation in the different DNA contexts and different regions of genes.

More specifically, *SaARS* gene (codifying for periplasmatic arylsulfatase) and *SaSULTR1* gene (codifying a high affinity sulfate transporter of the $H^+/SO_4^{2-}$ family) were expressed in S-sufficient conditions only in the Cr-t strain allowing to hypothesize a constitutive higher sulfur uptake in this strain respect to the wt. Furthermore, in the Cr-t strain, *SaSULTR1* induction, due to hypomethylation on promoter of this gene, overlaps to *SaSULTR2* expression (codifying a low affinity sulfate transporter of the $H^+/SO_4^{2-}$ family) supporting the evidence of a different S-perception or S-exploitation in this strain. Conversely, the low expression of genes involved in sulfur assimilation (*SaSabc, SaOASTL3, SaSAT1* and *SaGSH1)* due to hypermethylation in the gene body, strengthens the hypothesis of a different regulation of sulfur assimilation in Cr-t strain. Since regulation of this pathway involve a complex network of interactions between different enzyme isoforms located in different cell compartments, this aspect deserves further investigation.

This study also shows evidence that the two strains likely adopt two different strategies to cope Cr(VI) in S-sufficient conditions: the wt by silencing the constitutive transporter SaSULTR2 to reduce chromium entrance, the Cr-t by inducing the high affinity transporter SaSULTR1 to enhance S uptake. So, Cr(VI) exposure induces a reduction in

wt and an increase in Cr-t strain in S assimilation, strengthening the hypothesis that the two strains cope with chromium stress in a different manner and have a different basal sulfur request.

Finally, the transient tolerance increase observed after 3-days of S-starvation, resulting in an enhanced sulfur uptake and assimilation as well an improved cell defense capacity, is putatively due by the induction of expression of *SaSULTR1* gene which probably encodes for a high affinity sulfate transporter. A graphical summary of the key results is reported in Fig. 5.1.

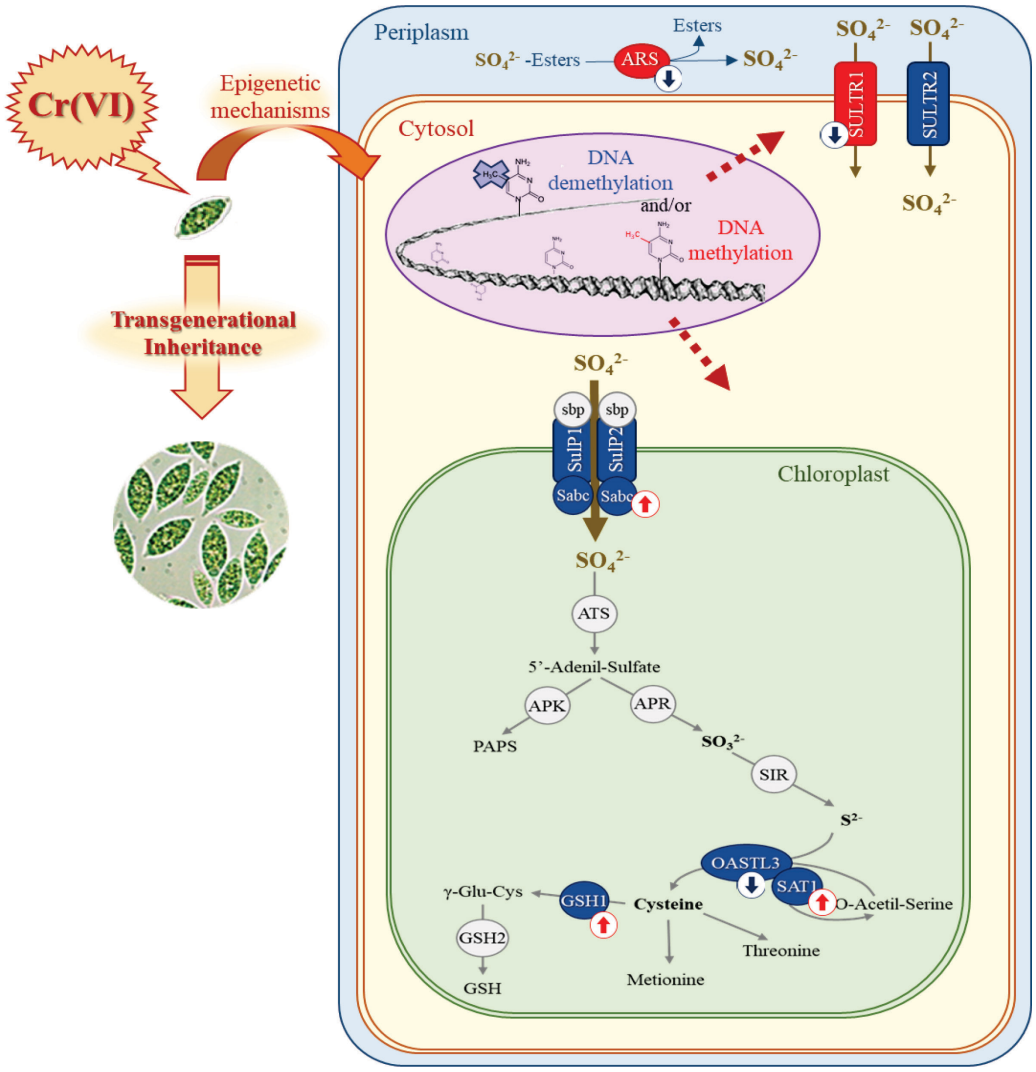


**Figure 5.1** - **Epigenomic marks of resistance to metal stress in Cr-t strain**. Adaptative responses to Cr(VI) stress occur through epigenomic modifications in sulfur uptake/assimilation pathway genes; hypomethylation or hypermethylation at DNA specific loci are transmitted to the Cr-t progeny. In the figure are reported the ⬇ hypomethylated, ⬆ hypermethylated, ● downregulated and ● upregulated genes in Cr-t *vs* wt.

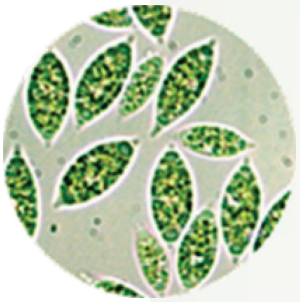

# References

Abd-El-Monem, H., Corradi, M.G., & Gorbi, G. (1998). Toxicity of copper and zinc to two strains of Scenedesmus acutushaving different sensitivity to chromium. Environmental and Experimental Botany, 40: 59-66. doi: 10.1016/S0098-8472(98)00021-5

Aceituno, F. F., Moseyko, N., Rhee, S. Y., & Gutiérrez, R. A. (2008). The rules of gene expression in plants: organ identity and gene body methylation are key factors for regulation of gene expression in Arabidopsis thaliana. *BMC genomics*, *9*, 438. doi:10.1186/1471-2164-9-438

Aina, R., Sgorbati, S., Santagostino, A., Labra, M., Ghiani, A., & Citterio, S. (2004). Specific hypomethylation of DNA is induced by heavy metals in white clover and industrial hemp. *Physiologia Plantarum*, *121*(3), 472–480. https://doi.org/10.1111/j.1399-3054.2004.00343.x

Akalin, A., Kormaksson, M., Li, S., Garrett-Bakelman, F. E., Figueroa, M. E., Melnick, A., & Mason, C. E. (2012). MethylKit: a comprehensive R package for the analysis of genome-wide DNA methylation profiles. *Genome Biology*, *13*(10). https://doi.org/10.1186/gb-2012-13-10-R87

Akgul, F., Tuney Kizilkaya, I., Akgul, R., & Erdugan, H. (2017). Morphological and Molecular Characterization of Scenedesmus-Like Species from Ergene River Basin (Thrace, Turkey). *Turkish Journal of Fisheries and Aquatic Sciences, 17(3).* doi:10.4194/1303-2712-v17_3_17

Ali, S., M. A. Farooq, T. Yasmeen, S. Hussain, M. S. Arif, F. Abbas, S. A. Bharwana, and G. Zhang 2013. The influence of silicon on barley growth, photosynthesis and ultra-structure under chromium stress. *Ecotoxicology and Environmental Safety*, 89:66–72. DOI: 10.1016/j.ecoenv.2012.11.015

Allmer, J., Naumann, B., Markert, C., Zhang, M., & Hippler, M. (2006). Mass spectrometric genomic data mining: Novel insights into bioenergetic pathways in *Chlamydomonas reinhardtii*. *Proteomics*, 6(23):6207–20. https://doi.org/10.1002/pmic.200600208

Andosch, A., Höftberger, M., Lütz, C., & Lütz-Meindl, U. (2015). Subcellular Sequestration and Impact of Heavy Metals on the Ultrastructure and Physiology of the Multicellular Freshwater Alga Desmidium swartzii. *International journal of molecular sciences*, *16*(5), 10389–10410. doi:10.3390/ijms160510389

Angers, B., Castonguay, E., & Massicotte, R. (2010). Environmentally induced phenotypes and DNA methylation: how to deal with unpredictable conditions until the next generation and after. *Molecular Ecology*, *19*(7), 1283–1295. https://doi.org/10.1111/j.1365-294X.2010.04580.x

Appenroth, K. (2008). Modification of chromate toxicity by sulphate in duckweeds (Lemnaceae). *Aquatic Toxicology, 89(3), 167–171.* doi:10.1016/j.aquatox.2008.06.012

Ashraf, A., Bibi, I., Niazi, N. K., Ok, Y. S., Murtaza, G., Shahid, M., … Mahmood, T. (2016). Chromium(VI) sorption efficiency of acid-activated banana peel over organo-montmorillonite in aqueous solutions. *International Journal of Phytoremediation, 19(7), 605–613.* doi:10.1080/15226514.2016.1256372

Babinger, P., Völkl, R., Cakstina, I., Maftei, A., & Schmitt, R. (2007). Maintenance DNA methyltransferase (Met1) and silencing of CpG-methylated foreign DNA in Volvox carteri. *Plant Molecular Biology*, *63*(3), 325–336. https://doi.org/10.1007/s11103-006-9091-1

Becker, C., Hagmann, J., Müller, J., Koenig, D., Stegle, O., Borgwardt, K., & Weigel, D. (2011). Spontaneous epigenetic variation in the Arabidopsis thaliana methylome. *Nature*, *480*(7376), 245–249. https://doi.org/10.1038/nature10555

Bernatavichute, Y. V, Zhang, X., Cokus, S., Pellegrini, M., & Jacobsen, S. E. (2008). Genome-wide association of histone H3 lysine nine methylation with CHG DNA methylation in Arabidopsis thaliana. *PLoS ONE*, *3*(9). https://doi.org/10.1371/journal.pone.0003156

Blevins, T., Podicheti, R., Mishra, V., Marasco, M., Wang, J., Rusch, D., … Pikaard, C. S. (2015). Identification of pol IV and RDR2-dependent precursors of 24 nt siRNAs guiding de novo DNA methylation in Arabidopsis. *ELife*, *4*, 1–22. https://doi.org/10.7554/eLife.09591

Bloem, E., Haneklaus, S., & Schnug, E. (2015). Milestones in plant sulfur research on sulfur-induced-resistance (SIR) in Europe. *Frontiers in plant science*, *5*, 779. doi:10.3389/fpls.2014.00779

Bohnert, H. J., Ostrem, J. A., Cushman, J. C., Michalowski, C. B., Rickers, J., Meyer, G., … Schmitt, J. M. (1988). *Mesembryanthemum crystallinum*, a higher plant model for the study of environmentally induced changes in gene expression. *Plant Molecular Biology Reporter*, *6*(1), 10–28. https://doi.org/10.1007/BF02675305

Bolchi, A., Petrucco, S., Tenca, P.L., Foroni, C., Ottonello, S. (1999). Coordinate modulation of maize sulfate and ATP sulfurylase mRNAs in response to variations in sulfur nutritional status: stereospecific down-regulation by cysteine. Plant Mol. Biol. 39,527–537. DOI:10.1023/a:1006148815106

Boudsocq, M., Barbier-Brygoo, H., & Laurière, C. (2004). Identification of nine sucrose nonfermenting 1-related protein kinases 2 activated by hyperosmotic and saline stresses in Arabidopsis thaliana. *Journal of Biological Chemistry*, *279*(40), 41758–41766. https://doi.org/10.1074/jbc.M405259200

Boyko A, Kovalchuk I. 2008. Epigenetic control of plant stress response. Environmental and Molecular Mutagenesis 49: 61–72. DOI: 10.1002/em.20347

Brauer, S.L., Hneihen, A.S., McBride, J.S., Wetterhahn, K.E., 1996. Chromium(VI)forms thiolate complexes with γ-glutamylcysteine, N-acetylcysteine, cysteineand methyl ester of N-acetylcysteine. Inorg. Chem. 35, 373–381. https://doi.org/10.1021/ic941452d

Brauer, S. L., & Wetterhahn, K. E. (1991). Chromium(VI) forms a thiolate complex with glutathione. *Journal of the American Chemical Society, 113(8), 3001–3007.* doi:10.1021/ja00008a031

Breuer, G., Lamers, P. P., Martens, D. E., Draaisma, R. B., & Wijffels, R. H. (2012). The impact of nitrogen starvation on the dynamics of triacylglycerol accumulation in nine microalgae strains. *Bioresource Technology, 124, 217–226.* doi:10.1016/j.biortech.2012.08.003

Brunold, C., & Schiff, J. A. (1976). Studies of sulfate utilization of algae: 15. Enzymes of assimilatory sulfate reduction in euglena and their cellular localization. *Plant physiology*, *57*(3), 430–436. doi:10.1104/pp.57.3.430

Cao, X., Aufsatz, W., Zilberman, D., Mette, M. F., Huang, M. S., Matzke, M., & Jacobsen, S. E. (2003). Role of the DRM and CMT3 Methyltransferases in RNA-Directed DNA Methylation. *Current Biology*, *13*(24), 2212–2217. https://doi.org/10.1016/j.cub.2003.11.052

Carfagna, S., Salbitani, G., Vona, V., & Esposito, S. (2011). Changes in cysteine and O-acetyl-l-serine levels in the microalga Chlorella sorokiniana in response to the S-nutritional status. *Journal of Plant Physiology, 168(18), 2188–2195.* doi:10.1016/j.jplph.2011.07.012

Carreres, B. M., de Jaeger, L., Springer, J., Barbosa, M. J., Breuer, G., van den End, E. J., … Martens, D. E. (2017). Draft genome sequence of the oleaginous green alga Tetradesmus obliquus UTEX 393. *Genome Announcements*, *5*(3), 1–2. https://doi.org/10.1128/genomeA.01449-16

Cerutti H., Johnson A. M., Gillham N. W., Boynton J. E. (1997) Epigenetic silencing of a foreign gene in nuclear transformants of Chlamydomonas. Plant Cell 9: 925–945

Cervantes, C., Campos-García, J., Devars, S., Gutiérrez-Corona, F., Loza-Tavera, H., Torres-Guzmán, H. C., & Moreno-Sánchez R. (2001). Interactions of chromium with microorganisms and plants, *FEMS Microbiology Reviews*, 25(3), 335–347, https://doi.org/10.1111/j.1574-6976.2001.tb00581.x

Chinnusamy, V., & Zhu, J.-K. (2009). Epigenetic regulation of stress responses in plants. *Current Opinion in Plant Biology*, *12*(2), 133–139. https://doi.org/10.1016/j.pbi.2008.12.006

Cobbett, C., & Goldsbrough, P. (2002). PHYTOCHELATINS AND METALLOTHIONEINS: Roles in Heavy Metal Detoxification and Homeostasis. *Annual Review of Plant Biology* 53(1):159–82. DOI: 10.1146/annurev.arplant.53.100301.135154

Cokus, S. J., Feng, S., Zhang, X., Chen, Z., Merriman, B., Haudenschild, C. D., … Jacobsen, S. E. (2008). Shotgun bisulphite sequencing of the Arabidopsis genome reveals DNA methylation patterning. *Nature,* 452(7184), 215–219. https://doi.org/10.1038/nature06745

Coleman-Derr, D., & Zilberman, D. (2012). Deposition of Histone Variant H2A.Z within Gene Bodies Regulates Responsive Genes. *PLOS Genetics*, *8*(10), e1002988. Retrieved from https://doi.org/10.1371/journal.pgen.1002988

Corradi, M. G., Gorbi, G., Ricci, A., Torelli, A., & Bassi, M. (1995). Chromium-induced sexual reproduction gives rise to a cr-tolerant progeny in scenedesmus acutus. *Ecotoxicology and Environmental Safety*, *32*(1), 12–18. https://doi.org/10.1006/eesa.1995.1079

Cozza, D., Torelli, A., Veltri, A., Ferrari, M., Marieschi, M., & Cozza, R. (2016). Ultrastructural features, chromium content and in situ immunodetection of 5-methyl-cytosine following Cr (VI) treatment in two strains of Scenedesmus acutus M. (Chlorophyceae) with different chromium sensitivity. *European Journal of Phycology*, *51*(3), 294–306. https://doi.org/10.1080/09670262.2016.1157902

Davidian, J. C., & Kopriva, S. (2010). Regulation of sulfate uptake and assimilation - The same or not the same? *Molecular Plant*, *3*(2), 314–325. https://doi.org/10.1093/mp/ssq001

de Cambiaire, J. C., Otis, C., Lemieux, C., & Turmel, M. (2006). The complete chloroplast genome sequence of the chlorophycean green alga Scenedesmus obliquus reveals a compact gene organization and a biased distribution of genes on the two DNA strands. *BMC Evolutionary Biology*, *6*, 1–15. https://doi.org/10.1186/1471-2148-6-37

de Hostos, E. L., Togasaki, R. K., & Grossman, A. (1988). Purification and biosynthesis of a derepressible periplasmic arylsulfatase from Chlamydomonas reinhardtii. *The Journal of cell biology*, *106*(1), 29–37. doi:10.1083/jcb.106.1.29

Del Fabbro, C., Scalabrin, S., Morgante, M., & Giorgi, F. M. (2013). An extensive evaluation of read trimming effects on Illumina NGS data analysis. *PloS one*, *8*(12), e85024. doi:10.1371/journal.pone.0085024

Ding, G., Jin, Z., Han, Y., Sun, P., Li, G., & Li, W. (2019). Mitigation of chromium toxicity in Arabidopsis thaliana by sulfur supplementation. *Ecotoxicology and Environmental Safety*, *182*(June), 109379. https://doi.org/10.1016/j.ecoenv.2019.109379

Diwan, H., Khan, I., Ahmad, A., Iqbal, M. (2010). Induction of phytochelatins and antioxidant defence system in *Brassica juncea* and *Vigna radiata* in response to chromium treatments. *Plant Growth Regul*. 61, 97–107. https://doi.org/10.1007/s10725-010-9454-0

Dotaniya, M. L., Das, H., & Meena, V. D. (2014). Assessment of chromium efficacy on germination, root elongation, and coleoptile growth of wheat *(Triticum aestivum L.*) at different growth periods. *Environmental Monitoring and Assessment, 186(5), 2957–2963.* doi:10.1007/s10661-013-3593-5

Dowen, R. H., Pelizzola, M., Schmitz, R. J., Lister, R., Dowen, J. M., Nery, J. R., … Ecker, J. R. (2012). Widespread dynamic DNA methylation in response to biotic stress. *Proceedings of the National Academy of Sciences*, *109*(32), E2183–E2191. https://doi.org/10.1073/pnas.1209329109

Du, J., Johnson, L. M., Jacobsen, S. E., & Patel, D. J. (2015). DNA methylation pathways and their crosstalk with histone methylation. *Nature reviews. Molecular cell biology*, *16*(9), 519–532. doi:10.1038/nrm4043

Dubey, S., Misra, P., Dwivedi, S., Chatterjee, S., Bag, S. K., Mantri, S., … Tuli, R. (2010). Transcriptomic and metabolomic shifts in rice roots in response to Cr (VI) stress, (Vi).

Dyachenko, O. V., Zakharchenko, N. S., Shevchuk, T. V., Bohnert, H. J., Cushman, J. C., & Buryanov, Y. I. (2006). Effect of hypermethylation of CCWGG sequences in DNA of *Mesembryanthemum crystallinum* plants on their adaptation to salt stress. *Biochemistry (Moscow)*, *71*(4), 461–465. https://doi.org/10.1134/S000629790604016X

Dzhambazov, B., Belkinova, D., & Mladenov R. (2002). Sind Scenedesmus obtusiusculus Chod. und Scenedesmus obliquus (Turp.) Kütz. (Chlorophyta, Chlorococcales) verschiedene Arten?. *Arch. Hydrobiol./Algolog. Studies 106: 141–150.*

Ebbs, M. L., Bartee, L., & Bender, J. (2005). H3 Lysine 9 Methylation Is Maintained on a Transcribed Inverted Repeat by Combined Action of SUVH6 and SUVH4 Methyltransferases. *Molecular and Cellular Biology*, *25*(23), 10507–10515. https://doi.org/10.1128/mcb.25.23.10507-10515.2005

Emamverdian, A., Ding, Y., Mokhberdoran, F., & Xie, Y. (2015). Heavy metal stress and some mechanisms of plant defense response. *Scientific World Journal*, *2015*, 7–9. https://doi.org/10.1155/2015/756120

Emanuelsson, O., Nielsen, H., & von Heijne, G. (1999). ChloroP, a neural network-based method for predicting chloroplast transit peptides and their cleavage sites. *Protein Sci. 8(5):978-84*

Fang, H., Liu, Z., Jin, Z., Zhang, L., Liu, D., & Pei, Y. (2016). An emphasis of hydrogen sulfide-cysteine cycle on enhancing the tolerance to chromium stress in Arabidopsis. *Environmental Pollution*, *213*, 870–877. https://doi.org/10.1016/j.envpol.2016.03.035

Feng, S., Cokus, S. J., Zhang, X., Chen, P.-Y., Bostick, M., Goll, M. G., … Jacobsen, S. E. (2010). Conservation and divergence of methylation patterning in plants and animals. *Proceedings of the National Academy of Sciences*, *107*(19), 8689–8694. https://doi.org/10.1073/pnas.1002720107

Finnegan, J. E., & Dennis, E. S. (1993). Isolation and identification by sequence homology of a putative cytosine methyltransferase from Arabidopsis thaliana. *Nucleic Acids Research*, *21*(10), 2383–2388. https://doi.org/10.1093/nar/21.10.2383

Flora, S. J. S., Mittal, M., & Mehta, A. (2008) Heavy metal induced oxidative stress & its possible reversal by chelation therapy. *Indian Journal of Medical Research*, vol. 128, no. 4, pp. 501–523

Fu, Y., Luo, G. Z., Chen, K., Deng, X., Yu, M., Han, D., … He, C. (2015). N6-methyldeoxyadenosine marks active transcription start sites in Chlamydomonas. *Cell*, *161*(4), 879–892. https://doi.org/10.1016/j.cell.2015.04.010

Gao, Z., Liu, H., Daxinger, L., Pontes, O., He, X., Qian, W., … Biochemistry, C. (2010). HHS Public Access, *465*(7294), 106–109. https://doi.org/10.1038/nature09025.An

Gigolashvili, T., & Kopriva, S. (2014). Transporters in plant sulfur metabolism. *Frontiers in Plant Science*, *5*(September), 1–16. https://doi.org/10.3389/fpls.2014.00442

Gill, R. A., Ali, B., Cui, P., Shen, E., Farooq, M. A., Islam, F., … Zhou, W. (2016). Comparative transcriptome profiling of two *Brassica napus* cultivars under chromium toxicity and its alleviation by reduced glutathione. *BMC Genomics*, *17*(1), 1–25. https://doi.org/10.1186/s12864-016-3200-6

Gill, R. A., Zang, L., Ali, B., Farooq, M. A., Cui, P., Yang, S., … Zhou, W. (2015). Chromium-induced physio-chemical and ultrastructural changes in four cultivars of *Brassica napus L. Chemosphere, 120, 154–164.* doi:10.1016/j.chemosphere.2014.06.029

Giordano, M. & Prioretti L. (2016). Sulphur and Algae: Metabolism, Ecology and Evolution. in The Physiology of Microalgae*, M.A. Borowitzka et al. (eds.), Developments in Applied Phycology 6, DOI 10.1007/978-3-319-24945-2_9*

Giordano, M., Norici, A., & Hell, R. (2005). Sulfur and phytoplankton: Acquisition, metabolism and impact on the environment. *New Phytologist*, *166*(2), 371–382. https://doi.org/10.1111/j.1469-8137.2005.01335.x

Goll, M. G., Kirpekar, F., Maggert, K. A., Yoder, J. A., Hsieh, C., Zhang, X., … Bestor, T. H. (2006). Methylation of tRNA Asp by the DNA Methyltransferase Homolog Dnmt2, *311*(January), 395–399.

Goll, M. G., & Bestor, T. H. (2005). EUKARYOTIC CYTOSINE METHYLTRANSFERASES. *Annual Review of Biochemistry*, *74*(1), 481–514. https://doi.org/10.1146/annurev.biochem.74.010904.153721

Gong, Z., Morales-Ruiz, T., Ariza, R. R., Rold_an-Arjona, T., David, L., & Zhu, J. K. (2002). ROS1, a repressor of transcriptional gene silencing in Arabidopsis, encodesa DNA glycosylase/lyase. Cell, 111(6), 803-14. DOI: 10.1016/s0092-8674(02)01133-9

Gonzalez-Ballester, D., & Grossman, A. R. (2009). Sulfur. The Chlamydomonas Sourcebook*, 159–187.* doi:10.1016/b978-0-12-370873-1.00013-7

González-Ballester, D., Casero, D., Cokus, S., Pellegrini, M., Merchant, S. S., & Grossman, A. R. (2010). RNA-seq analysis of sulfur-deprived Chlamydomonas cells reveals aspects of acclimation critical for cell survival. *The Plant cell*, *22*(6), 2058–2084. doi:10.1105/tpc.109.071167

Gorbi, G., Zanni, C., & Corradi, M. G. (2007). Sulfur starvation and chromium tolerance in Scenedesmus acutus: A possible link between metal tolerance and the regulation of sulfur uptake/assimilation processes. *Aquatic Toxicology*, *84*(4), 457–464. https://doi.org/10.1016/j.aquatox.2007.07.006

Gorbi, G., Torricelli, E., Pawlik-Skowrońska, B., Toppi, L. S. di, Zanni, C., & Corradi, M. G. (2006). Differential responses to Cr(VI)-induced oxidative stress between Cr-tolerant and wild-type strains of *Scenedesmus acutus* (Chlorophyceae). *Aquatic Toxicology*, *79*(2), 132–139. https://doi.org/10.1016/j.aquatox.2006.06.002

Gorbi, G., & Corradi, M. G. (1993). *Chromium Toxicity on Two Linked Trophic Levels I. Effects of Contaminated Algae on Daphnia magna. Ecotoxicology and Environmental Safety, 25(1), 64–71.* doi:10.1006/eesa.1993.1007

Greco, M., Chiappetta, A., Bruno, L., & Bitonti, M. B. (2012). In *Posidonia oceanica* cadmium induces changes in DNA methylation and chromatin patterning. *Journal of Experimental Botany*, *63*(2), 695–709.

Green, L. S., & Grossman, A. R. (1988). Changes in sulfate transport characteristics and protein composition of Anacystis nidulans R2 during sulfur deprivation. *Journal of Bacteriology*, *170*(2), 583 LP – 587. https://doi.org/10.1128/jb.170.2.583-587.1988

Guo, X., Feng, L., Lemos, B., & Lou, J. (2019). DNA methylation modifications induced by hexavalent chromium. *Journal of Environmental Science and Health - Part C Environmental Carcinogenesis and Ecotoxicology Reviews*, *37*(3), 133–145. https://doi.org/10.1080/10590501.2019.1592640

Haag, J. R., & Pikaard, C. S. (2011). Multisubunit RNA polymerases IV and V: purveyors of non-coding RNA for plant gene silencing. Nature Reviews Molecular Cell Biology, 12(8), 483-492. doi: 10.1038/nrm3152

Haas, F. H., Heeg, C., Queiroz, R., Bauer, A., Wirtz, M., & Hell, R. (2008). Mitochondrial Serine Acetyltransferase Functions as a Pacemaker of Cysteine Synthesis in Plant Cells. *Plant Physiology*, *148*(2), 1055 LP – 1067. https://doi.org/10.1104/pp.108.125237

Hagelueken, G., Adams, T. M., Wiehlmann, L., Widow, U., Kolmar, H., Tümmler, B., … Schubert, W. D. (2006). The crystal structure of SdsA1, an alkylsulfatase from Pseudomonas aeruginosa, defines a third

class of sulfatases. *Proceedings of the National Academy of Sciences of the United States of America*, *103*(20), 7631–7636. doi:10.1073/pnas.0510501103

Hatzfeld, Y., Cathala, N., Grignon, C., & Davidian, J. C. (1998). Effect of ATP sulfurylase overexpression in bright yellow 2 tobacco cells. Regulation Of atp sulfurylase and SO4(2-) transport activities. *Plant physiology*, *116*(4), 1307–1313. doi:10.1104/pp.116.4.1307

Hawkesford, M. J. (2003). Transporter gene families in plants: the sulphate transporter gene family - redundancy or specialization? *Physiologia Plantarum, 117(2), 155–163.* doi:10.1034/j.1399-3054.2003.00034.x

Heeg, C., Kruse, C., Jost, R., Gutensohn, M., Ruppert, T., Wirtz, M., & Hell, R. (2008). Analysis of the <em>Arabidopsis O</em>-Acetylserine(thiol)lyase Gene Family Demonstrates Compartment-Specific Differences in the Regulation of Cysteine Synthesis. *The Plant Cell*, *20*(1), 168 LP – 185. https://doi.org/10.1105/tpc.107.056747

Hegewald, E., & Wolf, M. (2003). Phylogenetic relationships of Scenedesmus and Acutodesmus (Chlorophyta, Chlorophyceae) as inferred from 18S rDNA and ITS-2 sequence comparisons, *241*, 185–191. https://doi.org/10.1007/s00606-003-0061-7

Heid, C. A., Stevens, J., Livak, K. J., & Williams, P. M. (1994). Real Time Quantitative PCR, 986–994.

Henderson, I. R., & Jacobsen, S. E. (2007). Epigenetic inheritance in plants, *Nature 447*. https://doi.org/10.1038/nature05917

Hesse, Trachsel, H. N., Suter, M., Kopriva, S., Von Ballmoos, P., Rennenberg H., & Brunold C. (2003). Effect of glucose on assimilatory sulphate reduction in Arabidopsis thaliana roots. *Journal of Experimental Botany, 54(388), 1701–1709.* doi:10.1093/jxb/erg177

Hofmann, K., & Stoffel, W. (1993). TMbase - A database of membrane spanning proteins segments. *Biol. Chem. Hoppe-Seyler 374,166*

Holland, S. L., & Avery, S. V. (2011). Chromate toxicity and the role of sulfur. *Metallomics*, *3*(11), 1119–1123. https://doi.org/10.1039/c1mt00059d

Höller, K., Király, L., Künstler, A., Müller, M., Gullner, G., Fattinger, M., Zechmann, B. (2010). Enhanced glutathione metabolism is correlated with sulfur-induced resistance in Tobacco mosaic virus-infected genetically susceptible Nicotiana tabacum plants. Mol. Plant-Microbe Interact. 11, 1448–1459. doi: 10.1094/MPMI-05-10-0117

Hörcsik, Z. T., Kovács, L., Láposi, R., Mészáros, I., Lakatos, G., & Garab, G. (2007). Effect of chromium on photosystem 2 in the unicellular green alga, *Chlorella pyrenoidosa. Photosynthetica, 45(1), 65–69.* doi:10.1007/s11099-007-0010-8

Huang, X. Y., Li, M., Luo, R., Zhao, F. J., Salt, D. E., & Takahashi, H. (2019). Epigenetic regulation of sulfur homeostasis in plants. *Journal of Experimental Botany*, *70*(16), 4171–4182. https://doi.org/10.1093/jxb/erz218

Huang, X., Chao, D., Koprivova, A., Danku, J., & Wirtz, M. (2016). Nuclear Localised MORE SULPHUR ACCUMULATION1 Epigenetically Regulates Sulphur Homeostasis in Arabidopsis thaliana, 1–29. https://doi.org/10.1371/journal.pgen.1006298

Huff, J. T., & Zilberman, D. (2014). Dnmt1-independent CG methylation contributes to nucleosome positioning in diverse eukaryotes. *Cell*, *156*(6), 1286–1297. https://doi.org/10.1016/j.cell.2014.01.029

Iyer, A., Mody, K., & Jha, B. (2004). Accumulation of hexavalent chromium by an exopolysaccharide producing marine Enterobacter cloaceae. *Marine Pollution Bulletin, 49(11-12), 974–977.* doi:10.1016/j.marpolbul.2004.06.023

Jackson, J. P., Lindroth, A. M., Cao, X., & Jacobsen, S. E. (2002). Control of CpNpG DNA methylation by the KRYPTONITE histone H3 methyltransferase, *416*(April), 2–6.

Jez, J. M., & Kopriva, S. (2019). Structural biology of plant sulfur metabolism: From sulfate to glutathione. *Journal of Experimental Botany*, *70*(16), 4089–4103. https://doi.org/10.1093/jxb/erz094

Jiang, C., Mithani, A., Belfield, E. J., Mott, R., Hurst, L. D., & Harberd, N. P. (2014). Environmentally responsive genome-wide accumulation of *de novo Arabidopsis thaliana* mutations and epimutations. *Genome Research*, *24*(11), 1821–1829. https://doi.org/10.1101/gr.177659.114

Johnson, L. M., Bostick, M., Zhang, X., Kraft, E., Henderson, I., Callis, J., & Jacobsen, S. E. (2007). The SRA Methyl-Cytosine-Binding Domain Links DNA and Histone Methylation. *Current Biology*, *17*(4), 379–384. https://doi.org/10.1016/j.cub.2007.01.009

Kahnert, A., & Kertesz, M. A. (2000). Characterization of a Sulfur-regulated Oxygenative Alkylsulfatase from *Pseudomonas putida S-313. Journal of Biological Chemistry, 275(41), 31661–31667.* doi:10.1074/jbc.m005820200

Kalisz, S., & Purugganan, M. D. (2004). Epialleles via DNA methylation: consequences for plant evolution. *Trends in Ecology & Evolution, 19(6)*, 309 – 314 https://doi.org/10.1016/j.tree.2004.03.034

Kamran, M.A., Eqani, S.A.M.A.S., Katsoyiannis, A., Xu, R.-K., Bibi, S., Benizri, E., Chaudhary, H.J. (2016). Phytoextraction of chromium (Cr) and influence of *Pseudomonas putida* on Eruca sativa growth. *J. Geochem. Explor.* http://dx.doi.org/10.1016/j.gexplo.2016.09.005.

Kaplan, D., Christiaen, D., & Arad, S. M. (1987). Chelating Properties of Extracellular Polysaccharides from Chlorella spp. *Applied and environmental microbiology*, *53*(12), 2953–2956.

Kelley, L. A., Mezulis, S., Yates, C. M., Wass, M. N., & Sternberg, M. J. E. (2015). The Phyre2 web portal for protein modeling, prediction and analysis. *Nature Protocols*, *10*(6), 845–858. https://doi.org/10.1038/nprot.2015.053

Kolb, D., Müller, M., Zellnig, G., & Zechmann, B. (2010). Cadmium induced changes in subcellular glutathione contents within glandular trichomes of Cucurbita pepo L. *Protoplasma*, *243*(1-4), 87–94. doi:10.1007/s00709-009-0043-x

Kopriva, S., Mugford, S. G., Matthewman, C., & Koprivova, A. (2009). Plant sulfate assimilation genes: Redundancy versus specialization. *Plant Cell Reports*, *28*(12), 1769–1780. https://doi.org/10.1007/s00299-009-0793-0

Koprivova, A., & Kopriva, S. (2016). *Sulfur metabolism and its manipulation in crops. Journal of Genetics and Genomics, 43(11), 623–629.* doi:10.1016/j.jgg.2016.07.001

Koprivova, A., Suter, M., den Camp, R. O., Brunold, C., & Kopriva, S. (2000). Regulation of sulfate assimilation by nitrogen in Arabidopsis. *Plant physiology*, *122*(3), 737–746. doi:10.1104/pp.122.3.737

Kranner, I., & Colville, L. (2011). Metals and seeds: Biochemical and molecular implications and their significance for seed germination. *Environmental and Experimental Botany, 72(1), 93–105.* doi:10.1016/j.envexpbot.2010.05.005

Kulik, A., Wawer, I., Krzywińska, E., Bucholc, M., & Dobrowolska, G. (2011). SnRK2 protein kinases--key regulators of plant response to abiotic stresses. *Omics: a journal of integrative biology*, *15*(12), 859–872. doi:10.1089/omi.2011.0091

Kumar, S., Cheng, X., Klimasauskas, S., Mi, S., Posfai, J., Roberts, R. J., & Wilson, G. G. (1994). The DNA (cytosine-5) methyltransferases. *Nucleic Acids Research*, *22*(1), 1– 10.

Kumar, S., Stecher, G., Li, M., Knyaz, C., & Tamura, K. (2018). MEGA X: Molecular Evolutionary Genetics Analysis across Computing Platforms, *35*(6), 1547–1549. https://doi.org/10.1093/molbev/msy096

Kumar, S., Stecher, G., Li, M., Knyaz, C., & Tamura, K. (2018). MEGA X : Molecular Evolutionary Genetics Analysis across Computing Platforms, *35*(6), 1547–1549. https://doi.org/10.1093/molbev/msy096

Labra, M., Grassi, F., Imazio, S., Di Fabio, T., Citterio, S., Sgorbati, S., & Agradi, E. (2004). Genetic and DNA-methylation changes induced by potassium dichromate in Brassica napus L. *Chemosphere*, *54*(8), 1049–1058. https://doi.org/10.1016/j.chemosphere.2003.10.024

Lappartient, A. G., & Touraine, B. (1996). Demand-Driven Control of Root ATP Sulfurylase Activity and SO42- Uptake in Intact Canola (The Role of Phloem-Translocated Glutathione). *Plant Physiology*, *111*(1), 147 LP – 157. https://doi.org/10.1104/pp.111.1.147

Laudenbach, D. E., & Grossman, A. R. (1991). Characterization and mutagenesis of sulfur-regulated genes in a cyanobacterium: evidence for function in sulfate transport. *Journal of bacteriology*, *173*(9), 2739–2750. doi:10.1128/jb.173.9.2739-2750.1991

Lauria, M., & Rossi, V. (2011). Epigenetic control of gene regulation in plants. *Biochimica et Biophysica Acta - Gene Regulatory Mechanisms*, *1809*(8), 369–378. https://doi.org/10.1016/j.bbagrm.2011.03.002

Law, J. A., & Jacobsen, S. E. (2010). Establishing, maintaining and modifying DNA methylation patterns in plants and animals. *Nature Reviews Genetics*, *11*(3), 204–220. https://doi.org/10.1038/nrg2719

Law, J. A., Du, J., Hale, C. J., Feng, S., Krajewski, K., Palanca, A. M. S., . . . Jacobsen, S. E. (2013). Polymerase IV occupancy at RNA-directed DNA methylation sites requires SHH1. Nature, 498(7454), 385-389. doi: 10.1038/nature12178

Lei, M., Zhang, H., Julian, R., Tang, K., Xie, S., & Zhu, J.-K. (2015). Regulatory link between DNA methylation and active demethylation in *Arabidopsis*. *Proceedings of the National Academy of Sciences*, *112*(11), 3553–3557. https://doi.org/10.1073/pnas.1502279112

Leliaert, F., Smith, D. R., Moreau, H., Herron, M. D., Verbruggen, H., Delwiche, C. F., … Clerck, O. De. (2012). Critical Reviews in Plant Sciences Phylogeny and Molecular Evolution of the Green Algae Phylogeny and Molecular Evolution of the Green Algae, *2689*. https://doi.org/10.1080/07352689.2011.615705

Li, Q., Song, J., West, P. T., Zynda, G., Eichten, S. R., Vaughn, M. W., & Springer, N. M. (2015). Examining the Causes and Consequences of Context-Specific Differential DNA Methylation in Maize 1 [ OPEN ], *168*(August), 1262–1274. https://doi.org/10.1104/pp.15.00052

Li, X., Zhu, J., Hu, F., Ge, S., Ye, M., Xiang, H., … Wang, W. (2012). Single-base resolution maps of cultivated and wild rice methylomes and regulatory roles of DNA methylation in plant gene expression. *BMC Genomics*, *13*(1), 1–15. https://doi.org/10.1186/1471-2164-13-300

Liang, L., Chang, Y., Lu, J., Wu, X., Liu, Q., Zhang, W., … Zhang, B. (2019). Global methylomic and transcriptomic analyses reveal the broad participation of DNA methylation in daily gene expression regulation of Populus trichocarpa. *Frontiers in Plant Science*, *10*(February), 1–10. https://doi.org/10.3389/fpls.2019.00243

Lindberg, P., & Melis, A. (2008). The chloroplast sulfate transport system in the green alga Chlamydomonas reinhardtii. *Planta*, *228*(6), 951–961. https://doi.org/10.1007/s00425-008-0795-0

Lindroth, A. M., Cao, X., Jackson, J. P., & Jacobsen, S. E. (2001). Requirement of CHROMOMETHYLASE3 for Maintenance of CpXpG Methylation, *292*(June), 2077–2081.

Lira-Silva, E., Ramírez-Lima, I.S., Olín-Sandoval, V., García-García, J.D., García-Contreras R., Moreno-Sánchez R., & Jasso-Chávez, R. (2011). Removal, accumulation and resistance to chromium in heterotrophic Euglena gracilis. J Hazard Mater. Oct;193 216-224. doi:10.1016/j.jhazmat.2011.07.056.

Lister, R., Mukamel, E. A., Nery, J. R., Urich, M., Puddifoot, C. A., Johnson, N. D., …Ecker, J. R. (2013). Global epigenomic reconfiguration during mammalian brain development. *Science (New York, N.Y.)*, *341*(6146), 1237905. https://doi.org/10.1126/science.1237905

Lopez, D., Hamaji, T., Kropat, J., Hoff, P. De, Morselli, M., Rubbi, L., … Pellegrini, M. (2015). Dynamic Changes in the Transcriptome and Methylome of Chlamydomonas reinhardtii throughout Its Life Cycle 1, *169*(December), 2730–2743. https://doi.org/10.1104/pp.15.00861

Luco, R. F., Pan, Q., Tominaga, K., Blencowe, B. J., Pereira-Smith, O. M., & Misteli, T. (2010). Regulation of alternative splicing by histone modifications. *Science*, *327*(5968), 996–1000. doi:10.1126/science.1184208

Ma, J., Lv, C., Xu, M., Chen, G., Lv, C., & Gao, Z. (2015). Photosynthesis performance, antioxidant enzymes, and ultrastructural analyses of rice seedlings under chromium stress. *Environmental Science and Pollution Research, 23(2), 1768–1778.* doi:10.1007/s11356-015-5439-x

Ma, X., Kim, E. J., & Cerutti, H. (2017). Gene silencing in archaeplastida algae. In *Plant Gene Silencing: Mechanisms and Applications* (Vol. 27, pp. 75–93). https://doi.org/10.1079/9781780647678.0075

Madulung, A., & Comai, L. (2004). The effect of stress on genome regulation and structure. *Annals of Botany*, *94*(4), 481–495. https://doi.org/10.1093/aob/mch172

Mallick, N. & Rai, L. C. (2002). Physiological responses of non-vascular plants to heavy metals. In *Physiology and Biochemistry of Metal Toxicity and Tolerance in Plants*, M. N. V. Prasad & K. Strzałka, eds., 111–147. Dordrecht: Kluwer.

Mao, X., Cai, T., Olyarchuk, J. G., & Wei, L. (2005). Automated genome annotation and pathway identification using the KEGG Orthology (KO) as a controlled vocabulary. *Bioinformatics, 21(19), 3787–3793.* doi:10.1093/bioinformatics/bti430

Marieschi, M., Gorbi, G., Zanni, C., Sardella, A., & Torelli, A. (2015). Increase of chromium tolerance in Scenedesmus acutus after sulfur starvation: Chromium uptake and compartmentalization in two strains with different sensitivities to Cr(VI). *Aquatic Toxicology*, *167*, 124–133. https://doi.org/10.1016/j.aquatox.2015.08.001

Maruyama-Nakashita, A., Nakamura, Y., Tohge, T., Saito, K., & Takahashi, H. (2006). Arabidopsis SLIM1 is a central transcriptional regulator of plant sulfur response and metabolism. *The Plant cell*, *18*(11), 3235–3251. doi:10.1105/tpc.106.046458

Marzluf, G. A. (1970) Genetic and metabolic controls for sulfate metabolism in *Neurospora crassa*: isolation and study of chromate-resistant and sulfate transport-negative mutants. *Journal of Bacteriology*, 102(3):716–721.

Mathieu, O., Reinders, J., Čaikovski, M., Smathajitt, C., & Paszkowski, J. (2007). Transgenerational stability of the *Arabidopsis* epigenome is coordinated by CG Methylation. *Cell*, *130*(5), 851–862. https://doi.org/10.1016/j.cell.2007.07.007

Matzke, M. A., & Mosher, R. A. (2014). RNA-directed DNA methylation: An epigenetic pathway of increasing complexity. *Nature Reviews Genetics*, *15*(6), 394–408. https://doi.org/10.1038/nrg3683

Matzke, M., Kanno, T., Daxinger, L., Huettel, B., & Matzke, A. J. (2009). RNA-mediated chromatin-based silencing in plants. *Current Opinion in Cell Biology*, *21*(3), 367–376. https://doi.org/10.1016/j.ceb.2009.01.025

Maunakea, A. K., Nagarajan, R. P., Bilenky, M., Ballinger, T. J., D'Souza, C., Fouse, S. D., … Costello, J. F. (2010). Conserved role of intragenic DNA methylation in regulating alternative promoters. *Nature*, *466*(7303), 253–257. doi:10.1038/nature09165

McCue, A. D., Nuthikattu, S., Reeder, S. H., & Slotkin, R. K. (2012). Gene Expression and Stress Response Mediated by the Epigenetic Regulation of a Transposable Element Small RNA. PLoS Genetics, 8(2), e1002474. https://doi.org/10.1371/journal.pgen.1002474

McCue, A. D., Panda, K., Nuthikattu, S., Choudury, S. G., Thomas, E. N., & Slotkin, R. K. (2015). ARGONAUTE 6 bridges transposable element mRNA-derived siRNAs to the establishment of DNA methylation, *34*(1).

Medeiros, M. G., Rodrigues, A. S., Batoréu, M. C., Laires, A., Rueff, J., & Zhitkovich, A. (2003) Elevated levels of DNA-protein crosslinks and micronuclei in peripheral lymphocytes of tannery workers exposed to trivalent chromium. *Mutagenesis*,18(1):19–24.

Melis, A., & Chen, H. C. (2005). Chloroplast sulfate transport in green algae - Genes, proteins and effects. *Photosynthesis Research*, *86*(3), 299–307. https://doi.org/10.1007/s11120-005-7382-z

Merchant, S. S., Prochnik, S. E., Vallon, O., Harris, E. H., Karpowicz, S. J., Witman, G. B., … Grossman, A. R. (2007). The Chlamydomonas genome reveals the evolution of key animal and plant functions. *Science (New York, N.Y.)*, *318*(5848), 245–250. doi:10.1126/science.1143609

Metsalu, T., & Vilo, J. (2015). ClustVis: A web tool for visualizing clustering of multivariate data using Principal Component Analysis and heatmap. *Nucleic Acids Research*, *43*(W1), W566–W570. https://doi.org/10.1093/nar/gkv468

Metsalu, T., & Vilo, J. (2015). ClustVis: A web tool for visualizing clustering of multivariate data using Principal Component Analysis and heatmap. *Nucleic Acids Research*, *43*(W1), W566–W570. https://doi.org/10.1093/nar/gkv468

Moran, J. F., Iturbe-Ormaetxe, I., Matamoros, M. A., Rubio, M. C., Clemente, M. R., Brewin, N. J., & Becana, M. (2000). Glutathione and homoglutathione synthetases of legume nodules. Cloning, expression, and subcellular localization. *Plant physiology*, *124*(3), 1381–1392. doi:10.1104/pp.124.3.1381

Moseley, J. L., Gonzalez-Ballester, D., Pootakham, W., Bailey, S., & Grossman, A. R. (2009). Genetic interactions between regulators of Chlamydomonas phosphorus and sulfur deprivation responses. *Genetics*, *181*(3), 889–905. doi:10.1534/genetics.108.099382

Nazar, R., Iqbal, N., Masood, A., Syeed, S., Khan, N.A. (2011). Understanding the significance of sulphur in improving salinity tolerance in plants. *Environ. Exp. Bot*. 70, 80–87

Niederhuth, C. E., Bewick, A. J., Ji, L., Alabady, M. S., Kim, K. Do, Li, Q., … Schmitz, R. J. (2016). Widespread natural variation of DNA methylation within angiosperms. *Genome Biology*, 1–19. https://doi.org/10.1186/s13059-016-1059-0

Nies, D. H., Koch, S., Wachi, S., Peitzsch, N., & Saier, M. H., Jr (1998). CHR, a novel family of prokaryotic proton motive force-driven transporters probably containing chromate/sulfate antiporters. *Journal of bacteriology*, *180*(21), 5799–5802.

Nishiyama, R., Wada, Y., Mibu, M., Yamaguchi, Y., Shimogawara, K., & Sano, H. (2004). of Chloroplast Genes in the Green Alga, Chlamydomonas reinhardtii, *1*. https://doi.org/10.1534/genetics.104.030775

Nocito, F.F., Lancilli, C., Crema, B., Fourcoy, P., Davidian, J.C., Sacchi, G.A., (2006). Heavy metal stress and sulfate uptake in maize roots. Plant Physiol. 141,1138–1148. DOI: https://doi.org/10.1104/pp.105.076240

Nriagu, J.O., 1988. Production and Uses of Chromium. Chromium in the Natural and Human Environments. Wiley, New York, pp. 81e104.

Nuthikattu, S., McCue, A. D., Panda, K., Fultz, D., DeFraia, C., Thomas, E. N., & Slotkin, R. K. (2013). The initiation of epigenetic silencing of active transposable elements is triggered by RDR6 and 21-22 nucleotide small interfering RNAs. Plant physiology, 162(1), 116-31. doi: 10.1104/pp.113.216481

Ou, X., Zhang, Y., Xu, C., Lin, X., Zang, Q., Zhuang, T., … Liu, B. (2012). Transgenerational Inheritance of Modified DNA Methylation Patterns and Enhanced Tolerance Induced by Heavy Metal Stress in Rice (Oryza sativa L.). *PLoS ONE*, *7*(9). doi.org/10.1371/journal.pone.0041143

Paietta J. V. (1990). Molecular cloning and analysis of the scon-2 negative regulatory gene of Neurospora crassa. *Molecular and cellular biology*, *10*(10), 5207–5214. doi:10.1128/mcb.10.10.5207

Panda, K., Ji, L., Neumann, D. A., Daron, J., Schmitz, R. J., & Slotkin, R. K. (2016). Full-length autonomous transposable elements are preferentially targeted by expression-dependent forms of RNA-directed DNA methylation. *Genome Biology*, 1–19. https://doi.org/10.1186/s13059-016-1032-y

Panda, S. K. (2007). Chromium-mediated oxidative stress and ultrastructural changes in root cells of developing rice seedlings. *Journal of Plant Physiology, 164(11), 1419–1428.* doi:10.1016/j.jplph.2007.01.012

Panda, S. K., & Choudhury, S. (2005). Chromium stress in plants. *Brazilian Journal of Plant Physiology*, *17*(1), 95–102. https://doi.org/10.1590/s1677-04202005000100008

Pandey, N., & Sharma, C. P. (2003) Chromium interference in iron nutrition and water relations of cabbage. *Environmental and Experimental Botany, 49(3), 195–200.* doi:10.1016/s0098-8472(02)00088-6

Patron, N. J., Durnford, D. G., & Kopriva, S. (2008). Sulfate assimilation in eukaryotes: fusions, relocations and lateral transfers. *BMC evolutionary biology*, *8*, 39. doi:10.1186/1471-2148-8-39

Pavlopoulou, A., & Kossida, S. (2007). Plant cytosine-5 DNA methyltransferases: Structure, function, and molecular evolution. *Genomics*, *90*(4), 530–541. https://doi.org/10.1016/j.ygeno.2007.06.011

Peng, H., & Zhang, J. (2009). Plant genomic DNA methylation in response to stresses: Potential applications and challenges in plant breeding. *Progress in Natural Science*, *19*(9), 1037–1045. https://doi.org/https://doi.org/10.1016/j.pnsc.2008.10.014

Pereira, Y., Lagniel, G., Godat, E., Baudouin-Cornu, P., Junot, C., & Labarre, J. (2008). Chromate Causes Sulfur Starvation in Yeast. *Toxicological Sciences, 106(2), 400–412.* doi:10.1093/toxsci/kfn193

Pérez-Castiñeira, J. R., Prieto, J. L., González-Arroyo, J. G., & Vega, J. M. (1998). Kinetic properties of sulfate uptake in two types of eukaryotic green microalgae. *Journal of Plant Physiology, 153(3-4), 324–331.* doi:10.1016/s0176-1617(98)80158-2

Pfaffl, M. W., Horgan, G. W., & Dempfle, L. (2002). Relative expression software tool (REST) for group-wise comparison and statistical analysis of relative expression results in real-time PCR. *Nucleic acids research*, *30*(9), e36. doi:10.1093/nar/30.9.e36

Pikaard, C. S., & Scheid, O. M. (2014). Epigenetic regulation in plants. *Cold Spring Harbor Perspectives in Biology*, *6*(12), 1–31. https://doi.org/10.1101/cshperspect.a019315

Pinto, E., Sigaud-kutner, T. C. S., Leitao, M. A. S., Okamoto, O. K., Morse, D., & Colepicolo, P. (2003). HEAVY METAL-INDUCED OXIDATIVE STRESS IN ALGAE. *Journal of Phycology, 39(6), 1008–1018.* doi:10.1111/j.0022-3646.2003.02-193.x

Ponger, L., & Li, W. H. (2005). Evolutionary diversification of DNA methyltransferases in eukaryotic genomes. *Molecular Biology and Evolution*, *22*(4), 1119–1128. https://doi.org/10.1093/molbev/msi098

Pootakham, W., Gonzalez-Ballester, D., & Grossman, A. R. (2010). Identification and Regulation of Plasma Membrane Sulfate Transporters in Chlamydomonas. *Plant Physiology*, *153*(4), 1653–1668. https://doi.org/10.1104/pp.110.157875

Prioretti, L., Gontero, B., Hell, R., & Giordano, M. (2014). Diversity and regulation of ATP sulfurylase in photosynthetic organisms. *Frontiers in plant science*, *5*, 597. doi:10.3389/fpls.2014.00597

Rai, V., Vajpayee, P., Singh, S. N., & Mehrotra, S. (2004). Effect of chromium accumulation on photosynthetic pigments, oxidative stress defense system, nitrate reduction, proline level and eugenol content of *Ocimum tenuiflorum* L. *Plant Science, 167(5), 1159–1169.* doi:10.1016/j.plantsci.2004.06.016

Rambani, A., Rice, J. H., Liu, J., Lane, T., Ranjan, P., Mazarei, M., … Hewezi, T. (2015). The methylome of soybean roots during the compatible interaction with the soybean cyst nematode. *Plant Physiology*, *168*(4), 1364–1377. https://doi.org/10.1104/pp.15.00826

Ramsahoye, B. H., Biniszkiewicz, D., Lyko, F., Clark, V., Bird, A. P., & Jaenisch, R. (2000). Non-CpG methylation is prevalent in embryonic stem cells and may be mediated by DNA methyltransferase 3a. *Proceedings of the National Academy of Sciences of the United States of America*, *97*(10), 5237–5242. https://doi.org/10.1073/pnas.97.10.5237

Ravina, C. G., Chang, C. I., Tsakraklides, G. P., McDermott, J. P., Vega, J. M., Leustek, T., … Davies, J. P. (2002). The sac mutants of Chlamydomonas reinhardtii reveal transcriptional and posttranscriptional control of cysteine biosynthesis. *Plant physiology*, *130*(4), 2076–2084. doi:10.1104/pp.012484

Razin, A., & Cedar, H. (1993). DNA methylation and embryogenesis. *EXS*, *64*, 343–357.

Reale, L., Ferranti, F., Mantilacci, S., Corboli, M., Aversa, S., Landucci, F., Baldisserotto, C., Ferroni, L., Pancaldi, S., Venanzoni, R. (2016). Cyto-histological and morpho-physiological responses of common duckweed (*Lemna minor* L.) to chromium. *Chemosphere 145*, 98-105.

Regulski, M., Lu, Z., Kendall, J., Donoghue, M. T., Reinders, J., Llaca, V., … Martienssen, R. A. (2013). The maize methylome influences mRNA splice sites and reveals widespread paramutation-like switches guided by small RNA. *Genome research*, *23*(10), 1651–1662. doi:10.1101/gr.153510.112

Reynolds, C. R., Islam, S. A., & Sternberg, M. J. E. (2018). EzMol: A Web Server Wizard for the Rapid Visualization and Image Production of Protein and Nucleic Acid Structures. *Journal of Molecular Biology*, *430*(15), 2244–2248. https://doi.org/10.1016/j.jmb.2018.01.013

Rodríguez, M. C., Barsanti, L., Passarelli, V., Evangelista, V., Conforti, V., & Gualtieri, P. (2007). Effects of chromium on photosynthetic and photoreceptive apparatus of the alga Chlamydomonas reinhardtii. *Environmental Research*, *105*(2), 234–239. https://doi.org/10.1016/j.envres.2007.01.011

Roudier, F., Ahmed, I., Bérard, C., Sarazin, A., Mary-Huard, T., Cortijo, S., … Colot, V. (2011). Integrative epigenomic mapping defines four main chromatin states in Arabidopsis. *The EMBO Journal*, *30*(10), 1928–1938. https://doi.org/10.1038/emboj.2011.103

Ryazanova, a Yu, L. a Abrosimova, T. S. Oretskaya, and E. a Kubareva. 2012. "Diverse Domains of (Cytosine-5) -DNA Methyltransferase: Structural and Functional Characterization." *Methylation - From DNA, RNA and Histones to Diseases and Treatment* 29–69.

Sahu, P. P., Pandey, G., Sharma, N., Puranik, S., Muthamilarasan, M., & Prasad, M. (2013). Epigenetic mechanisms of plant stress responses and adaptation. *Plant Cell Reports*, *32*(8), 1151–1159. https://doi.org/10.1007/s00299-013-1462-x

Sanchez, D. H., & Paszkowski, J. (2014). Heat-induced release of epigenetic silencing reveals the concealed role of an imprinted plant gene. *PLoS Genetics*, *10*(11), e1004806. https://doi.org/10.1371/journal.pgen.1004806

Sardella, A., Marieschi, M., Mercatali, I., Zanni, C., Gorbi, G., & Torelli, A. (2019). The relationship between sulfur metabolism and tolerance of hexavalent chromium in Scenedesmus acutus (Spheropleales): Role of ATP sulfurylase. *Aquatic Toxicology*, *216*(July), 105320. https://doi.org/10.1016/j.aquatox.2019.105320

Saroussi, S., Sanz-Luque, E., Kim, R. G., & Grossman, A. R. (2017). Nutrient scavenging and energy management: acclimation responses in nitrogen and sulfur deprived Chlamydomonas. *Current Opinion in Plant Biology*, *39*, 114–122. https://doi.org/10.1016/j.pbi.2017.06.002

Saze, H., Scheid, O. M., & Paszkowski, J. (2003). Maintenance of CpG methylation is essential for epigenetic inheritance during plant gametogenesis. *Nature Genetics*, *34*(1), 65. https://doi.org/10.1038/ng1138

Schiavon, M., Pilon-Smits, E. A. H., Wirtz, M., Hell, R., & Malagoli, M. (2008). Interactions between chromium and sulfur metabolism in Brassica juncea. *Journal of Environmental Quality*, *37*(4), 1536–1545. https://doi.org/10.2134/jeq2007.0032

Schiavon, M., Wirtz, M., Borsa, P., Quaggiotti, S., Hell, R., & Malagoli, M. (2007). Chromate Differentially Affects the Expression of a High-Affinity Sulfate Transporter and Isoforms of Components of the Sulfate Assimilatory Pathway in Zea mays (L.). *Plant Biol (Stuttg)*, *9*(05), 662–671. https://doi.org/10.1055/s-2007-965440

Schmitz, R. J., Schultz, M. D., Lewsey, M. G., O'Malley, R. C., Urich, M. A., Libiger, O., … Ecker, J. R. (2011). Transgenerational epigenetic instability is a source of novel methylation variants. *Science*, *334*(6054), 369–373. https://doi.org/10.1126/science.1212959

Shahid, Muhammad, Saliha Shamshad, Marina Rafiq, Sana Khalid, Irshad Bibi, Nabeel Khan Niazi, Camille Dumat, and Muhammad Imtiaz Rashid. (2017) Chromium Speciation, Bioavailability, Uptake, Toxicity and Detoxification in Soil-Plant System: A Review. *Chemosphere* 178:513–33.

Shanker, A. K., Cervantes, C., Loza-Tavera, H., & Avudainayagam, S. (2005). Chromium toxicity in plants. *Environment International*, *31*(5), 739–753. https://doi.org/10.1016/j.envint.2005.02.003

Shaw, W.H., & Anderson, J.W. (1974). The enzymology of adenosine triphosphate sulphurylase from spinach leaf tissue. Biochem J 139:27–35

Shi, X., & Dalal, N. S. (1992). The role of superoxide radical in chromium(VI)-generated hydroxyl radical: The Cr(VI) haber-weiss cycle. *Archives of Biochemistry and Biophysics, 292(1), 323–327.* doi:10.1016/0003-9861(92)90085-b

Shibagaki, N., & Grossman, A. R. (2010). Binding of cysteine synthase to the STAS domain of sulfate transporter and its regulatory consequences. *Journal of Biological Chemistry*, *285*(32), 25094–25102. https://doi.org/10.1074/jbc.M110.126888

Shibagaki, N. & Grossman, A. R. (2006). The role of the STAS domain in the function and biogenesis of a sulfate transporter as probed by random mutagenesis. *Journal of Biological Chemistry*, 281(32):22964–22973. doi: 10.1074/jbc.M603462200

Sirko, A., Hryniewicz, M., Hulanicka, D., & Böck, A. (1990). Sulfate and thiosulfate transport in Escherichia coli K-12: nucleotide sequence and expression of the cysTWAM gene cluster. *Journal of bacteriology*, *172*(6), 3351–3357. doi:10.1128/jb.172.6.3351-3357.1990

Smith, F. W., Ealing, P. M., Hawkesford, M. J., & Clarkson, D. T. (1995). Plant members of a family of sulfate transporters reveal functional subtypes. *Proceedings of the National Academy of Sciences of the United States of America*, *92*(20), 9373–9377. doi:10.1073/pnas.92.20.9373

Stanke, M., Diekhans, M., Baertsch, R., & Haussler, D. (2008). Sequence analysis Using native and syntenically mapped cDNA alignments to improve de novo gene finding, *24*(5), 637–644. https://doi.org/10.1093/bioinformatics/btn013

Starkenburg, S. R., Polle, J., Hovde, B., Daligault, H. E., Davenport, K. W., Huang, A., … McKie-Krisberg, Z. (2017). Draft Nuclear Genome, Complete Chloroplast Genome, and Complete Mitochondrial Genome for the Biofuel/Bioproduct Feedstock Species *Scenedesmus obliquus* Strain DOE0152z. *Genome announcements*, *5*(32), e00617-17. doi:10.1128/genomeA.00617-17

Stroud, H., Greenberg, M. V. C., Feng, S., Bernatavichute, Y. V, & Jacobsen, S. E. (2013). Comprehensive analysis of silencing mutants reveals complex regulation of the *Arabidopsis* methylome. *Cell*, *152*(1–2), 352–364. https://doi.org/10.1016/j.cell.2012.10.054

Takahashi, H., Buchner, P., Yoshimoto, N., Hawkesford, M. J., & Shiu, S. H. (2012). Evolutionary relationships and functional diversity of plant sulfate transporters. *Frontiers in Plant Science*, *2*(JAN), 1–9. https://doi.org/10.3389/fpls.2011.00119

Takahashi, H., Kopriva, S., Giordano, M., Saito, K., & Hell, R. (2011). Sulfur Assimilation in Photosynthetic Organisms: Molecular Functions and Regulations of Transporters and Assimilatory Enzymes. *Annual Review of Plant Biology, 62(1), 157–184.* doi:10.1146/annurev-arplant-042110-103921

Tang, K., Lang, Z., Zhang, H., & Zhu, J.-K. (2016). The DNA demethylase ROS1 targets genomic regions with distinct chromatin modi_cations. Nature Plants, 2(11), 16169. doi: 10.1038/nplants.2016.169

Tchounwou, P. B., Yedjou, C. G., Patlolla, A. K., & Sutton, D. J. (2012). Environmental Toxicology. *Molecular, Clinical and Environmental Toxicology*, *101*, 133–164. https://doi.org/10.1007/978-3-7643-8340-4

Thacker, U., & Madamwar, D. (2005). *Reduction of Toxic* Chromium and Partial Localization of Chromium Reductase Activity in Bacterial Isolate DM1. *World Journal of Microbiology and Biotechnology, 21(6-7), 891–899.* doi:10.1007/s11274-004-6557-7

Toledo-Cervantes, A., Garduño, G., Campos, J. E., Martínez-garcía, M., & Morales, M. (2018). Characterization of Scenedesmus obtusiusculus AT-UAM for high-energy molecules accumulation : deeper insight into biotechnological potential of strains of the same species. *Biotechnology Reports*, *17*, 16–23. https://doi.org/10.1016/j.btre.2017.11.009

Torricelli, E., Gorbi, G., Pawlik-Skowronska, B., Di Toppi, L. S., & Corradi, M. G. (2004). Cadmium tolerance, cysteine and thiol peptide levels in wild type and chromium-tolerant strains of Scenedesmus acutus (Chlorophyceae). *Aquatic Toxicology*, *68*(4), 315–323. https://doi.org/10.1016/j.aquatox.2004.03.020

Umen, J. G., & Goodenough, U. W. (2001). Chloroplast DNA methylation and inheritance in Chlamydomonas. *Genes and Development*, *15*(19), 2585–2597. https://doi.org/10.1101/gad.906701

Upadhyay, R. & Panda, S. K. (2010). Influence of chromium salts on increased lipid peroxidation and differential pattern in antioxidant metabolism in *Pistia stratiotes* L. *Brazilian Archives of Biology and Technology*, 53(5):1137–1144. DOI: 10.1590/S1516-89132010000500018

Vandegehuchte, M. B., & Janssen, C. R. (2014). Epigenetics in an ecotoxicological context. *Mutation Research - Genetic Toxicology and Environmental Mutagenesis*, *764–765*, 36–45. https://doi.org/10.1016/j.mrgentox.2013.08.008

Veluchamy, A., Lin, X., Maumus, F., Rivarola, M., Bhavsar, J., Creasy, T., … Tirichine, L. (2013). Insights into the role of DNA methylation in diatoms by genome-wide profiling in *Phaeodactylum tricornutum*. *Nature Communications*, *4*. https://doi.org/10.1002/jpln.19851480105

Vignati, D. A. L., J. Dominik, M. L. Beye, M. Pettine, & B. J. D. Ferrari (2010). Chromium(VI) is more toxic than chromium(III) to freshwater algae: A paradigm to revise? *Ecotoxicology and Environmental Safety*, 73(5):1034–1045.

Volland, S., Bayer, E., Baumgartner, V., Andosch, A., Lütz, C., Sima, E., & Lütz-Meindl, U. (2014). Rescue of heavy metal effects on cell physiology of the algal model system *Micrasterias* by divalent ions. *Journal of Plant Physiology, 171(2), 154–163.* doi:10.1016/j.jplph.2013.10.002

Volland, S., Lütz, C., Michalke, B., & Lütz-Meindl, U. (2012). Intracellular chromium localization and cell physiological response in the unicellular alga *Micrasterias. Aquatic Toxicology, 109, 59–69.* doi:10.1016/j.aquatox.2011.11.013

Wang, Y., Zhang, C., Zheng, Y., & Ge, Y. (2017). Phytochelatin synthesis in Dunaliella salina induced by arsenite and arsenate under various phosphate regimes. *Ecotoxicology and Environmental Safety*, *136*(July 2016), 150–160. https://doi.org/10.1016/j.ecoenv.2016.11.002

Warren, Schultz, Bancroft, Bennett, Abbott, & Rogers (1981) Mutagenicity of a series of hexacoordinate chromium(iii) compounds. *Mutation Research/Genetic Toxicology*, 90(2):111 – 118.

Watanabe, M., Kusano, M., Oikawa, A., Fukushima, A., Noji, M., & Saito, K. (2008a). Physiological Roles of the *β*-Substituted Alanine Synthase Gene Family in Arabidopsis. *Plant Physiology*, *146*(1), 310 LP – 320. https://doi.org/10.1104/pp.107.106831

Watanabe, M., Mochida, K., Kato, T., Tabata, S., Yoshimoto, N., Noji, M., & Saito, K. (2008b) Comparative Genomics and Reverse Genetics Analysis Reveal Indispensable Functions of the Serine Acetyltransferase Gene Family in *Arabidopsis*. *The Plant Cell*, *20*(9), 2484 LP – 2496. https://doi.org/10.1105/tpc.108.060335

Westerman, S., Stulen, I., Suter, M., Brunold, C., & De Kok, LJ. (2001). Atmospheric H2S as sulphur source for Brassica oleracea: Consequences for the activity of the enzymes of the assimilatory sulphate reduction pathway. *Plant Physiology and Biochemistry*, *39*(5), 425-432. https://doi.org/(...)0981-9428(01)01258-X

Whelan, J. A., Russell, N. B., & Whelan, M. A. (2003). A method for the absolute quantification of cDNA using real-time PCR. *Journal of Immunological Methods, 278(1-2), 261–269.* doi:10.1016/s0022-1759(03)00223-0

Williams, B. P., Pignatta, D., Henikoff, S., & Gehring, M. (2015). Methylation-Sensitive Expression of a DNA Demethylase Gene Serves As an Epigenetic Rheostat.PLOS Genetics, 11(3), e1005142. doi: 10.1371/journal.pgen.1005142

Wirtz, M., & Hell, R. (2007). Dominant-Negative Modification Reveals the Regulatory Function of the Multimeric Cysteine Synthase Protein Complex in Transgenic Tobacco. *The Plant Cell*, *19*(2), 625 LP – 639. https://doi.org/10.1105/tpc.106.043125

Wynne, M. J., & Hallan, J. K. (2016). Reinstatement of Tetradesmus G. M. Smith (Sphaeropleales, Chlorophyta). *Feddes Repertorium*, *126*(3–4), 83–86. https://doi.org/10.1002/fedr.201500021

Xie, Y., Ye, S., Wang, Y., Xu, L., Zhu, X., Yang, J., … Liu, L. (2015). Transcriptome-based gene profiling provides novel insights into the characteristics of radish root response to Cr stress with next-generation sequencing. *Frontiers in Plant Science*, *6*(March), 1–12. https://doi.org/10.3389/fpls.2015.00202

Yadav, B. S., Singh, S., Srivastava, S., & Mani, A. (2019). Analysis of chickpea gene co-expression networks and pathways during heavy metal stress. *Journal of Biosciences*, *44*(4), 1–10. https://doi.org/10.1007/s12038-019-9899-x

Yadav, B. S., Singh, S., Srivastava, S., Singh, N. K., & Mani, A. (2019). Whole transcriptome expression profiling and biological network analysis of chickpea during heavy metal stress. *Journal of Plant Biochemistry and Biotechnology*, *28*(3), 345–352. https://doi.org/10.1007/s13562-019-00486-3

Yildiz, F. H., Davies, J. P., & Grossman, A. (1996). Sulfur Availability and the SAC1 Gene Control Adenosine Triphosphate Sulfurylase Gene Expression in Chlamydomonas reinhardtii. *Plant Physiology*, *112*(2), 669 LP – 675. https://doi.org/10.1104/pp.112.2.669

Zechmann, B., Mauch, F., Sticher, L., & Müller, M. (2008). Subcellular immunocytochemical analysis detects the highest concentrations of glutathione in mitochondria and not in plastids. *Journal of experimental botany*, *59*(14), 4017–4027. doi:10.1093/jxb/ern243

Zemach, A., Kim, M. Y., Hsieh, P.-H., Coleman-Derr, D., Eshed-Williams, L., Thao, K., … Zilberman, D. (2013). The nucleosome remodeler DDM1 allows DNA methyltransferases to access H1-containing heterochromatin. *Cell*, *153*(1), 193–205. https://doi.org/10.1016/j.cell.2013.02.033

Zemach, A., McDaniel, I. E., Silva, P., Zilberman, D., Goll, M. G., Bestor, T. H., … Bestor, T. H. (2010). Genome-Wide Evolutionary Analysis of Eukaryotic DNA Methylation. *Science*, *328*(5980), 916–919. https://doi.org/10.1126/science.1186366

Zhang, B., Tieman, D. M., Jiao, C., Xu, Y., Chen, K., Fei, Z., … Klee, H. J. (2016). Chilling-induced tomato flavor loss is associated with altered volatile synthesis and transient changes in DNA methylation. *Proceedings of the National Academy of Sciences of the United States of America*, *113*(44), 12580–12585. https://doi.org/10.1073/pnas.1613910113

Zhang, H., Lang, Z., & Zhu, J. K. (2018). Dynamics and function of DNA methylation in plants. *Nature Reviews Molecular Cell Biology*, *19*(8), 489–506. https://doi.org/10.1038/s41580-018-0016-z

Zhang, Z., Shrager, J., Jain, M., Chang, C. W., Vallon, O., & Grossman, A. R. (2004). Insights into the survival of Chlamydomonas reinhardtii during sulfur starvation based on microarray analysis of gene expression. *Eukaryotic cell*, *3*(5), 1331–1348. doi:10.1128/EC.3.5.1331-1348.2004

Università degli Studi di Ferrara

# Dottorati di ricerca

Il tuo indirizzo e-mail

frrmhl1@unife.it

Oggetto:

Dichiarazione di conformità della tesi di Dottorato

Io sottoscritto Dott. (Cognome e Nome)

Ferrari Michele

Nato a:

Cosenza

Provincia:

Cosenza

Il giorno:

25/01/1987

Avendo frequentato il Dottorato di Ricerca in:

BIOLOGIA EVOLUZIONISTICA ED ECOLOGIA

Ciclo di Dottorato

32

Titolo della tesi:

DNA methylation and Cr(VI) stress responses in Scenedesmus acutus: a focus in Sulfur pathway

Titolo della tesi (traduzione):

Tesi in inglese: Metilazione del DNA e risposte al Cr(VI) in Scenedesmus acutus: un focus nel patway del solfato

Tutore: Prof. (Cognome e Nome)

Torelli Anna

Settore Scientifico Disciplinare (S.S.D.)

BIO/01

Parole chiave della tesi (max 10):

DNA methylation, Metilazione del DNA, Sulfur pathway, Pathway del solfato, Scenedesmus acutus, Cr(VI) stress responses, Risposte allo stress da Cr(VI), Transporters, Trasportatori

Consapevole, dichiara

CONSAPEVOLE: (1) del fatto che in caso di dichiarazioni mendaci, oltre alle sanzioni previste dal codice penale e dalle Leggi speciali per l'ipotesi di falsità in atti ed uso di atti falsi, decade fin dall'inizio e senza necessità di alcuna formalità dai benefici conseguenti al provvedimento emanato sulla base di tali dichiarazioni; (2) dell'obbligo per l'Università di provvedere al deposito di legge delle tesi di dottorato al fine di assicurarne la conservazione e la consultabilità da parte di terzi; (3) della procedura adottata dall'Università di Ferrara ove si richiede che la tesi sia consegnata dal dottorando in 2 copie, di cui una in formato cartaceo e una in formato pdf non modificabile su idonei supporti (CD-ROM, DVD) secondo le istruzioni pubblicate sul sito : http://www.unife.it/studenti/dottorato alla voce ESAME FINALE – disposizioni e modulistica; (4) del fatto che l'Università, sulla base dei dati forniti, archivierà e renderà consultabile in rete il testo completo della tesi di dottorato di cui alla presente dichiarazione attraverso l'Archivio istituzionale ad accesso aperto "EPRINTS.unife.it" oltre che attraverso i Cataloghi delle

Biblioteche Nazionali Centrali di Roma e Firenze. DICHIARO SOTTO LA MIA RESPONSABILITA': (1) che la copia della tesi depositata presso l'Università di Ferrara in formato cartaceo è del tutto identica a quella presentata in formato elettronico (CD-ROM, DVD), a quelle da inviare ai Commissari di esame finale e alla copia che produrrà in seduta d'esame finale. Di conseguenza va esclusa qualsiasi responsabilità dell'Ateneo stesso per quanto riguarda eventuali errori, imprecisioni o omissioni nei contenuti della tesi; (2) di prendere atto che la tesi in formato cartaceo è l'unica alla quale farà riferimento l'Università per rilasciare, a mia richiesta, la dichiarazione di conformità di eventuali copie. PER ACCETTAZIONE DI QUANTO SOPRA RIPORTATO

Dichiarazione per embargo

36 mesi

Richiesta motivata embargo

5. Tutela della proprietà intellettuale

Liberatoria consultazione dati Eprints

Consapevole del fatto che attraverso l'Archivio istituzionale ad accesso aperto "EPRINTS.unife.it" saranno comunque accessibili i metadati relativi alla tesi (titolo, autore, abstract, ecc.)

Firma del dottorando

Ferrara, li 18/02/2020 Firma del Dottorando _____

Firma del Tutore

Visto: Il Tutore Si approva Firma del Tutore _____

# Università degli Studi di Ferrara

**UFFICIO DOTTORATI DI RICERCA**

**AL MAGNIFICO RETTORE**
UNIVERSITÀ DEGLI STUDI DI FERRARA
UFFICIO DOTTORATO
Via delle Scienze, n. 41/B – 44121 Ferrara

| **Richiesta di embargo della tesi di dottorato oltre i 12 mesi**<br>(da allegare alla dichiarazione di conformità) | |
|---|---|
| **Nome e cognome del dottorando:** | **Michele Ferrari** |
| **Corso di dottorato:** | BIOLOGIA EVOLUZIONISTICA ED ECOLOGIA |
| **Matricola:** | 131522 |
| **Ciclo:** | XXXII |
| **E-mail per contatti:** | frrmhl1@unife.it |
| **Anno dell'esame finale:** | **2020** |
| **Nome e cognome del Tutore:** | **Anna Torelli** |

**Titolo della tesi:**

DNA methylation and Cr(VI) stress responses in Scenedesmus acutus: a focus in Sulfur pathway

| **Periodo di secretazione:** | ☐ **18 mesi** | ☐ **24 mesi** | ☑ **36 mesi** |
|---|---|---|---|

**Motivo dell'embargo:**

| | | |
|---|---|---|
| **Tesi in corso di pubblicazione** | ☐ | Tesi già sottoposte a un editore che non consenta l'accesso aperto prima dell'avvenuta pubblicazione |
| **Motivi di pubblica sicurezza** | ☐ | Quando la tesi può mettere a rischio la sicurezza pubblica e/o nazionale o per motivi di rispetto della Legge vigente |
| **Tutela della proprietà intellettuale** | ☑ | Diritto d'autore, brevetti, copyright etc. |
| **Tesi previo accordo con terze parti** | ☐ | Lavoro prodotto nell'ambito di un progetto di ricerca per il quale sia stato stipulato un accordo con un ente di ricerca esterno o con un ente finanziatore che preveda la divulgazione della tesi solo dopo il completamento dell'intero progetto di ricerca |
| **Privacy** | ☐ | Qualora la ricerca verta su una o più persone per cui si tema di violare il diritto alla riservatezza |

**Descrizione dettagliata della richiesta di secretazione:**

*Indicare in modo esaustivo le ragioni per cui si chiede l'embargo, citando gli estremi di eventuali accordi editoriali, contratti commerciali, progetti di ricerca etc. per cui sia richiesta la non accessibilità temporanea ai contenuti del lavoro*

**I dati contenuti nella presente tesi saranno oggetto di pubblicazioni in via di preparazione.**

| | |
|---|---|
| **Data:** | **18/02/2020** |
| **Firma del dottorando:** | |
| **Firma del Tutore:** | |

Come previsto dal Regolamento in materia di Dottorato di Ricerca dell'Università di Ferrara, che stabilisce l'obbligo di deposito delle tesi di Dottorato nell'archivio istituzionale d'Ateneo ad accesso aperto, la presente istanza dovrà essere sottoposta all'eventuale approvazione da parte del Consiglio di "IUSS Ferrara 1391"